Analysis of Programmed Cell Death in the Amnioserosa, an Extra-embryonic Epithelium in *Drosophila melanogaster*

by

Nilufar Mohseni

A thesis
presented to the University of Waterloo
in fulfillment of the
thesis requirement for the degree of
Master of Science
in
Biology

Waterloo, Ontario, Canada, 2008

I hereby declare that I am sole author of this thesis. This is a true copy of the thesis, including any required final revisions, as accepted by my examiners. I understand that my thesis may be electronically available to the public.

Abstract

The amnioserosa (AS) is an epithelium that plays major roles in two crucial morphogenetic processes during *Drosophila* embryogenesis: Germ Band Retraction (GBR) and Dorsal Closure (DC). The AS is extra-embryonic and as such, it does not contribute to the mature embryo but is eliminated during development by programmed cell death. In this thesis, a comprehensive investigation of the timing and characteristics of the AS death and degeneration is performed. It is demonstrated that AS elimination occurs in two phases: "cell extrusion" during DC, embryonic stages 12 to 14, and "tissue dissociation" following DC, embryonic stages 15 to 16. Ten percent of AS cells are eliminated during phase one while the remaining ninety percent are removed during phase two. It is found that both cell extrusion and tissue dissociation are absent in apoptotic defective backgrounds, as well as in genetic backgrounds associated with increased class I phosphoinositide 3-kinase (PI3K) activity, a key regulator of autophagy. It is also found that extrusion is enhanced two-fold in embryos expressing the pro-apoptotic *reaper* gene product, and that tissue dissociation also accelerates in this background. Interestingly, our observations suggest that the activation of caspase cascade is not complete until AS cells have lost apical contacts with neighboring cells. Shortly after the loss of apical contact, an apoptotic morphology including membrane blebbing, cell fragmentation, and macrophage engulfment is readily observed. Measurements of the rate of DC demonstrate that this process is protracted in backgrounds lacking extrusion, leading to the conclusion that extrusion contributes towards generating adequate AS tension required for normal DC rates. Overall, our data suggest that phase one extrusion and phase two dissociation are manifestations of the same cellular event and that both are caspase dependent.

It is also demonstrated that autophagy is a key component of AS death that acts upstream of apoptosis. Strikingly, our results lead to the suggestion that autophagy may function to trigger apoptosis during the programmed elimination of this extra-embryonic tissue.

Acknowledgment

I would like to thank my supervisor, Dr. Bruce H. Reed for giving me the opportunity to work in his laboratory. Bruce's tremendous support, enormous knowledge and tireless effort devoted to my project are greatly appreciated. Thank you for believing in me and my abilities, and for your patience for my endless questions. It has been a wonderful experience to pursue science in your laboratory.

I would like to express my gratitude to my committee members, Prof. Niels Bols, and Dr. Mungo Marsden, for their valuable suggestions and guidance throughout this work.

I am also grateful to Dale Weber, for his extensive help with confocal and Transmission Electron Microscopy. He was a great support during my tough time obtaining the TEM skill.

A big “Thank you” to my lab members from past to present. I specially want to thank Roopali Chaudhary and Stephanie McMillan for their wonderful friendship, and helping me to become better acquainted with my new hometown.

I would like to thank my family, my mom, Sudabeh Firozabadi, my dad, Prof. Hossein Mohseni, and my brother, Salman Mohseni, for their unconditional love and encouragement, and my husband, Arash Abghari, whose love, support and faith in me helped me to accomplish this work.

Table of Contents

List of Figures

List of Tables

Abbreviations

AEL	After Egg Laying
AO	Acridine Orange
ΔαInR	Activated Insulin Receptor
APAF-1	Apoptosis Protease Activating Factor 1
APF	After Pupae Formation
AS	Amnioserosa
ATG	Autophagy (gene)
BIR	Baculoviral IAPs Repeat
CAD	Caspase Activated DNAase
CARD	Caspase Recruitment Domain
CNS	Central Nervous System
Crq	Croquemort
cyt-c	Cytochrome c
DC	Dorsal Closure
DIABLO	Direct IAP-Binding protein with Low pl
DIAP	Drosophila Inhibitor of Apoptosis
DISC	Death Inducing Signaling Complex
E/A	Epan/Araldyde
FASL	Fas Ligand
GBR	Germ Band Retraction
GFP	Green Fluorescent Protein
Grm	Grim
HI	Head Involution
Hid	Head involution defective
IAP	Inhibitor of Apoptosis
ICAD	Inhibitor of CAD
InR	Insulin Receptor
LC3	Light Chain 3
PAS	Pre Autophagosomal Structure
PCD	Programmed Cell Death
PDK1	Phosphoinositide Dependent Kinase 1
PI3K	Phosphoinositide 3-Kinase

PS	Phosphatidylserine
PTT	Protein Transposon Trap
Rpr	Reaper
SGs	Salivary Glands
Skl	Sickle
Smac	Second mitochondria derived activator of caspaes
TEM	Transmission Electron Microscopy
TUNEL	Terminal Deoxynucleotidyl Transferase mediated dUTP

Chapter 1

Introduction

Cells die through two distinct morphological pathways: accidental cell death, generally described as necrosis, and programmed cell death (PCD). PCD is divided into three distinct forms of cell death: apoptotic, autophagic, and non-lysosomal cell death. Apoptotic and autophagic cell death are the most common and the most studied forms of cell death, particularly during animal development. Non-lysosomal cell death, however, is unusual and is not well described (Lockshin and Zakeri, 2004).

1.1 Necrosis

Necrosis, from the Greek word "nekros" meaning dead body, describes the morphology of cells that are injured due to severe stress such as mechanical damage, exposure to toxins, or infection. Necrosis is usually a multi-step process. Primarily, various physiological stimuli can increase mitochondria permeability, causing the mitochondria to cease functioning. Dysfunctional mitochondria in turn, cause the collapse of cell and/or organelle potential, leading to the disruption of membrane integrity (Zamzami et al., 1997). The loss of organelle membrane integrity, particularly lysosomes, leads to the release of proteolytic enzymes and results in the digestion and breakdown of intracellular as well as extra-cellular components and structures. Significant hallmarks of necrosis include cellular swelling and cell membrane leakage, which, unlike apoptosis (see below), occur in the absence of nuclear fragmentation. Also, unlike PCD, necrosis invokes an immune response and localized inflammation, leading to further tissue damage (Cruchten and Broeck, 2002).

1.2 Apoptosis

Apoptosis, a Greek term meaning “leaves falling off the trees”, is the best understood and the most well defined form of PCD. Apoptosis has significant roles in sculpting structures during embryonic development, eliminating damaged or unwanted cells, and maintaining tissue homeostasis in multi-cellular organisms (Lockshin and Zakeri , 2004; Baehrecke, 2002). Apoptosis was first described as a unique form of cellular death, and is distinct from necrotic cell death on the basis of morphology. In addition, and in contrast to necrosis, apoptosis is genetically regulated. The morphological manifestation of apoptosis comprises cell shrinkage, chromatin condensation, organelle preservation, nuclear fragmentation, cytoplasmic budding, and cell fragmentation (Figure 1.1).

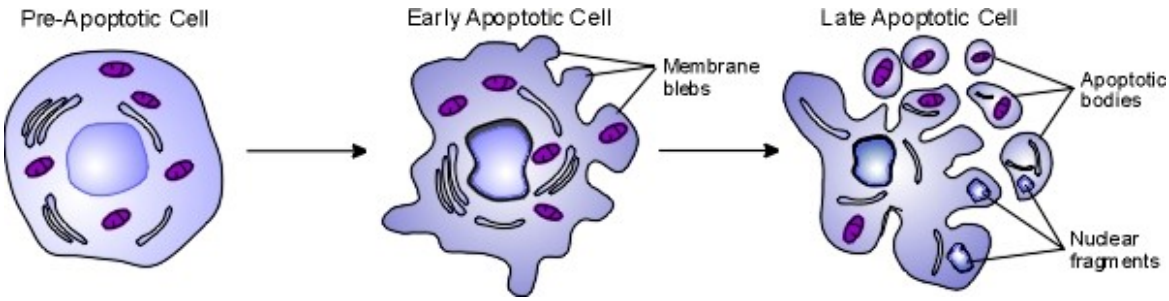

Figure 1.1 The main morphological manifestation of apoptosis (Walker NI, 1988)**.**

Apoptotic cells send “eat me” signals to the macrophages in order to provoke the rapid engulfment of apoptotic corpses and prevent inflammatory response (Martin and Baehrecke, 2004). Exposed phosphatidylserine (PS) in the outer leaflet of the apoptotic cell membrane for instance, functions as an “eat me” signal for macrophage engulfment (Williamson et al., 2001). Macrophages, on the other hand, carry receptors to recognize apoptotic cells and their signals.

Apoptosis can be activated through two distinct pathways: extrinsic or intrinsic. The former, exemplified by the removal of undesired tissues or cells during embryonic development, is induced by different external signals such as death ligands which bind to death receptors in the

plasma membrane, whereas the latter is triggered by internal signals such as DNA damage, viral infection, activation of oncogenes, or other factors leading to permeation of the outer mitochondrial membrane (Shiozaki and Shi, 2004). Both the extrinsic and intrinsic pathways ultimately activate the hallmark molecules of apoptosis, the caspases.

Caspases are site-specific proteases, which contain cysteine within their active sites and cleave substrate peptides c-terminal to an aspartic acid residue (Lockshin and Zakeri, 2004). Caspases are classified into two groups, according to their order and mechanism of activation. Both groups exist as inactive precursors or zymogens in all the cells. The first caspases to be activated in response to cell death stimuli are known as initiator caspases. Once activated, the initiator caspases, in turn, act on the second group of caspases, which are known as effector caspases. This system creates a caspase cascade activation mechanism (Shi, 2004). Activated effector caspases are responsible for all apoptotic events via the cleavage of death substrates. Death substrates include other caspase precursors, anti-apoptotic regulatory proteins, and numerous (over forty are known at present) other proteins; e.g. ICAD, an inhibitor of a deoxyribonuclease, or nuclear lamins, the destruction of which can be directly linked to the physical manifestations, described for apoptosis (Mukae et al., 1998; Rao et al., 1996).

Initially, the role of caspases in PCD was elucidated through analysis of the *Caenorhabditis elegans* gene CED-3, a homolog of mammalian caspase-9, and homolog of the *Drosophila melanogaster* caspase DRONC (Yuan et al., 1993). CED-3 is the only caspase found in *C.elegans*, which possibly operates as both an initiator and an effector caspase. To date, at least 14 caspases are found in mammals, among them four initiator and three effector caspases contribute most to cell death (Bao and Shi, 2007).

In mammals, caspase-8 and 9 are the crucial initiator caspases which are activated through two distinct pathways; caspase-8 is associated with extrinsic apoptosis in which external signals are required for the initiation of the recruitment, whereas caspase-9 is connected with intrinsic apoptosis and requires internal signals to be activated. Procaspase-9 carries a Caspase

Recruitment Domain (CARD), which is essential for its activation; upon activation, the CARD domain of procaspase-9 assembles on the CARD domain of APAF-1 (Apoptotic Protease Activating Factor 1), which is only available for interaction when assembled into an oligomeric wheel-like structure called the apoptosome. An apoptosome consists of APAF-1, the orthologue of CED-4 in *C.elegans* and Dark or DAPAF-1 in *Drosophila,* and cofactors, including cytocrome c (cyt-c), and dATP (Li et al., 1997; Qin et al., 1999). Interaction of procaspase-9 with the assembled apoptosome leads to auto-catalyzation and activation of this caspase.

Caspase-8, on the other hand, is the best representative of the initiator caspases involved in the extrinsic pathway mediated by the activation of death receptors on the cell surface. The death receptors belong to the family of tumor necrosis factor receptor such as Fas. Fas receptors oligomerize through binding with the FAS ligand (FASL). After a series of adaptors are recruited, procaspase-8 sequesters in a complex known as the Death Inducing Signaling Complex (DISC) and becomes activated through auto-catalysis (Bao and Shi, 2007).

Both excessive and insufficient apoptosis are devastating to organisms and lead to severe pathological conditions. Many neurodegenerative disorders are the consequence of upregulated apoptosis (Yuan and Yankner, 2000) whereas cancer and some autoimmune diseases are sometimes the result of apoptosis suppression (Hanahan and Weinberg, 2000; Thompson, 1995). Therefore, caspases, as vital components of the apoptotic machinery, are strictly regulated in all multi-cellular organisms. Some of the controlling mechanisms for caspases include transcriptional regulation, post-translational modification (Earnshaw et al., 1999), and the degradation of activated caspases by 26S proteasomes (Huang et al., 2000).

The Inhibitor of Apoptosis (IAP) proteins act as the principal regulators of apoptosis (Deveraux and Reed, 1999). In mammals, eight IAP molecules are found but not all initiator and effector caspases are inhibited by these molecules; caspase-6 and 8, for instance, are not suppressed by IAPs.

The functional unit of the IAP molecules, the Baculoviral IAPs Repeat (BIR) domain,

contains eighty amino acids. In mammals, for example, XIAP, c-IAP1 and c-IAP2 contain three BIR domains. In all of them, BIR3 inhibits caspase-9, whereas the linker section between BIR1 and BIR2 bind selectively with caspase-3 and -7 (Fesik and Shi, 2001). Upon receiving death signals, the outer membranes of the mitochondria form pores, become permeable, and release pro-apoptotic proteins such as cyt-c and Smac (Second mitochondria-derived activator of caspases) (Du et al., 2000) / DIABLO (Direct IAP-Binding protein with Low pl) (Verhagen et al., 2000) into the cytosol. cyt-c binds to APAF-1 and eventually activates caspase-9 through assembly of the apoptosome; meanwhile Smac/DIABLO binds to the BIR domains of IAPs and thereby liberates the active initiator and effector caspases, leading to caspase cascade and apoptosis. It has been demonstrated that active caspase-9 contains an exposed IAP-binding tetra-peptide motif to which XIAP can bind and results in suppression of caspase-9 activity (Srinivasula et al., 2001). Since proteolytic processing is required for the tetra-peptide motif exposure, procaspase-9 is unable to interact with the XIAP molecule, suggesting that IAPs suppress activated caspases, not procaspases. Smac/DIABLO is the only IAP inhibitor protein identified in mammals. Reaper, Grim, Hid, and Sickle, are the functional homologs of Smac/DIABLO in *Drosophila* (Wang et al., 1999).

Based on the primary features of apoptotic cells, different techniques have been developed to detect apoptotic cells over the years. These methods include DNA fragmentation detection, cleaved caspase substrate recognition, caspase activity measurement, the exposure of phosphatidylserine, and mitochondria membrane depolarization detection. TUNEL assay, anti-cleaved caspase-3 antibody and acridine orange staining are some common tools to detect apoptosis.

1.3 Autophagy and Autophagic PCD

Autophagy is a normal cellular event and occurs in all cells at a low basal rate to maintain homeostasis, but up-regulates quickly in the absence of energy producing resources. Autophagy can also act as a pro-death mechanism, especially in cells with damaged apoptotic machinery (Levine and Yuan, 2005), and when the elimination of an entire tissue is desired (Lockshin and Zakeri, 2004). Autophagy has also been implicated as a non-apoptotic form of PCD, in which there is self-cannibalization via a lysosomal degradation process. It is also the only known pathway for degrading organelles and certain macromolecules such as protein aggregates (Klionsky and Emr, 2000; Levine and Yuan, 2005).

In contrast to apoptosis, less is known of the molecular mechanism(s) regulating autophagy and its associated morphological events (Lockshin, and Zakeri, 2004). Most of what is known of the autophagy pathway has been derived from studies in budding yeast (*Saccharomyces cerevisiae*). The only hallmark cytological feature associated with autophagic cells is a double-membraned structure known as the autophagosome. The origin of the autophagosome remains something of a mystery. In yeast, the autophagosome is thought to originated from an isolation membrane that is derived from a preautophagosomal (PAS) structure (a distinct cellular region), and envelops cytoplasmic components (Rusten et al., 2004) (Figure 1.2). In mammals, however, one study suggests that the autophagosome is derived from the endoplasmic reticulum (ER) (Dunn, 1990), whereas other studies suggest that the sequestering membranes are not derived directly from the ER (Stromhaug et al., 1998), lysosomes (Stromhaug et al., 1998), or golgi apparatus (Ueno et al., 1991), but from a unique organelle called the phagophore (Stromhaug et al., 1998).

To date, twenty genes required for autophagy have been identified in *Saccharomyces cerevisiae*. Among theses, ATG12, a small ubiquitin-like protein, is covalently bound to ATG5, forming an ATG12-ATG5 complex. ATG8, another ubiquitin-like protein, localizes to the PAS

through association with the ATG12-ATG5 complex. All three genes (ATG5, ATG8, and ATG12) are essential for the progression of autophagy (Levine and Yuan, 2005), and are conserved from yeast to mammals (Mizushima et al., 2001). ATG5 and ATG8 (mammalian homologs ATG5 and LC3, respectively) localize to the emerging autophagic double membranes. Once membrane closure is complete, forming the autophagosome, ATG5 is shed from autophagosome membrane, while LC3 remains attached. After fusing with the lysosome to form the autolysosome, LC3 is lost from the inner membrane but is still detected in the lysosomal lumen (Figure 1.2) (Rusten et al., 2004).

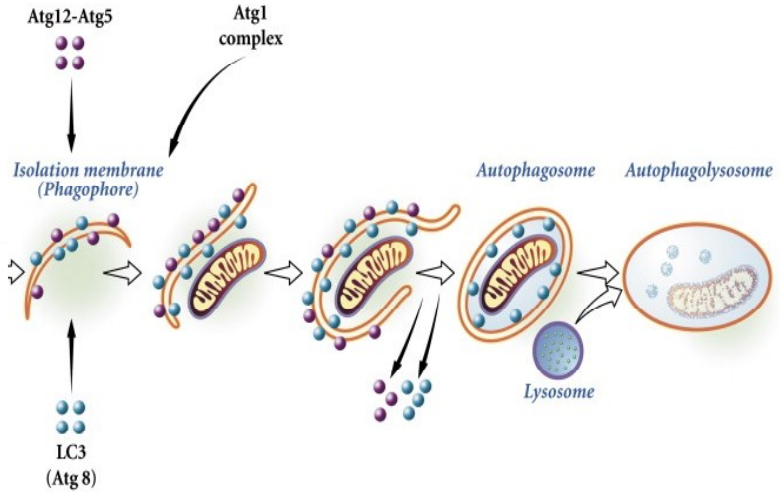

Figure 1.2 Different stages of the autophagic process (Pattingre et al., 2007)**.**

Based on the main features of autophagic cells, which include the presence of autophagosomes and autolysosomes, different techniques have been developed to detect autophagic cells. LC3-GFP (section 2.9), Transmission Electron Microscopy (TEM) (described in section 2.10), and LysoTracker staining are among the most common tools to detect autophagy in cells and tissues. LysoTracker is a red fluorescent permeant vital dye for staining the acidic compartments in a cell, including lysosomes and autolysosomes. The dye has been proven to be a useful complementary method to LC3-GFP for autophagy (Rusten et al., 2004).

Autophagic cell death describes a second form of PCD that can result from excessive levels of autophagy (Levine and Yuan, 2005). Sometimes described as "histolysis", autophagic cell death morphologically differs from apoptosis. The principal hallmark of autophagy, the autophagosome and autolysosomes, are abundant in cells undergoing autophagic PCD. In autophagic cells the cytoskeletal elements remain intact until the very late stages of cell death, whereas the degradation of the organelles is an early event. In apoptosis, the converse is true; there being an early collapse of the cytoskeletal elements but intact organelles until very late stages (Lockshin and Zakeri,, 2004). Apoptosis is also distinct from autophagic cell death based on the location and role of lysosomes. Moreover, apoptotic cells are usually engulfed by macrophages or, in some cases, by neighboring cells. In either scenario, however, the degradation of the apoptotic corpse occurs in the macrophage vacuoles, but in autophagic cells the cytoplasmic components are ultimately found inside their own lysosomes. In effect, autophagic cells are degenerated and eliminated without phagocytes (Baehrecke, 2003). Autophagic cell death and apoptosis are similar in that neither evokes an inflammatory response (Levine and Yuan, 2005). In some cases, certain features of apoptosis such as DNA fragmentation are also observed in cells committed to autophagic PCD.

Apoptotic and autophagic PCD appear to be prominent features in both vertebrate and insect development and are used in tissue remodeling (Wyllie, 1980). Autophagic PCD is more commonly seen when a group of associated cells or an entire tissue is eliminated (Lockshin and Zakeri, 2004). Apoptosis, however, is frequently observed when individual cells within a tissue undergo PCD.

The apoptotic and autophagic molecular machinery are both well conserved from yeast to mammals. Although autophagic PCD occurs during development and plays an important role in tumorogenesis and neurodegenerative diseases, the genetic regulatory pathways are not well understood (Gorski et al., 2003). Moreover, the difference in morphological characteristics between apoptosis and autophagic PCD suggests that these two forms of PCD utilize distinct

mechanisms (Clarke, 1990). Some interdependence, however, is suggested by the discovery that there is some overlap with respect to the molecules involved in autophagic cell death and apoptosis (Lee et al., 2000).

It is possible that cells normally destined to die by apoptosis, will die by autophagic cell death if the apoptotic machinery has been disabled**.** A related possibility is that since apoptotic death happens much faster than autophagic cell death, autophagy is only observed as the cause of death in apoptotic deficient cells (Lockshin and Zakeri, 2004).

Although the connection between apoptosis and autophagic PCD is still unclear, there is evidence that suggests autophagy leads to apoptosis. For example, it has been shown that the over-expression of ATG1, an autophagy regulator in *Drosophila,* leads to apoptosis. Programmed cell death, caused by the over-expression of ATG1, is a direct effect of autophagy induction and not due to the over-expression of ATG1 per se; over-expression of this gene in an ATG8 mutant background, suffering from suppressed autophagic machinery (no autophagosome formation), inhibits apoptosis (Scott et al., 2007). In addition, cell death resulting from ATG1 over-expression is suppressed by ectopic expression of the caspase inhibitor protein p35, and cells over-expressing ATG1 exhibit an elevated rate of activated caspase-3 and positive TUNEL staining (Scott et al., 2007). Scott *et al*.[2007] indicate that the over-expression of ATG1 causes a programmed cell death with characteristics of both apoptosis and autophagy that is caspase-dependent and demonstrates DNA fragmentation. Consequently, the authors conclude that excessive levels of autophagy can lead to apoptosis (Scott et al., 2007).

Other lines of evidence support the cross-talk between apoptotic and autophagic PCD. For example, the over-expression of Bcl-2, an anti-apoptotic element, inhibits autophagy through interaction with ATG6 (yeast Beclin 1 ortholog) in yeast and mammalian cell lines (Pattingre et al., 2005). In addition, it has been shown that autophagy genes, can be required for the induction of caspase dependent PCD in mammalian cell lines (Yu et al., 2004),(Pyo et al., 2005).

During embryogenesis numerous cells must be removed at specific times and

macrophages might not be sufficient to clear massive numbers of dying cells (Levine and Yuan, 2005). It is also possible that a high level of autophagy in dying cells can be a self-clearance mechanism in apoptotic cells. In such cases, autophagy may be triggered and cellular contents digested by using their own lysosomes.

1.4 *Drosophila*: A Useful Model Organism for the Analysis of PCD

Much of the pioneer work in the field of PCD has been carried out by using mammalian tissue cultures or the genetic analysis of free-living nematode *C. elegans*. *Drosophila melanogaster,* as a model to study the PCD components and pathways, provides a system of intermediate complexity that is situated somewhere between *C. elegans* and mammals. *Drosophila* shares many of the PCD components with mammals, more so than *C. elegans*, but due to a lower genetic redundancy than the mammalian systems, there is often a greater ease of functional analysis. Also, *Drosophila* offers the advantages of highly developed genetic analysis, molecular and developmental biology, as well as publicly available high-resolution genome databases, associated microarray, and cloning resources.

Many human pathological conditions, including cancer, several neurodegenerative diseases, and even heart failure and stroke, are associated with the disregulation of PCD. *Drosophila* is an appropriate model organism to provide a better understanding of the fundamental mechanisms governing PCD, and generating novel approaches to managing and treating these devastating conditions.

1.5 Regulation of Apoptosis in *Drosophila*

So far, seven caspases have been characterized in *Drosophila* and are classified into two groups: initiator caspases, with long N-terminal prodomains (DREDD, DRONC, and STRICA), and effector caspases, having short or no N-terminal prodomains (Dcp-1,DAMM, DECAY,and DRICE) (Kornbluth and White, 2005).

Also, the intrinsic and extrinsic cell death pathways are prominent in apoptosis induction in *Drosophila*. In the intrinsic cell death pathway, DRONC—the mammalian caspase-9 homolog, the principal initiator caspase, and the CARD domain carrying caspase in *Drosophila*—is activated through interaction with the *Drosophila* apoptosome. The *Drosophila* apoptosome contains mammalian APAF-1 homolog, DAPAF-1 or DARK, but does not necessarily require cyt-c for proper assembly and function (Dorstyn et al., 2004). Activated DRONC can further cleave and activate the primary effector caspase DRICE which executes cell death.

To protect against unwanted death, cells have systems of checks and balances. Inhibitors of Apoptosis Proteins (IAPs) in mammals and DIAPs in *Drosophila* are ubiquitously expressed proteins that guard against apoptosis. In *Drosophila,* DIAP1 and DIAP2 are two known IAPs which act by binding and inhibiting the active site of caspases (Shiozaki and Shi, 2004). The loss of DIAP1 leads to an early embryonic death due to massive apoptosis (Goyal et al., 2000). DIAP2 is less known and does not inhibit most of the *Drosophila* caspases.

Thus the accidental activation of initiator or effector caspases is prevented by anti–apoptotic molecules. Following the reception of a death signal, the effects of the DIAPs in *Drosophil*a are, in turn, countered by at least three apoptosis proteins: Reaper (Rpr), Grim (Grm), and Head-involution-defective (Hid). These proteins are thought to bind DIAPs, thereby relieving the DIAP-caspase inhibitory interaction (Wang et al., 1999). Therefore, each of these genes can be viewed as encoding an inhibitor of the inhibitor.

The *rpr*, *grm* and *hid* are located three-in-a-row and map to the left arm of the third

chromosome at 75C1-75C2. These three genes are removed by a small deletion, *Df(3L)H99*, and hence are frequently referred to as the *H99* genes. The deletion of a single *H99* gene has a very small effect on apoptosis, compared with the situation where two of them are deleted (Bangs et al., 2000). Embryos homozygous for the *H99* deletion are lethal and exhibit a complete absence of programmed cell death (Christich et al., 2002). *H99* deficient homozygous embryos also show a failure in the morphological process of head involution during the late stages of embryogenesis; the embryos still secrete cuticle but do not hatch from the egg case. In a cell, when the combined activity of *reaper*, *grim,* and *hid* exceeds a threshold, apoptosis is induced (Bangs et al., 2000).

The only similarity among Reaper, Grim*,* and Hid lies in a short stretch of homology at the N-terminus of each protein (Bangs et al., 2000), known as the tetra-peptide motif. Curiously, a very similar tetra-peptide motif has also been identified on the mammalian cell death regulatory protein Smac/DIABLO (Shiozaki and Shi, 2004). Smac/DIABLO is the only IAP inhibitor protein that is identified in mammals. Reaper, Grim, and Hid, which bind to the BIR2 domain in DIAP1 through their tetra-peptide motif and suppress the inhibitory effect of DIAP1 on the caspases, are the functional homologs of Smac/DIABLO in *Drosophila* (Wang et al., 1999).

Sickle (skl) is a fourth IAP binding protein in *Drosophila*. This gene maps 20 Kb proximal to the *H99* breakpoint and is transcribed in the same orientation as the *H99* genes. In addition, Sickle contains an N-terminal tetra-peptide motif and is associated with PCD in the embryo. Like the other *H99* genes, Sickle, also binds to the BIR2 domain in DIAP1. Unlike *reaper*, *grim* and *hid* that are expressed in all apoptotic cells throughout the embryo, the *sickle* expression is spatially restricted, being expressed in apoptotic cells only in certain tissues (Christich et al., 2002). Although *skl* is not removed by *Df(3L)H99*, the homozygous *H99* embryos reveal a complete absence of cell death. This observation suggests that the *skl* expression alone is insufficient for embryonic apoptosis, and that *skl* functions to enhance, rather than direct PCD (Christich et al., 2002).

The effects of the *H99* genes on PCD have been mostly studied in the CNS in

Drosophila. It has been demonstrated that the *rpr* null mutants do not suffer from many defects in developmental apoptosis. However, adult flies, lacking the functional *rpr* exhibit an enlarged central nervous system (Peterson et al., 2002). Usually, *rpr* and *hid* are expressed in dying midline cells in the CNS during embryogenesis. The ectopic expression of two copies of *rpr* and *hid* in the CNS results in rapid cell death in the midline cells during CNS development. It has been shown that the death induced by *rpr*+*hid*, *rpr,* or *hid* is dosage dependent; i.e., the expression of one copy of *rpr*+*hid*, *rpr,* or *hid* has less effect on the death of the midline cells in CNS compared to two copies (Zhou et al., 1997).

Many viruses express anti-apoptotic genes that efficiently inhibit apoptosis. These strategies likely evolved to ensure that host cells are kept alive long enough for the completion of viral replication (Tschopp et al., 1998). The insect baculovirus encodes a globally acting caspase inhibitor called p35. p35 is an unusual inhibitor because it presents itself as a substrate for caspases, but through partial cleavage, results in its own destruction while inactivating the caspase active site. Thus, p35 is known as a Trojan horse or suicide inhibitor. It is curious that p35 acts on almost all caspases, with the exception of the *Drosophila* initiator caspase DRONC which is refractory to p35 (Meier et al., 2000).

1.6 Regulation of Autophagy during Starvation in *Drosophila*

The InR (Insulin Receptor)/PI3K (class I phosphoinositide 3 kinase) signaling cascade regulates cell growth and proliferation by sensing nutrient availability through insulin. The over-expression of the InR, a member of the receptor tyrosine kinases, has been shown to inhibit starvation induced autophagy in *Drosophila* larval fat bodies (Scott et al., 2004). PI3K, which is activated through InR, catalyzes the formation of phosphatidylinositol-3,4,5-tris-phosphate (PIP_3) from phosphatidylinositol-4,5-bis-phosphate (PIP_2) in the cell membrane (Figure.1.3). A high level of PIP_3, in turn, recruits several kinases including Akt/PKB (protein kinase B) and PDK1 (3-Phosphoinositide-dependent protein kinase-1) which eventually inhibits autophagy. PDK1 activates Akt/PKB and S6K (ribosomal S6 kinase) (see below) through the phosphorylation of specific sites (Figure.1.3) (Chan et al., 1999). The PI3K signaling pathway is negatively regulated by a tumor suppressor gene, PTEN (phosphatase and tensin homolog deleted from chromosome 10) that reconverts PIP3 to PIP2 (Figure.1.3) (Neufeld, 2003).

In addition to the inhibitory effect of Akt on autophagy, Akt is also shown to function as an anti-apoptotic protein. Akt inactivates the members of the transcription family FOXO (Forkhead Box O, the homolog of DFOXO in *Drosophila*), a pro-apoptotic protein. Akt/PKB phosphorylates and inactivates FOXO. Phosphorylated FOXO is unable to enter the nucleus and regulate the transcription of its target genes. As a result of FOXO inactivation, the expression of some anti-apoptotic proteins such as Bcl-2 is up-regulated, whereas the expression of certain pro-apoptotic proteins such as Fas ligand is inhibited. Another anti-apoptotic effect of Akt is the suppression of several pro-apoptotic components; for example, caspase-9, through phosphorylation (Neufeld, 2003). DFOXO has also been proven to regulate the transcription of *hid* during UV-induced apoptosis in developing fly retina (Luo et al., 2007).

The Target of rapamycin (Tor), another regulator of autophagy, is a conserved kinase that inhibits autophagy during nutrient abundance (particularly amino acids) and induces cell growth,

transcription, and translation. Rapamycin, a macrolide antibiotic, induces autophagy through Tor inhibition (Rusten et al., 2004). Tor is the upstream activator of 6K p70 S6 kinase (S6) (Chung et al., 1992) S6K phosphorylates S6, a 40S ribosomal protein and induces translation, and, ultimately, cell growth (Kozma and Thomas, 1994), *Drosophila* DTor and DS6K mutants exhibit a smaller body size than that of the wild-type (Montagne et al., 1999; Zhang et al., 2000).

ATG1, a kinase regulating autophagy, negatively regulates the Tor/S6K pathway through the inhibition of S6K activation (Lee et al., 2007). On the other hand, Tor down-regulates ATG1 activity (Scott et al., 2004). A study of ATG1 in yeast indicates that this kinase is required for autophagosome/autolysosome formation during autophagy, as well as conducting autophagy itself (Shimizu et al., 2004; Kabeya et al., 2005).

Figure 1.3 Regulation of autophagy in *Drosophila*. The schematic demonstrates the various molecules involved in the regulation of autophagy through insulin receptor (InR) pathway. Activated InR activates the PI3-kinase homolog DP110 and its regulatory subunit p60 through the insulin receptor substrate, chico, and recruits the DP110 catalytic subunit of PI3-kinase to the plasma membrane. DP110 and its antagonized, DPTEN, are principal molecules in this pathway. The tumor suppressor protein DPTEN negatively regulates the levels of the phosphoinositide PIP3, and induces autophagy. High levels of PIP3, activates some kinases downstream of the pathway, such as DAkt and DPDK1. DPDK1 and DTor activate another kinase, S6K, which positively affects the cell and tissue growth. DTor is regulated by the abundance of the nutrients, particularly amino acids. The macrolide antibiotic, rapamycin, directly inhibits DTor, a negative regulator of autophagy. Also, ATG1 inhibits DTor and induces autophagy, particularly in the absence of nutrients. Ecdysone receptor is another positive regulator of autophagy, which induces autophagy through the inhibition of PI3K. The transcription factor, DFOXO, functions as a positive regulator of autophagy by regulating the expression of several genes involved in autophagy and apoptosis.

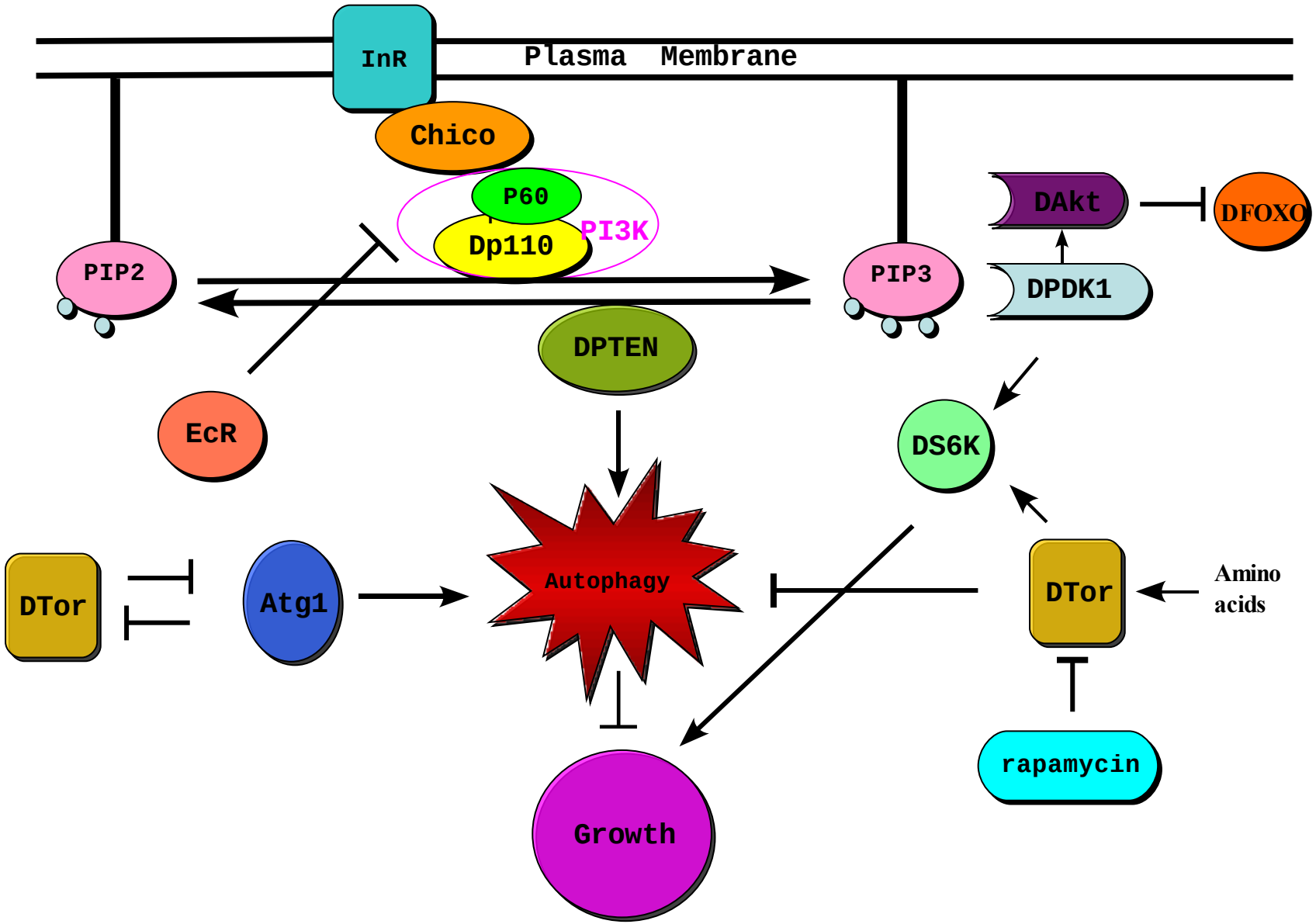
InR
Plasma Membrane
Chico
P60
Dp110
PI3K
PIP2
PIP3
DAkt
DFOXO
DPDK1
DPTEN
EcR
DS6K
DTor
Atg1
Autophagy
DTor
Amino acids
rapamycin
Growth

1.7 Regulation of Autophagic PCD in *Drosophila*

Ecdysone signaling induces autophagic cell death in larval tissue in *Drosophila* through the down-regulation of PI3K, the ortholog of *Drosophila* Dp110 (catalytic subunit) and p60 (regulatory subunit) (Figure 1.3). The ectopic expression of the dominant negative Dp110 as well as the loss of function of Akt results in extensive apoptosis during embryogenesis in *Drosophila* (Staveley et al., 1998). The larval salivary glands (SGs), midgut and fat bodies are the three principal larval structures that are eliminated during larval methamorphosis in *Drosophila.* Although these tissues are shown to be eliminated by autophagic PCD, some hallmarks of apoptotic PCD are also observed in these dying tissues making these larval structures useful tissue models to study the connection between the two forms of PCD.

Upon initiation of the pulses of steroid hormone 20-hydroxyecdysone (hereafter referred to as simply ecdysone) during metamorphosis, several genes, including *rpr* and *hid* are induced. Their induction removes the inhibitory effect of the high level of DIAP1 in the larval tissue, and trigger a rapid dissociation of the tissue, particularly SGs and midgut (Yin and Thummel, 2004). The loss of *hid* has been shown to inhibit SGs destruction, leading to persistent SGs. The loss of *rpr ,* though, does not prevent SG death but *rpr* cooperates with *hid* to eliminate the SGs (Yin and Thummel, 2004).

In contrast to the good knowledge about the role of ecdysone during *Drosophila* metamorphosis, the role of ecdysone during embryogenesis is less characterized. During embryogenesis, the titer of ecdysone peaks at the Germ Band Retraction (GBR), Dorsal Closure (DC) and Head Involution (HI) stage. The secretion of ecdysone is essential for cuticle deposition in the *Drosophila* embryo (Chavez et al., 2000). However, the role of ecdysone during embryogenesis is difficult to determine, because the mRNA and protein of the ecdysone are deposited maternally to the *Drosophila* eggs (Talbot et al., 1993).

1.8 *Drosophila* Salivary Glands, an Ideal Model Tissue to Study Autophagic PCD

Steroid hormones are important regulators of PCD during animal development. The *Drosophila* larval salivary gland (SG) is an excellent system to study the genetic response to steroid during PCD. Throughout *Drosophila* metamorphosis, the ecdysone titer rises 10-12 hr after puparium formation (APF) (Lee et al., 2000). This rise in ecdysone titer triggers a transcriptional cascade that culminates in the induction of PCD in the SGs, leading to a complete SG destruction by 16 hr APF. Within 4 hr of the ecdysone titer increase, SG cells exhibit several traits of apoptosis, including acridine orange positive cells, DNA fragmentation, and phosphatidylserine exposure on the outer leaflet of the plasma membrane (Jiang et al., 1997). Transcriptional upregulation of pro-apoptotic genes, including *rpr* and *hid*, has also been noted as an ecdysone response (Jiang et al., 2000). Although much data suggest that SGs die through apoptosis, dying cells possess autophagic vacuoles that contain organelles and do not appear to be associated with phagocytes during degradation, indicating that the cells achieve death using elements of both autophagic and apoptotic pathways (Lee et al., 2003).

Although the expression of p35, a caspase inhibitor, is sufficient to prevent DNA fragmentation and SG destruction (Lee and Baehrecke, 2001), the SG cells do not exhibit any significant change in the autophagic vacuolar structures. Similar experiments with the dominant-negative form of a *Drosophila* initiator caspase (DRONC) reveal that DRONC ^{DN} is capable of neither preventing vacuolar changes in persistent salivary glands nor changing the level of filamentous actin (Martin and Baehrecke, 2004). The interpretation of these studies is that while caspases are indeed involved in the destruction of the SGs in *Drosophila,* autophagic vacuole formation in SG cells is independent of caspase activity.

A recent model suggests that apoptosis and autophagy can play distinct roles during metamorphosis; autophagy is initially induced in the dying larval tissues to utilize the nutrients to

be used for differentiation and growth during metamorphosis. Then, the induction of apoptosis causes larval tissue removal (Yin and Thummel, 2005). The following evidence support this model: SG destruction and nuclear fragmentation is inhibited by the anti-apoptotic protein p35; however, p35 does not suppress autophagic vacuoles' formation in this tissue (Lee and Baehrecke, 2001), and the tissue degeneration is also interrupted in the main autophagy loss-of-function mutants, while DNA fragmentation persists in these mutants (Berry and Baehrecke, 2007).

Although it has been demonstrated that the two forms of cell death do not function absolutely independently, and that overlap exists with respect to the molecules involved in autophagic cell death and apoptosis, the cross-talk signaling between them is not well-characterized and needs further research.

1.9 The Amnioserosa: An Extra-embryonic Tissue in *Drosophila*

In *Drosophila*, the amnioserosa (AS) is an epithelium derived from the dorsal most region of the blastoderm (Campos-Ortega JA, 1997). This dorsal epithelium is extra-embryonic and, as such, does not contribute to the mature embryo.

The AS, though eventually discarded, is thought to play a major role in the morphogenetic processes of GBR and DC (Reed et al., 2004). During GBR (8-10 hr After Egg Laying (AEL)), the AS contracts along the anterior-posterior axis; this contraction may contribute part of the force that leads to the shortening (or retraction) of the germ band (Lamka and Lipshitz, 1999). During DC (10-13 hr AEL) the lateral epithelial sheets migrate, stretch, and fuse along the dorsal midline, a process that ultimately internalizes the AS and closes the dorsal hole of the embryo (Scuderi and Letsou, 2005). A premature loss of the AS is seen in several mutant backgrounds (Frank and Rushlow, 1996), or can be engineered through expression based cell ablation (Scuderi and Letsou, 2005). In either scenario, premature AS loss leads to clear defects

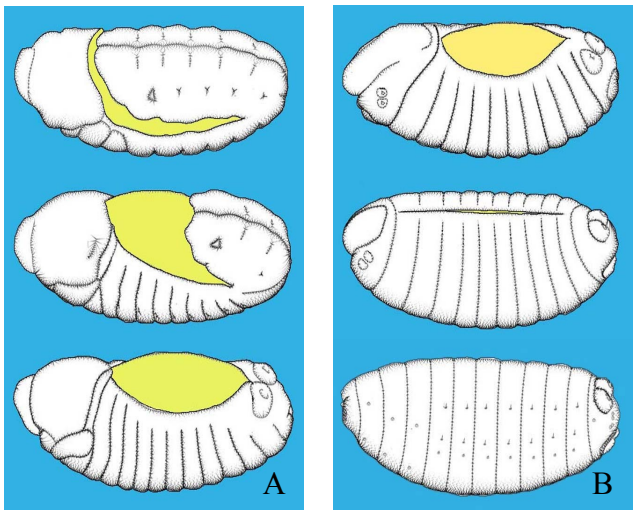

Figure 1.4 Embryogenesis stages in *Drosophila*. During GBR (A) the AS cells (yellow) change shape and contract along AP axis. During DC (B), the lateral epidermal sheets migrate, stretch and fuse along the dorsal midline. Embryos are anterior left, dorsal up (Hartenstein V., 1993).

in GBR and DC, demonstrating a role for the AS during these morphogenetic events (Lamka and Lipshitz, 1999; Reed et al., 2001). Possible AS functions include the generation of a force during the morphogenic movements of GBR and DC, as well as a cell signaling function (Lamka and Lipshitz, 1999). The interaction between the lateral epithelial sheets and the AS is crucial for GBR and DC.

Following DC, the AS degenerates. The cell death pathways involved in AS degeneration are unknown. However, it has been suggested that this tissue may be used as a model system for the analysis of anoikis (Reed et al., 2004). Anoikis is a term used to describe a type of caspase-dependent cell death that is activated when cells lose contact with their neighboring cells or the extra-cellular matrix. The study of anoikis has a significant relevance to tumor invasiveness and cancer metastasis.

The elimination of larval SGs, midgut and fat bodies are three main metamorphogenetic events in *Drosophila*. Although it has been shown that these tissues are removed by autophagic PCD, there are lines of evidence suggesting that apoptotic machinery is also active during the

death of these tissues. While studies on these tissues in *Drosophila* larvae have generated valuable information about the similarities and differences between apoptotic and autophagic PCD pathways, their components, and physical features (Lee and Baehrecke, 2001; Yin and Thummel, 2005; Rusten et al., 2004), less is known about the cross-talk between apoptotic and autophagic PCD during *Drosophila* embryogenesis. The AS and its role in morphogenetic events are well understood, however, not much is known about the removal mechanism(s) of this extra-embryonic tissue. We took advantage of the AS as a useful model tissue to study the connections between apoptotic and autophagic PCD during *Drosophila* embryogenesis.

1.10 Main Experimental Objectives of This Study

The AS, an extra-embryonic tissue which eventually falls apart during development, providing an excellent model to learn more about apoptotic and autophagic cell death, and the possible connections between these two forms of PCD.

The first objective in this study was to determine the timing and characteristics of the AS dissociation and death. This was achieved using a GFP-based live imaging approach. The confocal live imaging results presented suggest that the AS dissociation happens in two phases: cell extrusion (prior to DC), and tissue dissociation (following DC). Then the focus was to discern if these two phases are caspase dependent and if they represent manifestations of the same cellular event

Our second objective was to discover if autophagic cell death is involved in AS degeneration. Since the AS eventually shrinks in persistent AS backgrounds (apoptotic defective), it was assumed that autophagy is responsible for the shrinkage of this tissue. Ultra-structure analysis by TEM was performed to examine the AS in wild-type and mutant backgrounds.

At the onset of these studies we formulated four models regarding the relationship

between autophagic and apoptotic cell death in the AS. These are presented in figures 1.5-1.8.

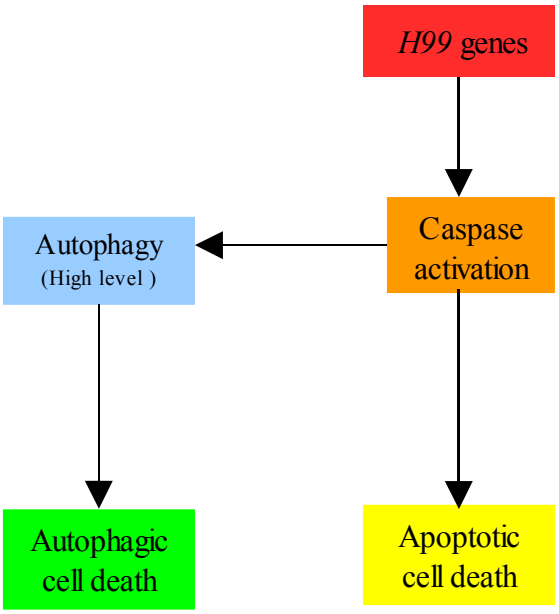

Figure 1.5 Model one: In the AS, autophagy, autophagic and apoptotic cell death are regulated by caspase activation which itself is downstream of *H99* genes.

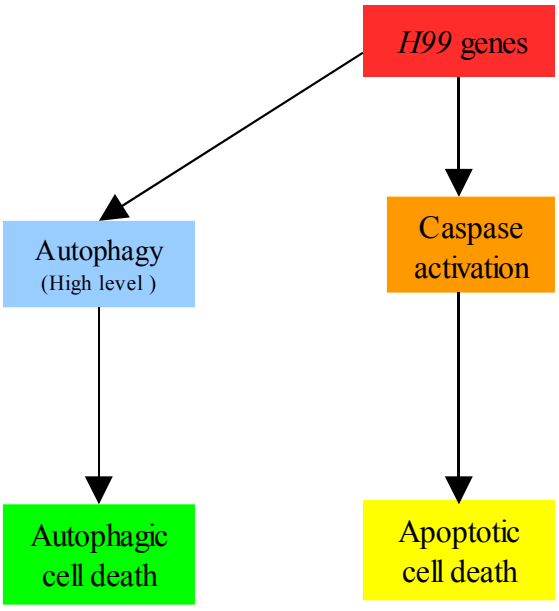

Figure 1.6 Model two: In the AS, apoptotic cell death is downstream of caspase activation and *H99* genes; autophagy (and consequently autophagic cell death) is also regulated by *H99* genes.

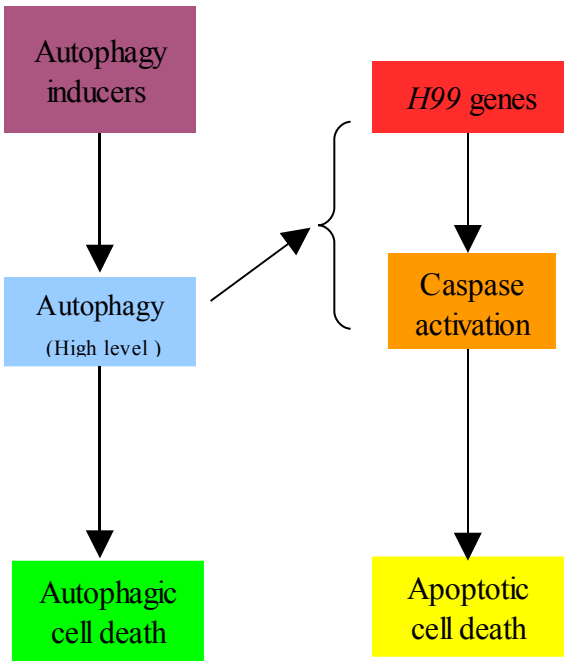

Figure 1.7 Model three: In the AS, high level of autophagy increases caspase activity and consequently apoptotic cell death, a similar regulation by *H99* genes. Autophagy inducers may include PI3K, ecdysone, and ATG1, as described in Section 1.6.

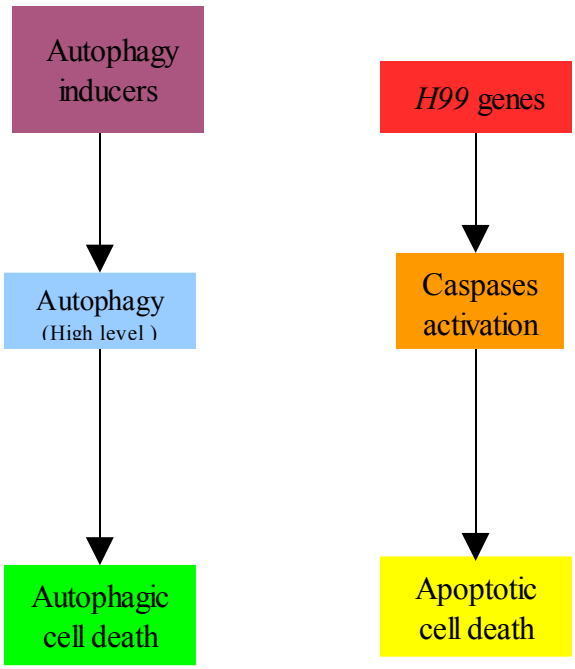

Figure 1.8 Model four: In the AS, apoptotic and autophagic cell death are regulated through independent pathways. Autophagy inducers may include PI3K, ecdysone, and ATG1, as described in Section 1.6.

Chapter 2

Materials and Methods

2.1 GAL4-UAS System

The GAL4/UAS expression system was used throughout these studies to promote ectopic gene expression, or to express gene constructs under spatial or temporal control (Phelps and Brand, 1998). GAL4 is a yeast transcription factor that binds to a target sequence called UAS (Upstream Activating Sequence). Since GAL4 responsive sequences are not found in the *Drosophila* genome, the UAS sequence can be used in combination with GAL4 to drive expression of transgenes (which are most frequently stable insertions of the *P* transposable element specifically developed for transgenic work in *Drosophila*). Numerous *P* element based GAL4 constructs or enhancer trap insertions are available, each having a unique GAL4 spatial/temporal expression pattern. These GAL4 insertions, or GAL4 drivers, place the expression of any gene downstream from a UAS sequence under GAL4 control, thereby confirming spatial/temporal expression. Generating a GAL4/UAS combination is often a simple matter of performing a genetic cross between a GAL4 driver line and a UAS expression line. Progeny of such a cross that carry both the GAL4 driver and the UAS construct will result in ectopic or over-expression of the gene of interest, housed in the UAS construct (Figure 2.1).

Figure 2.1 GAL4-UAS gene expression system. To activate target gene expression, a GAL4 enhancer trap line is crossed with a UAS target gene. In the progeny, the GeneX is expressed under spatial/temporal control conferred by the GAL4 expression.

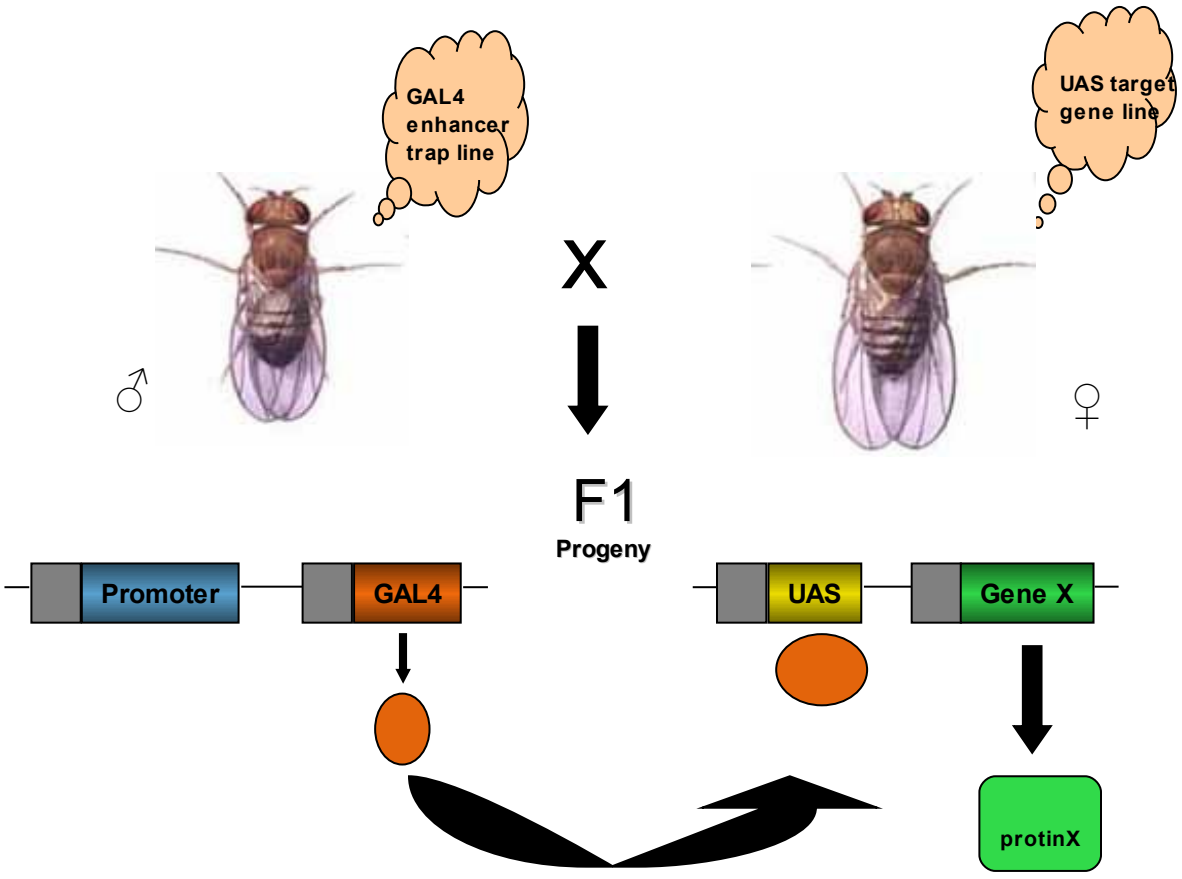
GAL4
enhancer
trap line
UAS target
gene line
X
♂
♀
F1
Progeny
Promoter
GAL4
UAS
Gene X
protinX

2.2 *Drosophila* mutants, Lines and Genetic Crosses

All *Drosophila* stock genotypes and genetic crosses used in this thesis are presented in Table 2.1. The mating scheme and system used to recognize the homozygous *Df(3L)H99* mutant embryos is presented in Figure 2.2.

2.3 Live Imaging

2.3.1 Confocal Microscopy

Eggs were collected at 3 hr intervals at 25°C on grape-juice agar plates using an automated *Drosophila* egg collector (Flymax Scientific Equipment Ltd.). Appropriately staged embryos were placed on double-sided sticky tape and manually dechorionated using jeweller's forceps. Dechorionated embryos were mounted on thin strip of double-sided sticky tape on a gas-permeable membrane as previously described (Reed et al., 2004). Mounted embryos were imaged at 2 min intervals for approximately 6 hr on a Ziess Axiovert 100 confocal microscope. NIH ImageJ software was used to compile the captured images and produce QuickTime movie files.

2.3.2 Stereoscope Microscopy

Embryos were collected every 3 hr between 6 pm and 6 am at 25°C using an automated *Drosophila* egg collector and dechorionated by hand as described in the previous section. Embryos were placed in a small drop of halocarbon oil on a coverslip, and over a hole previously cut on the bottom of an inverted plastic Petri dish to form a hanging drop. The chamber was humidified with moist paper to prevent dehydration. Embryos were imaged at 2 min intervals, and the images were complied using Leica Application Suite software.

Table 2.1 A summary of all crosses used to generate genotypes analyzed in this study. The parental genotypes, chromosomal locations of relevant genes or transgenes (where position is not evident from genotype description), as well as the source of the genetic stocks are described. *TwiG* is an abbreviation for "*Twist-GAL4+UAS-GFP*", "*Ubi-DEcad-GFP*" is an abbreviation for DEcadherin-GFP fusion transgene expressed under the control of a ubiquitin promoter. BC indicated stocks from the Bloomington stock centre.

	♀ Female Genotype	♂ Male Genotype
1	*yw*^{67} (X), BC	*yw*^{67} (X), BC
2	*yw*^{67} (X), BC	*Ubi-DEcad-GFP* (II), Lynn Cooley
3	*yw*^{67} (X), BC	Basigin-GFP,NP6293 (II), BC
4	*yw*^{67} (X), BC	*w;YET-1* (II), Alan Michaelson
5	*GAL4*$^{LP-1}$ (III), BC	*UAS-mCD8GFP* (III), BC
6	*GAL4*$^{LP-1}$ (III), BC	*UAS-α-catenin-GFP* (X), Nick Harden
7	*GAL4*$^{LP-1}$ (III), BC	*w*^{118}*;UAS-GFP*^{nls} (II), BC
8	*Zeus* (III), BC	*Ubi-DEcad-GFP* (II), Hiroki Oda
9	*y(w);+;GAL4*$^{LP-1}$*+Df(3L)H99* *TM6UW23-1* Reedlab	*y(w);+;UAS-mCD8GFP+Df(3L)H99* *TM6UW23-1* Reedlab
10	*y(w);+; GAL4*$^{LP-1}$ *+Df(3L)ED225* *TM6UW23-1* Reedlab	*y(w);+;UAS-mCD8GFP+Df(3L)H99* *TM6UW23-1* Reedlab
11	y(w);Ubi-*DEcad-GFP*; *Df(3L)ED225* *CyO* *TM3,TWI* Reedlab	*y(w);Ubi-DEcad-GFP; Df(3L)ED225* *CyO* *TM3,TwiG* Reedlab
12	*w; crqGAl4*^{79}*+UAS-mCD8GFP* *Gla* Reedlab	*w; crqGAl4*^{79}*+UAS-mCD8GFP* *Gla* Reedlab
13	*w;+;H99, GLA4*$^{LP-1}$ *TM6UW23-1* Reedlab	*w; crqGAl4*^{79}*;H99+UAS-mCD8GFP* + + Reedlab
14	*UAS-p35;UAS-p35* (X and II), BC	*w;Ubi-DEcad-GFP*; *daGal4* Reedlab
15	*UAS-rpr* (II), BC	*w;YET-1*; *daGal4* Reedlab
16	*UAS-rpr* (II), BC	*w;Ubi-DEcad-GFP*; *daGal4* Reedlab
17	*UAS-rpr* (II), BC	*yw;Ubi-DEcad-GFP, bsgGAL4* *CyO* Reedlab

	♀ Female Genotype	♂ Male Genotype
18	*UAS-grim* (II), JR.Nambu	*w;Ubi-DEcad-GFP*; *daGal4* Reedlab
19	*UAS-grim* (II), JR.Nambu	w;+; $\underline{GAL4^{LP\text{-}1}+GFP^{nls}}$ *TM3* Reedlab
20	*UAS-grim* (II), JR.Nambu	w;+;*Ubi-DEcad-GFP, bsgGAL4* *CyO* Reedlab
21	*UAS-hid* (X), Kristin White	*w;Ubi-DEcad-GFP*; *daGal4* Reedlab
22	*UAS-hid* (X), Kristin White	w;+; $\underline{GAL4^{LP\text{-}1}+GFP^{nls}}$ *TM3* Reedlab
23	*UAS-rpr +UAS-hid* (X), JR.Nambu	*w;Ubi-DEcad-GFP*; *daGAL4* Reedlab
24	*UAS-rpr +UAS-hid* (X), JR.Nambu	$\underline{GAL4^{LP\text{-}1}+GFP^{nls}}$ *TM3* Reedlab
25	*UAS-rpr +UAS-hid* (X), JR.Nambu	*yw;Ubi-DEcad-GFP, bsgGAL4* *CyO* Reedlab
26	*UAS-ΔαInR "G"* (III), BC	$\underline{Ubi\text{-}DEcad\text{-}GFP;GAL4^{LP\text{-}1}+GFP^{nls}}$ Reedlab
27	*UAS-ΔαInR "G"* (III), BC	*yw;Ubi-DEcad-GFP, bsgGAL4* *CyO* Reedlab
28	*UAS-LC3-GFP* (X), BC	$GAL4^{LP\text{-}1}$ (III), BC
29	*yw;UAS-ATG1*^{6A} (II), BC	*daGAL4* (III), BC
30	*yw;UAS-ATG1*^{6A} (II), BC	$GAL4^{LP\text{-}1}$ (III), BC
31	*yw;UAS-ATG1*^{6A} (II), BC	*yw;Ubi-DEcad-GFP, bsgGAL* *CyO* Reedlab
32	*UAS-ricin A* (III), BC	$GAL4^{LP\text{-}1}$ (III), BC
33	*w;+;*$\underline{th^4}$ *TM3.Twig* BC	*Ubi-DEcad-GFP* (II),BC
34	*w;+;*$\underline{tinman^{EC40}+Df(3L)ED225}$ *TM6UW23-1* Reedlab	*w;+;*$\underline{tinman^{EC40}+Df(3L)ED225}$ *TM6UW23-1* Reedlab

Figure 2.2 Cross scheme of obtaining and recognizing *Df(3L)H99* homozygous mutants. The homozygous deficiency for *H99 genes* is fully lethal, whereas the *H99* heterozygous mutants are viable; therefore, *Df(3L)H99* is maintained as a viable heterozygous stock using balancer chromosome *TM6UW23-1*. In order to separate the *H99* homozygous progeny from the siblings, two *H99* recombinant lines previously recovered in the Reedlab, were employed. The two lines were crossed, providing four genotypes. Only the *Df(3L)H99* homozygous progeny display AS GFP expression, as they are the only progeny that carry both the AS GAL4 driver ($GAL4^{LP\text{-}1}$) and the *UAS-mCD8-GFP* reporter.

♂ 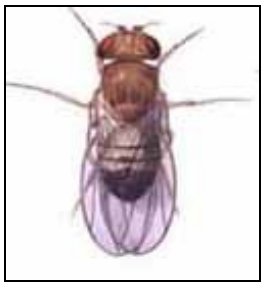 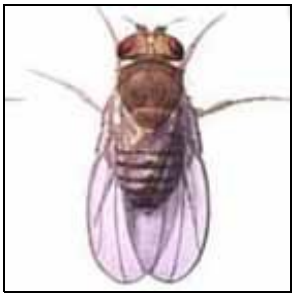 ♀

UAS-mCD8GFP+Df(3L)H99 **x** *GAL4^{LP-1}+Df(3L)H99*
TM6UW23-1 *TM6UW23-1*

F1 progeny

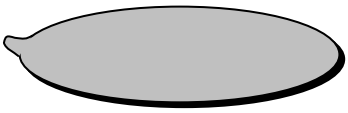

UAS-mCD8GFP+Df(3L)H99
TM6UW23-1

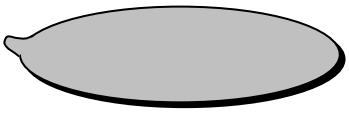

GAL4^{LP-1}+Df(3L)H99
TM6UW23-1

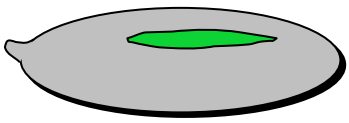

UAS-mCD8GFP+Df(3L)H99
GAL4^{LP-1} +Df(3L)H99

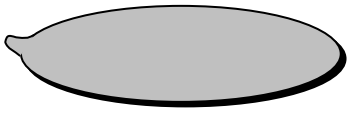

TM6UW23-1
TM6UW23-1

2.4 Calculation of the Rate of Extrusion

To measure the frequency of extrusion in different genetic backgrounds, the total number of AS cells was counted at the beginning of live imaging. Also, the number of the extruded cells was counted during the entire live imaging sequence. The percentage of the extruded AS cells was calculated for each embryo. The average of the extrusion was determined for each genotype.

2.5 Measurement of DC Progression

To plot the time course of DC, the areas of the dorsal hole were measured using NIH ImageJ software at 10 min interval, for the entire movie. The AS area vs. time was plotted with Matlab software (Figure 3.4).

2.6 Acridine Orange Staining

Acridine Orange (AO) is a simple but selective stain that labels apoptotic cells and not necrotic cells (Abrams et al., 1993). AO is weakly basic and has a tendency to bind to the acidic compartments of cell such as lysosomes and DNA. In a healthy cell, AO accumulates in the lysosomes in the cytoplasm, and thus, prevented from reaching the DNA (Clerc and Barenholz, 1998). After the death signals have been received, the mitochondria stop functioning, the pH gradient across the lysosome membrane is lost, and AO is discharged into the cytoplasm. In the absence of intact and functional lysosomes, AO enters the nucleus, binds to the DNA, and becomes extremely fluorescent (Delic et al., 1991).

To proceed with AO staining, over-night embryo collections were dechorionated in 50% bleach/50% dH2O for 3 min, and then washed thoroughly with dH2O. The acridine orange stock solution was diluted to 5μg/ml in 0.7%NaCl, and the embryos were transferred to a scintillation vial containing AO solution (5 μg/ml) topped with 10 ml heptane. The vial was shaken

vigorously by hand for 5 min. The aqua phase (AO and 0.7%NaCl) was then removed and replaced with heptane. The embryos were washed 3 times for 2 min in heptane, mounted in halocarbon oil on a slide, covered with a coverslip, and visualized with a Leica MZ16 microscope equipped with a Leica DFC350 FX camera and Leica Application suite software.

2.7 Cuticle Preparation

Embryo collections were aged for 24-36 hr to allow viable embryos to complete embryonic development. After the aged embryos were dechorionated in 50%bleach/50%PBS for 3 min, they were rinsed with dH2O. Dechorionated eggs were transferred with a clean artist's paint brush to a drop of Hoyer's mounting medium on a dust-free glass slide, covered with a coverslip, baked overnight at 60°C (Wieschaus and Nusslein-Volhard, 1986), and observed using a Zeiss axiovert 200 microscope equipped with a QIMAGING Retiga EXi fast 1394 camera and OpenLab software.

2.8 RNA *in situ* Hybridization

RNA *in situ* hybridization was applied to study the morphology and the fate of the AS using a probe for the gene CG12011. CG12011 is an RNA probe generated from cDNA clones housed in a pFLC-I vector. The CG12011 probe, which strongly labels AS cells, was obtained from the Canadian *Drosophila* Microarray Centre. All steps for *in situ* hybridization followed standard protocols (Henry M Krause, accessed 2008 January 5). Whole mount embryos were examined and photographed with a Zeiss axiovert 200 microscope equipped with QIMAGING Retiga EXi fast 1394 camera and OpenLab software

2.9 LC3-GFP

A transgenic line, expressing LC3-GFP, a mammalian homolog for ATG8, was recovered by Rusten *et al*. LC3-GFP is inserted downstream of the UAS sequence. In the absence of autophagic structures, LC3-GFP is observed to be uniformly distributed throughout the cytoplasm, whereas in the presence of autophagosomal/ autolysosomal structures LC3-GFP is as punctate GFP. This has been proven to be an efficient method for detection of autophagy in some tissues (Rusten et al., 2004).

To detect autophagy in the AS cells, *UAS-LC3-GFP* males were crossed with $GAL4^{LP\text{-}1}$ females. 3 hr embryo collections were aged for 6 to 12 hr and prepared for observation with confocal microscopy (as described in section 2.3.1.).

2.10 Transmission Electron Microscopy

Transmission Electron Microscopy (TEM) is used to study the occurrence of autophagosomes and autolysosomes in the cells as evidence of autophagy execution.

To prepare samples for TEM, 3 hr *Drosophila* embryo collections were aged 15 hr and dechorionated in 50% bleach/PBS (Phosphate Buffered Saline) for 3 min, and rinsed thoroughly in dH_2o. Dechorionated embryos were fixed in a mixture of 8 ml heptane and 2 ml 25% glutaraldehyde in 50mM sodium cacodylate buffer (PH=7.0) for 15-20 min. To devitellinize pre-fixed embryos, they were placed on double-sided tape covered with 2% glutaraldehyde in 50 mM cacodylate buffer. The vitelline membranes were removed manually using electrolytically sharpened tungsten needles. After the embryos were transferred to a mixture of 2% glutaraldehyde and 1% osmium tetroxide in 50 mM cacodylate buffer, they were fixed for 2 hr on ice, followed by several washes in 50 mM cacodylate. The post-fixation was performed in 1% osmium tetroxide buffer for 1 hr on ice. The fixed embryos were washed several times in 50 mM sodium cacodylate buffer and dehydrated in a graded series of ethanol and acetone as follows:

25% ethanol (10 min), 50% ethanol (10 min), 70% ethanol (2x10 min), 95% ethanol (10 min), 100% ethanol (2x10 min), 100% ethanol/100% acetone (2x 10 min), 100% acetone (15 min), 100% acetone first change (10 min), and 100% acetone second change (10 min). Gradually the embryos in acetone were transferred to Epan/Araldite (E/A) as follows: 75% acetone and 25% E/A (20 min), 50% acetone and 50% E/A (20 min), 25% acetone and 75% for 1 hr, 100% E/A on a rotator (overnight). After the embryos were embedded and oriented in fresh E/A in a flat embedding mold, they were heated at 60-65 °C for 24-48 hr to allow the plastic to be polymerized. Once embedded in E/A, ultra-thin sections (50-70nm) were obtained using a Reichert Ultracut E ultra microtome and glass knife. The sections were placed on 300 mesh copper grids (Canemco & Marivac), stained with lead citrate (0.04 g in 10 ml of boiled and cooled dH_2O with 0.1 NaOH 10 N), and uranyl acetate (0.05 g in 10 ml of 50% ethanol) and observed and photographed with Transmission Electron Microscopy (TEM) (Phillips CM10) using Philips photographic negative films. The negatives were scanned by a MICROTEK ScanMaker 6800 scanner. The images were processed and displayed with Photoshop software

Chapter 3

Results

3.1. Development of Systems to Analyze the Amnioserosa Degeneration

Initially, to determine the timing and characteristics of AS degeneration, a detailed analysis was performed in wild-type embryos. Using live imaging based techniques these studies revealed that AS degeneration occurs in two phases, possibly utilizing two distinct cell death mechanisms. These two phases are described as "cell extrusion" during DC, and "tissue dissociation" following DC. To visualize the AS prior to and following DC, different GFP reporters were tested as described below.

3.1.1 Visualizing the Amnioserosa

Two classes of transgenic lines, Protein Transposon Trap (PTT) and UAS-GFP fusion protein lines, were evaluated with respect to their utility in visualizing the AS in live embryos. These GFP constructs and reporters are listed in Table 3.1, and confocal microscope images are presented in Figure 3.1. Each GFP expressing background was found to be useful in visualizing the AS in live embryos. The *YET-1* line was found to be better suited to examining the late stages of the AS degeneration, while the *basigin* line was more suited to the earlier stages and visualizing AS/yolk membrane interactions. Also, the stock carrying *Zeus-GFP* with *Ubi-DEcad-GFP*, was found to be valuable; however, the strong GPF expression, especially in the leading edge of the epithelial cells, obscured the AS visualization. In addition, too much GFP expression can be harmful to the embryo. α-catenin-GFP labels the apical membrane of the AS cells and visualizes the apical shape of the cells, however, the level of expression, was much lower compared with the Ubi-DEcad-GFP. The Ubi-DEcad-GFP construct is co-localized to the apical adherens junctions and expressed throughout the *Drosophila* embryo.

Table 3.1 Description of approaches for attaining AS GFP expression, suitable for live imaging experiments.

Source of GFP expression	Description/Comments
GAL4$^{LP\text{-}1}$+UAS-GFP^{nls}	nuclear localized GFP expressed under AS driver control
YET-1	enhanced GFP expressed as an enhancer trap (strong expression in AS perimeter cells)
G270	protein Transposon Trap (PTT) lines expressing Basigin-GFP fusion protein under control of endogenous basigin promoter
Zeus+Ubi-DEcad-GFP	*Zeus+Ubi-DEcad-GFP* recombinant chromosome Zeus insert is a PTT line resulting in the expression of a microtubule-binding protein fused to GFP (under endogenous protein). *Ubi-DEcad-GFP* is described in Table 2.1 figure legend.
GAL4$^{LP\text{-}1}$+UAS-α-catenin-GFP	*α-catenin-GFP* fusion protein expressed under AS driver control
Ubi-DEcad-GFP	described in Table 2.1 figure legend
GAL4$^{LP\text{-}1}$+UAS-mCD8GFP	cytoplasmic localized GFP expressed under AS driver control

Figure 3.1 Different GFP reporters for visualizing the AS. Nuclear GFP expression in the AS using *UAS-GFP*^{nls} and *GAL4*$^{LP-1}$ (A), *YET-1* expression, a vital enhancer trap line (B), Basigin-GFP fusion protein expression from the endogenous basigin promoter (C), Zeus-GFP fusion protein and *Ubi-DEcad-GFP* expression (D), *UAS-α-catenin-GFP* expression driven by *GAL4*$^{LP-1}$(E), DEcadherin-GFP fusion protein under the control of a ubiquitin promoter (*Ubi-DEcad-GFP*) (F), and UAS-*mCD8GFP* expression driven by *GAL4*$^{LP-1}$(G).

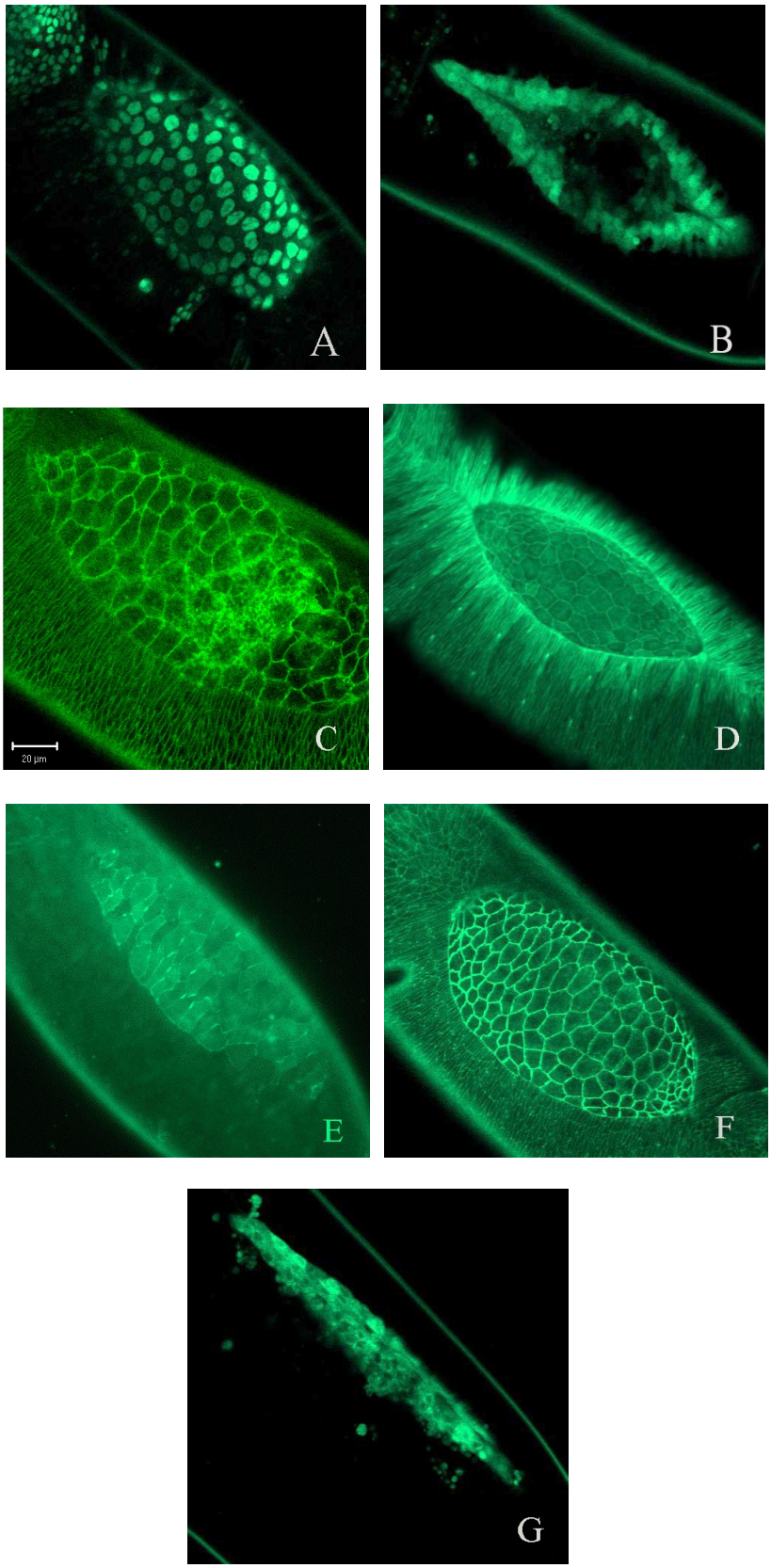
A
B
C
20 µm
D
E
F
G

Ubi-DEcad-GFP construct is particularly useful for visualizing the apical shapes of epithelial cells, especially the AS cells (Oda and Tsukita, 2001). Ubi-DEcad-GFP proved to be the best GFP marker for visualizing the AS, prior to the completion of DC (Figure 3.1 and 3.2). Following DC however, the DEcad-GFP is not useful for analysis of the AS as it is shed from the apical and lateral membranes.

To investigate the AS following DC, $GAL4^{LP\text{-}1}$ crossed with a myristoylated CD8-GFP construct under UAS control was found to be the best (Figure 3.1, Panel G).

In the course of this analysis, we also examined the timing of AS degeneration. We found the conspicuous midgut constrictions, which are readily visualized due to autofluorescence of the enveloped yolk, to be a reliable indicator of developmental stage. Muscle innervation, which is apparent by contractile activity, was also a useful marker of developmental stage.

3.2 Amnioserosa Death: Phase I Cell Extrusion

Live imaging analysis during DC stage (8 to 11 hr AEL) showed conspicuous extrusion of AS cells from the epithelium. Literature has presented that epithelial cells that are dying can be extruded, and we, therefore, wished to determine if these extrusion events are related to programmed cell death.

"Cell extrusion" is a process by which cell is squeezed out of an epithelium by the concerted contraction of its neighbors (Figure 3.3). Phalloidin staining on yw^{67} (the control embryos) revealed the accumulation of filamentous actin surrounding the extruding cell, suggesting the contribution of actin to the extrusion event (Reed Lab, unpublished data). Using confocal live imaging on Ubi-DEcad-GFP bearing embryos in a wild-type genetic background, we observed that some AS cells are extruded. This extrusion occurs exclusively in the basal direction. Strikingly, three min after losing apical contacts, the extruded cells exhibited the principal characteristics of apoptosis, including nuclear fragmentation, membrane blebbing, and

rapid removal by either the macrophage or yolk engulfment. Previous observations in our lab on Basigin-GFP carrying embryos also indicated that extruded cells exhibit a typical morphology of apoptosis (ReedLab, unpublished observations). To address the question as to whether AS epithelial extrusion is dependent on caspase-dependent cell death, we recovered genetic strains having either inhibited or over-activated apoptosis and evaluated the rate of extrusion in these backgrounds. To inhibit apoptosis in *Drosophila*, *Df(3L)ED225* mutants and the global expression of *p35*, an anti-apoptotic protein, using *daGAL4* were utilized. The activation of apoptosis, however, turned out to be more challenging, since the over-expression of the most pro-apoptotic proteins, in most cases, caused either malformed development or death prior to the desired stage (Table 3.2). After several attempts, the global over-expression of *reaper* using *daGAL4* proved to be a good tool to study the extrusion rate in an activated apoptosis background.

Figure 3.2 Confocal live image sequences during dorsal closure. The progression of dorsal closure in a wild-type embryo carrying DEcad-GFP. The lateral epithelial sheets are moving toward the dorsal midline, closing the dorsal hole and internalizing the AS.

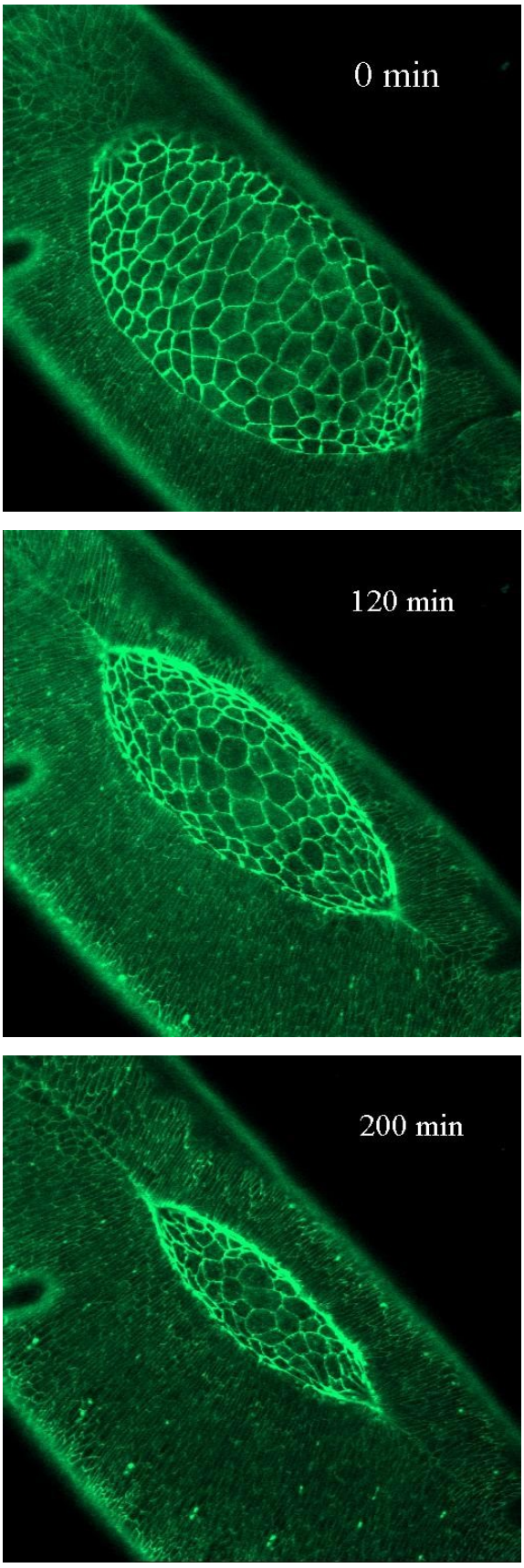
0 min
120 min
200 min

Figure 3.3: Cell extrusion in the amnioserosa. An AS cell (the marked cell) leaves the epithelium by basal extrusion during mid dorsal closure within 10 min. The genotype of the embryo is *yw*^{67}; *Ubi-DEcad-GFP*.

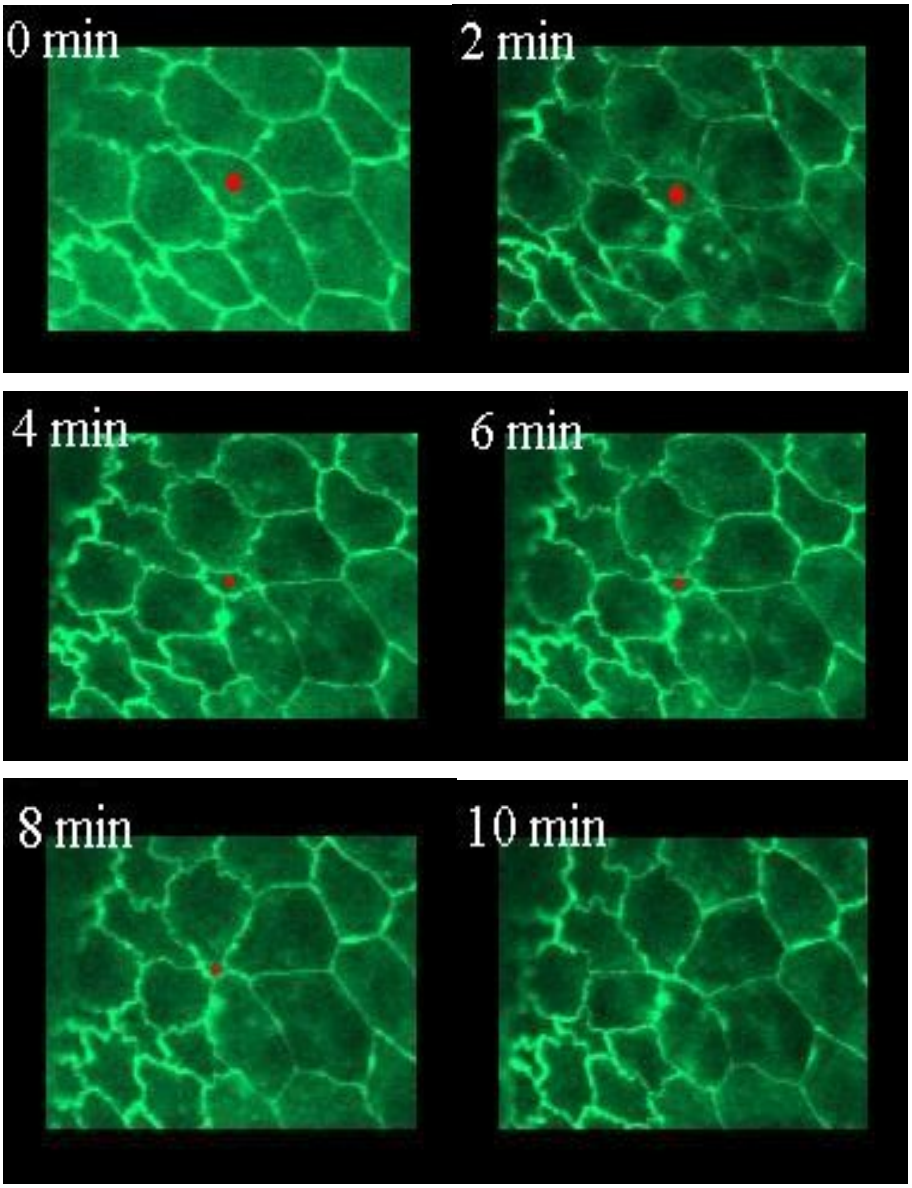
0 min
2 min
4 min
6 min
8 min
10 min

3.2.1 *Df(3L)ED225* Mutants and Extrusion

To address the question as to whether AS epithelial extrusion is truly a caspase dependent cell death, we attempted to create genetic strains that carry *Ubi-DEcad-GFP* in a *Df(3L)H99* mutant background. However, this proved problematic due to a second lethal mutation on the *H99* chromosome, leading to ambiguity in identifying the *H99* mutant embryos. To overcome this problem, a new mutant in which the principal pro-apoptotic genes including *rpr*, *grim* and *skl* as well as all but 1507 bp of 5' of *hid* have been deleted, was utilized. This new mutant is defined as *Df(3L)ED225.* Based on embryonic lethality, morphology, and acridine orange staining, *Df(3L)ED225* homozygous embryos are identical to *Df(3L)H99*. Live imaging of the AS during the early to late DC in the *Df(3L)ED225* homozygous mutants, carrying *Ubi-DEcad-GFP*, revealed significantly fewer extrusion events in this background, compared to wild-type (Table 3.3). These embryos failed head involution, an event also observed in *Df(3L)H99*, and DC occurred at a slower rate compared to wild-type embryos (Figure 3.4). Homozygous mutants for *Df(3L)ED225* were 100% embryonic lethal. The embryos never hatched and eventually died 24-25 hr AEL (i.e., 3 to 4 hr beyond the normal hatching time), and all exhibited a complete lack of acridine orange positive cells (i.e., indicative of a lack of apoptosis) (Figure 3.5).

3.2.2 Global Expression of *p35* and Extrusion

To confirm that the very low rate of cell extrusion observed in the homozygous *Df(3L)ED225* mutants was due to the defect of apoptosis in these embryos, we further attempted to disrupt apoptosis in the *Drosophila* embryos by expressing *UAS-p35*, an insect baculovirus caspase inhibitor. Different GAL4 drivers as well as different copy numbers of *UAS-p35* were examined. The global expression of two copies of *UAS-p35* (one copy on the X chromosome and another on the II chromosome) using the *daGAL4* (*daughterless GAL4* which expresses the target gene throughout the embryo) driver provided the best apoptotic inhibitory result. The acridine

orange staining on this background displayed essentially no acridine orange positive cells, the same observation as that in *Df(3L)H99* homozygous, indicating that apoptosis is completely inhibited in these embryos (Figure 3.5). Live imaging DC in the global expression of *p35* embryos indicated no extrusion (Table 3.3). Although some of these embryos failed head involution, the defect was not fully penetrant. DC occurred at slower rate, than that of the control (Figure 3.4).

Table 3.2 The effect of over-expression of *rpr*, *grm*, *hid*, or *rpr+hid* on the AS using different GAL4 drivers. To study the effect of the over-expression of *rpr*, *grm*, *hid*, or *rpr+hid* on the AS, $GAL4^{LP\text{-}1}$, *bsgGAL4* or *daGAL4* were utilized. Either *Ubi-DEcad-GFP* or GFP^{nls} were used to visualize the single AS cells.

Genotype	Phenotype
UAS-grim **x** *Ubi-DEcad-GFP*; *daGal4* (II)	GBR failure
UAS-grim **x** $\underline{GAL4^{LP\text{-}1}+GFP^{nls}}$ *TM3*	Normal GBR and DC
UAS-grim **x** *Ubi-DEcad-GFP, bsgGAL4* *CyO*	Normal GBR and DC
UAS-rpr **x** *Ubi-DEcad-GFP;* $GAL4^{LP\text{-}1}$ (II) *CyO*	Normal GBR and DC
UAS-rpr **x** *Ubi-DEcad-GFP, bsgGAL4* *CyO*	Normal GBR and DC
UAS-hid **x** *Ubi-DEcad-GFP*; *daGAL4* (X)	Malformed embryos. Staging was not possible due to extent of abnormalities.
UAS-hid **x** $\underline{GAL4^{LP\text{-}1}+GFP^{nls}}$ *TM3*	GBR failure, gut was partially misplaced in the head.
UAS-hid **x** *Ubi-DEcad-GFP, bsgGAL4* *CyO*	GBR failure
UAS-rpr +UAS-hid **x** *Ubi-DEcad-GFP*; *daGAL4* (X)	Malformed embryos. Staging was not possible due to sever abnormalities.
UAS-rpr +UAS-hid **x** $\underline{GAL4^{LP\text{-}1}+GFP^{nls}}$ *TM3*	GBR failure (fully penetrant)
UAS-*rpr* +UAS-*hid* **x** *Ubi-DEcad-GFP, bsgGAL4* *CyO*	GBR failure (not fully penetrant), rarely found some DC stage.

Table 3.3 Extrusion scores in various genetic backgrounds. The rate of extrusion was measured in four different backgrounds, each of which included the ubiquitous expression of apical DEcad-GFP to visualize the AS apical membrane. 10% of the AS cells are extruded during DC in the control while the extrusion rate drops dramatically in the apoptotic defective backgrounds. The global expression of the pro-apoptotic protein, Reaper, increases the rate of extrusion by 16%.

Genotype	Average extrusions/embryo (no. embryos)	% AS cells extruded
yw^{67}	21 (4)	10.0%
UAS-p35	0 (5)	0%
Df(3L)ED225	1(5)	0.5%
UAS-reaper	32(4)	26.0%

Figure 3.4 Time Course of Dorsal Closure in Different Genetic Backgrounds. The reduction of the AS surface in control (A), *Df(3L)ED225* mutants (B), global expression of *p35* (C), global expression of *rpr* (D), a representative embryo from each genotypes having the larger AS surface and longer run (E). The qualitative rate of DC was inferred from the steepness of the plots.

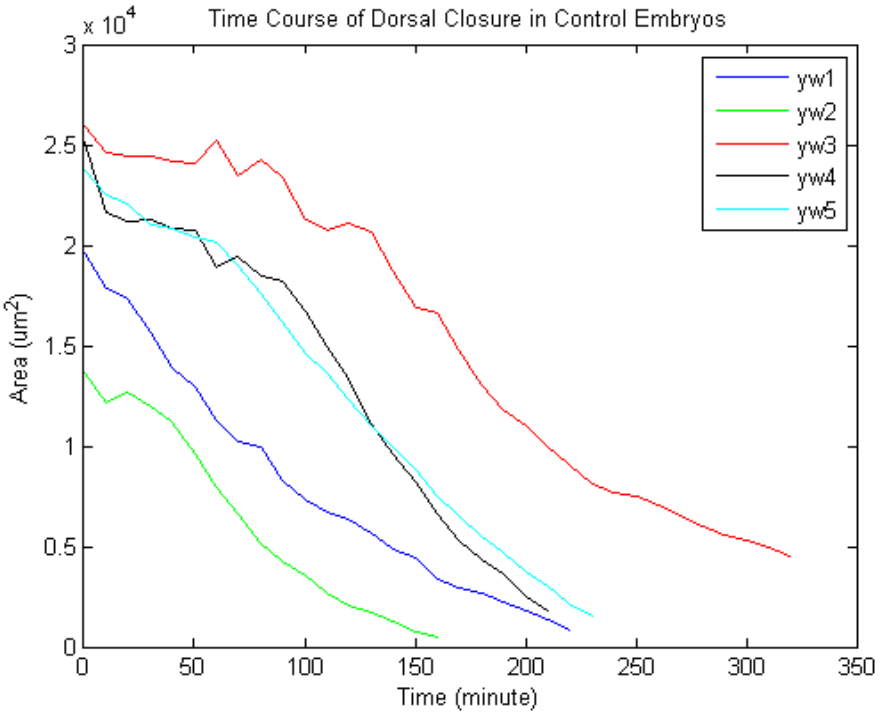
Time Course of Dorsal Closure in Control Embryos
x 10^4
Area (um^2)
Time (minute)
yw1
yw2
yw3
yw4
yw5

(A)

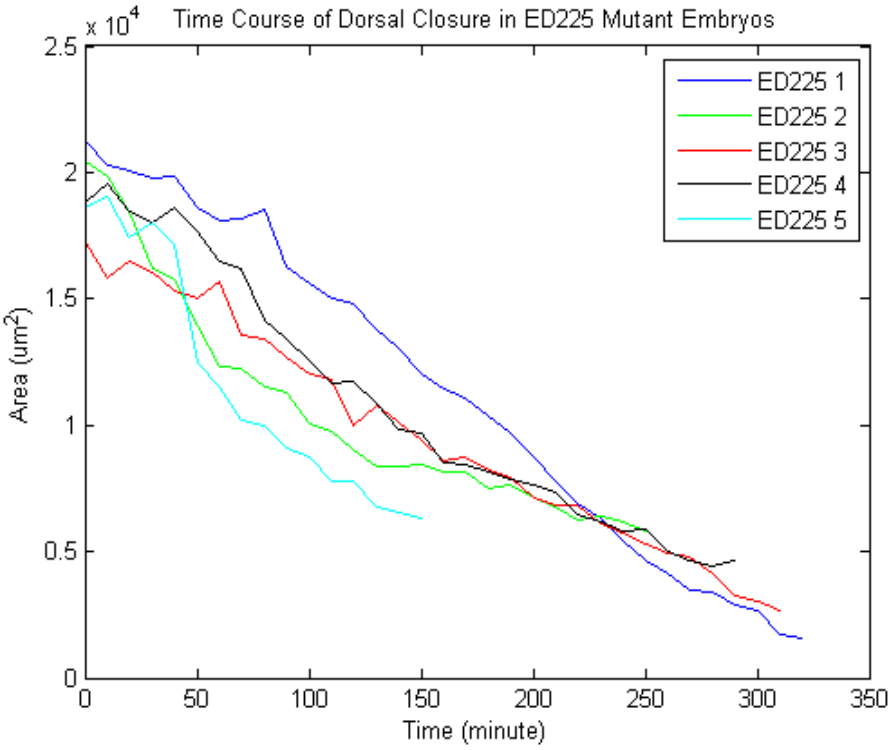
Time Course of Dorsal Closure in ED225 Mutant Embryos
x 10^4
Area (um^2)
Time (minute)
ED225 1
ED225 2
ED225 3
ED225 4
ED225 5

(B)

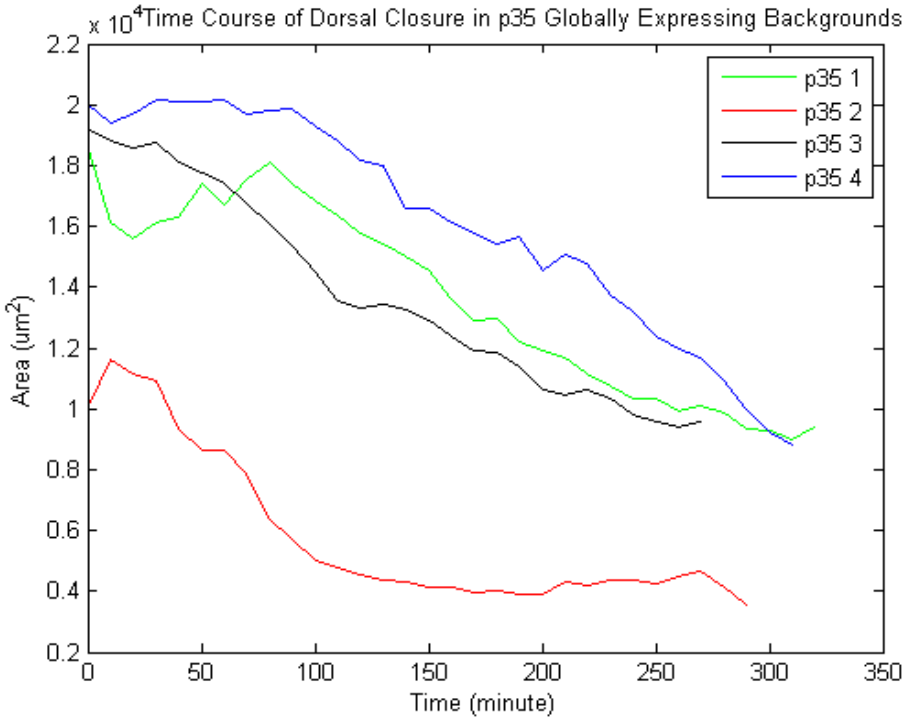
x 10^4 Time Course of Dorsal Closure in p35 Globally Expressing Backgrounds
p35 1
p35 2
p35 3
p35 4
Area (um^2)
Time (minute)
2.2
2
1.8
1.6
1.4
1.2
1
0.8
0.6
0.4
0.2
0
50
100
150
200
250
300
350

(C)

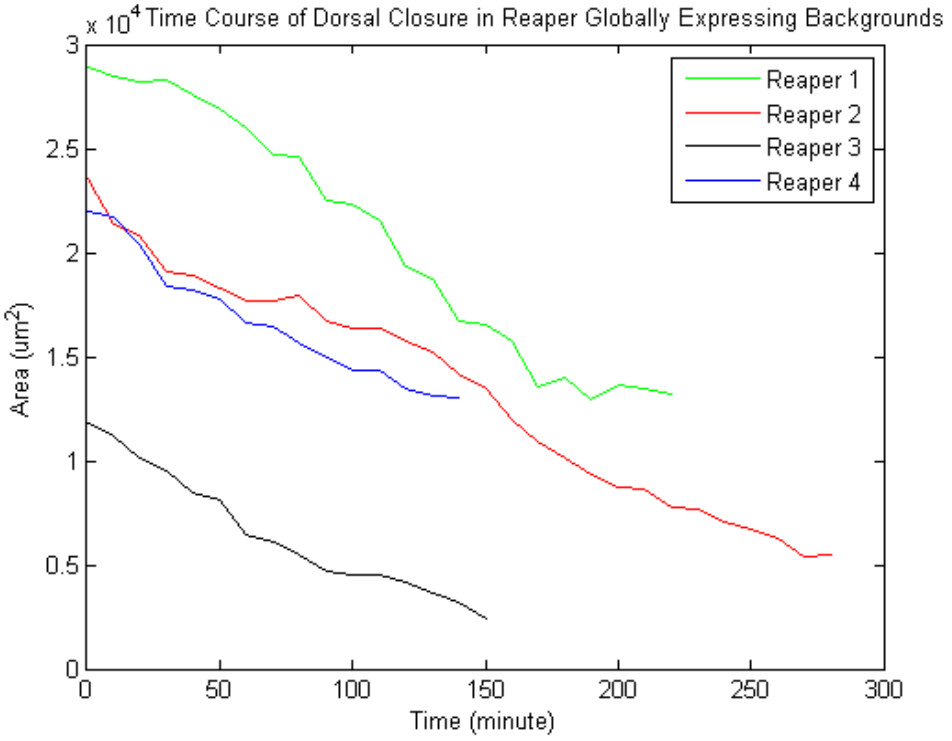
x 10^4 Time Course of Dorsal Closure in Reaper Globally Expressing Backgrounds
Reaper 1
Reaper 2
Reaper 3
Reaper 4
Area (um^2)
Time (minute)
3
2.5
2
1.5
1
0.5
0
50
100
150
200
250
300

(D)

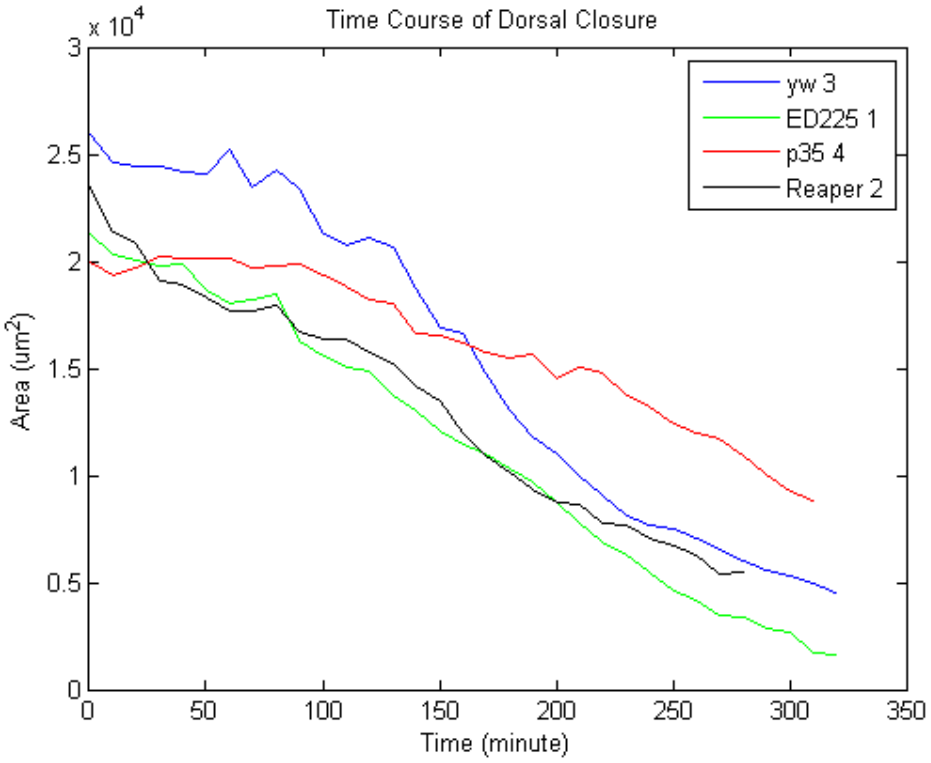
Time Course of Dorsal Closure
x 10^4
Area (um^2)
Time (minute)
yw 3
ED225 1
p35 4
Reaper 2
0
0.5
1
1.5
2
2.5
3
0
50
100
150
200
250
300
350

(E)

Figure 3.5 Acridine orange staining on different genotypes. *yw*^{67} (A), *Df(3L)H99* (B), UAS-*p35/+;UAS-p35+;daGAL4/+* (C), and *UAS-rpr/+;daGAL4/+* (D). Note the lack of apoptotic cells (AO positive cells) in *Df(3L)H99* and global expression of *p35* backgrounds, and the higher number of AO positive cells in global expression of *rpr*. The embryos are oriented anterior left, dorsal up.

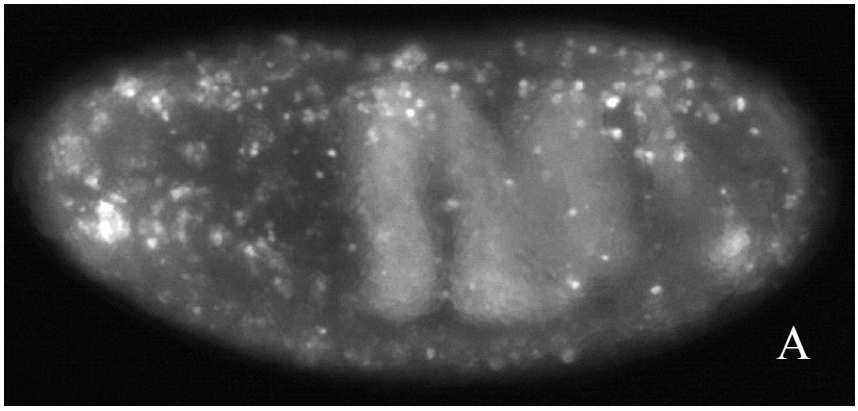
A

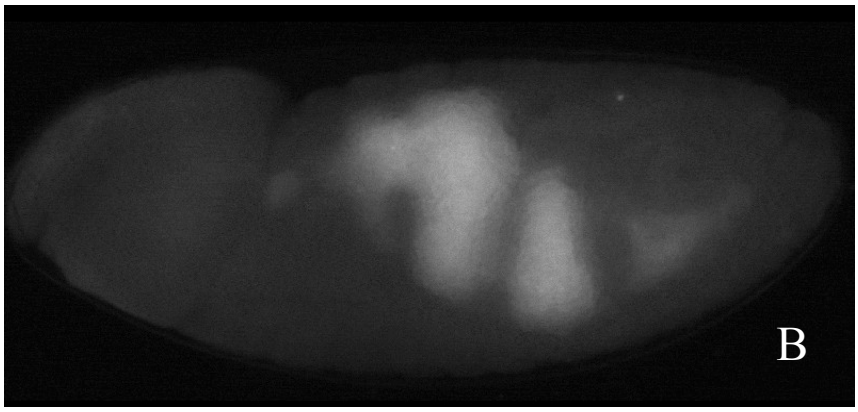
B

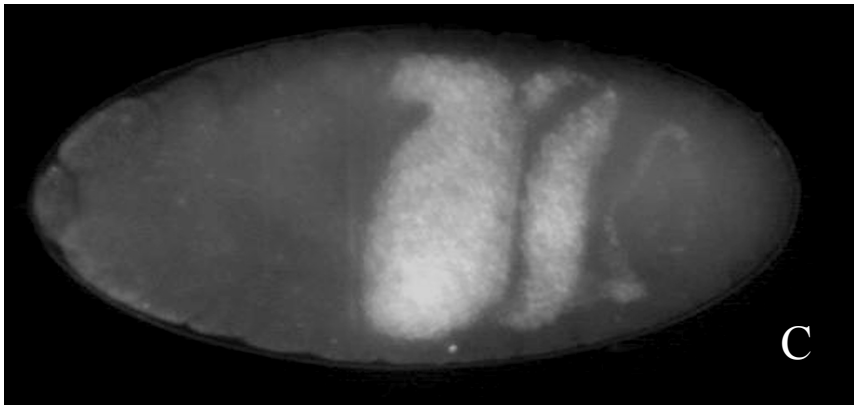
C

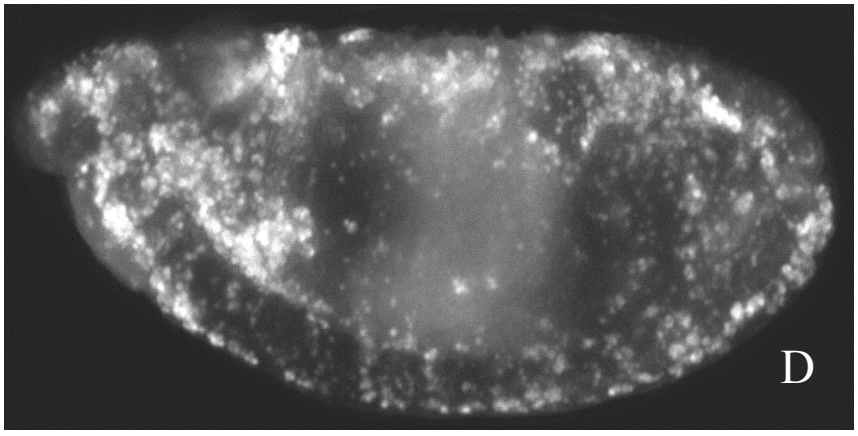
D

3.2.3 Global Expression of *reaper* and Extrusion

Following the inhibition of apoptosis and the decrease in extrusion in the two mentioned backgrounds, the next goal was to activate apoptosis and test if this increases extrusion rates. The over-expression effects of various pro-apoptotic genes, including *rpr, grm,* and *hid,* were tested using different GAL4 drivers. The effects were evaluated by either live imaging or cuticle preparation (Figure 3.6). The results are summarized in Table 3.2. The over-expression of *grim*, *hid,* or *rpr+hid* recombinant with *daGAL4* produced abnormal embryos. Over-expression of any of these genes using either $GAL4^{LP\text{-}1}$ (driving target gene expression in the AS and the SGs) or *bsgGAL4* a.k.a $bsg^{NP6293}GAL4$, (driving target gene expression in the AS and yolk), however, had weak effects on the developing embryos. We speculated that the level of expression varies between different GAL4 drivers; by evaluating UAS-GFP expression we found *daGAL4* to be stronger compared to the other two drivers (data not shown).

The global expression of *rpr* with the *daGAL4* driver resulted in embryos with high rates of extrusion (Table 3.3). Acridine orange staining on this background also confirmed elevated apoptosis compared to wild-type (Figure 3.5). The over-expression of *rpr* throughout the embryo resulted in 100% embryonic lethality. Interestingly, these embryos were more sensitive and many of them died during confocal imaging. The rate of DC, however, was normal in this background for those embryos which survived mounting preparation and imaging procedure (Figure 3.4). Over-expression of *rpr* using $GAL4^{LP\text{-}1}$ and *bsgGAL4* did not significantly increase the extrusion rate compared with that of the control. Unlike the control, the AS perimeter cells in this background were more prone to extrusion. In the wild type, perimeter cells were invariably the last cells to die.

3.3 Amnioserosa Death: Phase II Tissue Dissociation

Tissue dissociation following DC represents the second phase of cell death in the AS; it leads to the complete elimination of this extra-embryonic structure. AS dissociation starts upon the completion of DC (13 hr AEL) and is completely eliminated within 3 hr. Using our developmental reference points, we found that AS dissociation coincided very nicely with the formation of constrictions in the developing midgut. In wild-type embryos, AS dissociation was particularly active at the midgut four-lobe stage, and was completed before the events of midgut elongation and musculature innervation.

Live imaging of wild-type (yw^{67}), as well as *H99*, *ED225*, global expression of *p35* and *rpr* backgrounds revealed that as DC is completed, the AS is internalized and forms a tube beneath the epidermis, where it ultimately falls apart. To examine the degeneration of the AS in the control, the AS was illuminated with $GAL4^{LP\text{-}1}$ line crossed with *UAS-mCD8-GFP* (Figure 3.7). The control imaging sequences of the AS after DC denoted that this tissue initiated dissociation at the anterior and posterior end of the tissue. Ultimately, the entire tissue "fell apart" approximately 3 hr after the completion of DC (Figure 3.7). Interestingly, we were also able to see the GFP expressing AS apoptotic corpses within macrophages (Figure 3.7).

3.3.1 *Df(3L)H99* Homozygous Mutants and Tissue Dissociation

To study phase two of AS degeneration in *Df(3L)H99* homozygous mutants, we crossed two stocks, one carrying *H99* and $GAL4^{LP\text{-}1}$; and the other, *H99* and *UAS-mCD8-GFP* recombinant chromosomes (recovered in Reedlab). This system permitted the unambiguous identification of *H99* homozygous mutant embryos, since only *H99* homozygous mutant embryos express GFP (Figure 2.2). Live imaging of *H99* mutants revealed that the AS did not undergo tissue dissociation as observed in the wild-type. Following the stage at which the AS should begin to rapidly degenerate, the AS in the *H99* mutants gradually stretched and formed a very

long and persistent tube (Figure 3.7). Although the entire tissue persisted for several hours beyond its normal lifespan, the tissue eventually shrank to a small remnant (Figure 3.10). Interestingly, no GFP apoptotic corpses appeared inside the macrophages of *H99* mutants (Figures 3.7 and 3.8).

Live imaging of *Df(3L)ED225* homozygous mutants, as well as mutants carrying *Df(3L)ED225* over *Df(3L)H99*, also displayed lack of tissue dissociation. These deficiencies showed a head involution failure phenotype, however, gut development occurred normally.

Figure 3.6 The cuticle preparation in global expression of *UAS-rpr* +*UAS-hid* and UAS-*rpr*. Ubiquitous expression of a double insertion line (*UAS-rpr+UAS-hid*) using $GAL4^{LP\text{-}1}$ demonstrated a fully penetrant GBR failure mutants, suggesting that the over-expression of two pro-apoptotic proteins simultaneously led to premature AS cell death (A). The global expression of a single insertion line (*UAS-rpr*) exhibited AS degeneration during DC, leading to dorsal hole formation (B), which was fully penetrant (C). (A) and (B) embryos are anterior left, dorsal up.

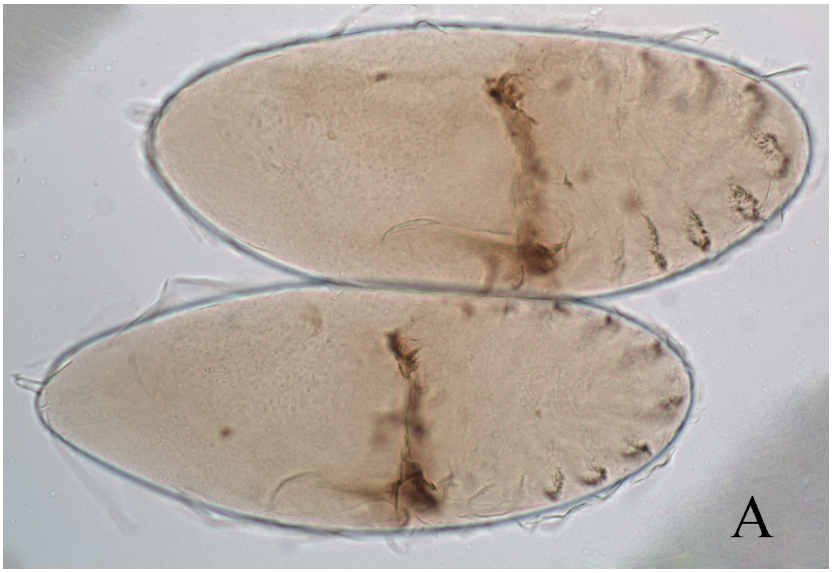
A


B

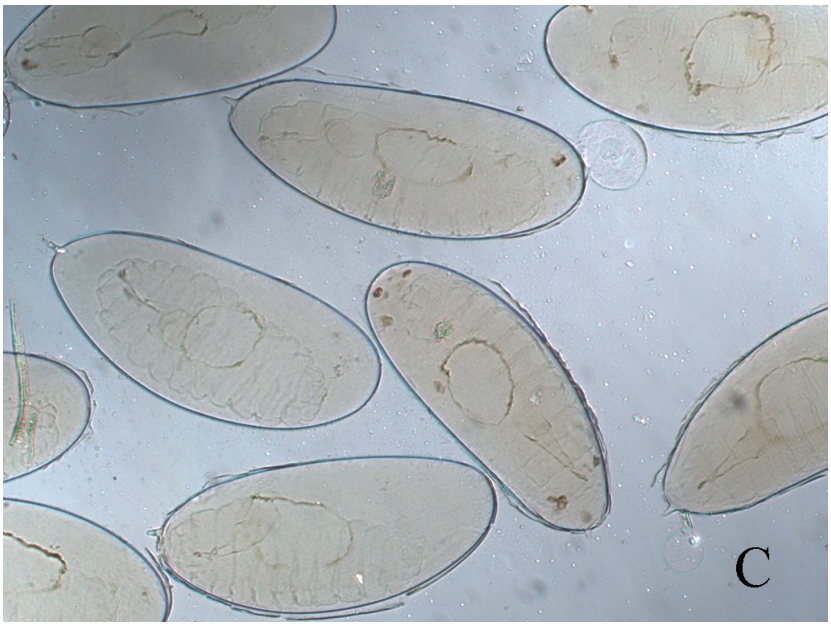
C

Figure 3.7 Phase II: Tissue dissociation following dorsal closure. Panels (A) to (C) denote the visualization of the AS in the control by *GAL4*$^{LP\text{-}1}$ and *UAS-mCD8GFP*. Note the normal degeneration of the AS in the control. The AS GFP expressing apoptotic corpses are engulfed by macrophages in the control but not in *H99*. In (D) to (F), the AS in *H99* homozygous backgrounds is illuminated. Note the persistent AS (beyond its normal life span) and the lack of apoptotic corpses in this mutant. AS (amnioserosa), YK (Yolk), MP (Macrophages).

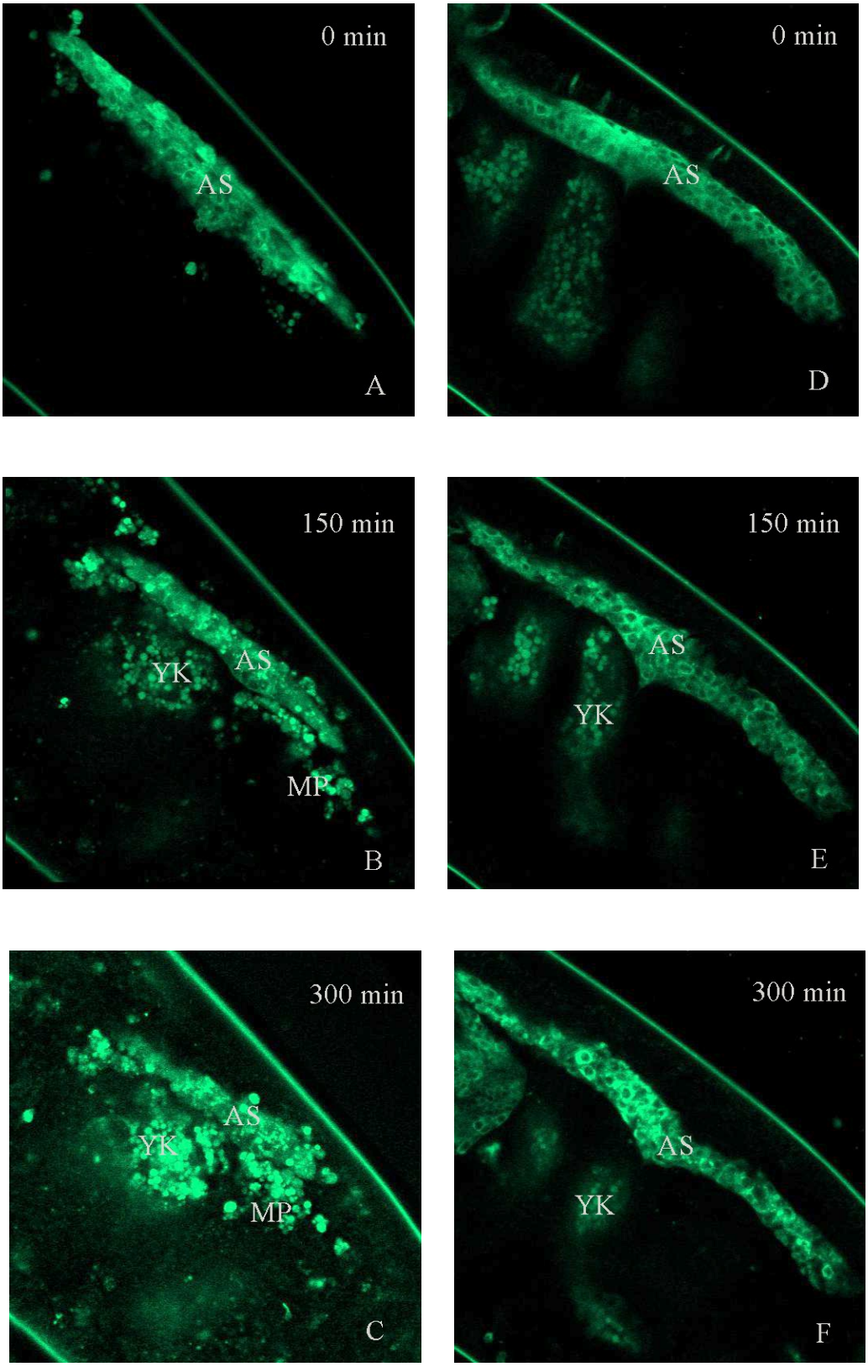
0 min
AS
A
0 min
AS
D
150 min
YK
AS
MP
B
150 min
AS
YK
E
300 min
AS
YK
MP
C
300 min
AS
YK
F

3.3.1.1 Macrophages in *H99* Mutant Background

To further address the apparent absence of macrophages in the *H99* mutant background, a macrophage specific driver, *croquemort*-GAL4, was crossed with UAS-mCD8GFP in an *H99* mutant background. *croquemort* (*crq*) encodes a CD36-related receptor, expressed exclusively in macrophages (Franc et al., 1996). The live imaging of *H99* mutants with illuminated macrophages revealed that macrophages were indeed present in the *H99* mutants (Figure 3.8). Strikingly, the macrophages of *H99* mutants were, generally, smaller than those of the wild-type, with no vacuoles and no engulfed GFP particles. The apparent absence of macrophages in the former *H99* background (without the macrophage specific driver, *croquemort*-GAL4) is explained not by the absence of the macrophages, but rather by the lack of GFP-filled apoptotic corpses. Furthermore, the imaging experiments revealed that macrophages were actively moving around the AS, and appeared to extend cellular projections towards the AS cells. It is possible that the AS in the *H99* mutants lacked "eat me" signals such as the phosphatidylserine exposure in the outer membrane leaflet, and, therefore, was refractory to the actions of the macrophages.

Figure 3.8 Macrophages are present in *H99* mutants. A macrophage specific driver, *croquemort-GAL4*, crossed to *UAS-mCD8GFP* in a wild-type (A) and the H99 mutant background (B). Confocal live imaging reveals that macrophages (arrows) are involved in the elimination of the AS in wild-type. *croquemort-GAL4* is also expressed in the AS, driving *UAS-mCD8GFP* weakly in the AS.

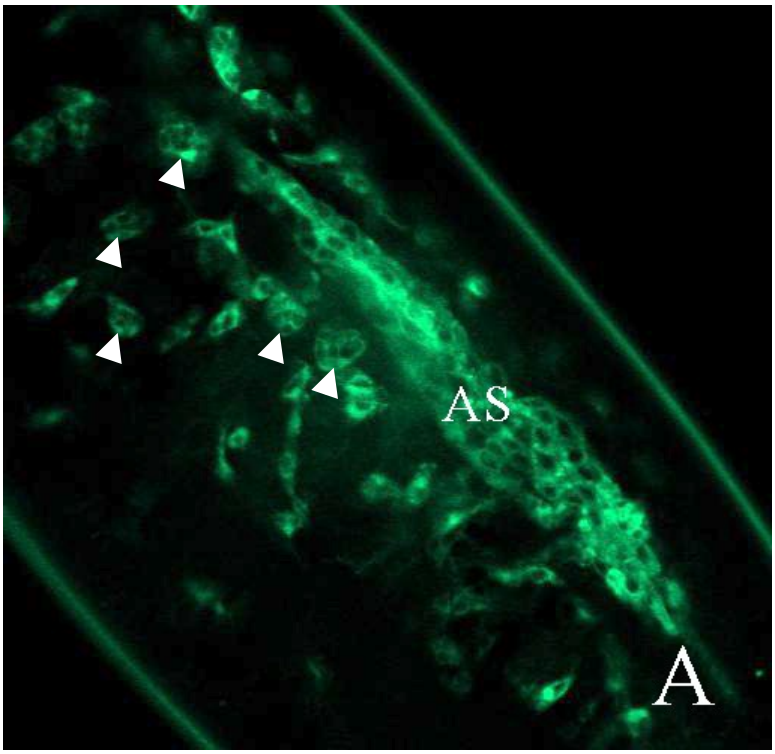
AS
A

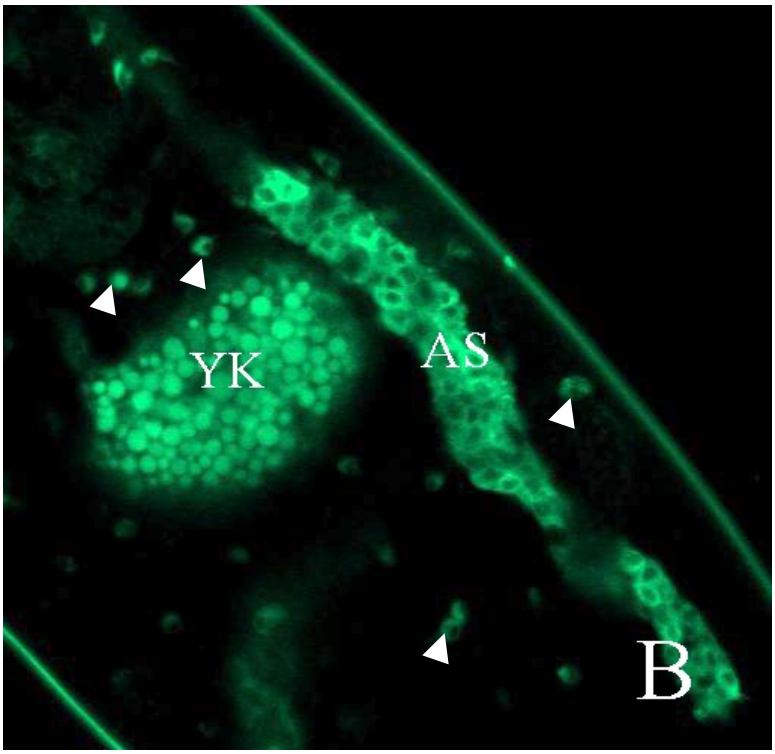
YK
AS
B

3.3.2 Global Expression of *p35* and Tissue Dissociation

To confirm that the lack of tissue dissociation observed in *Df(3L)H99* was the consequence of the lack of apoptotic death, a second apoptotic defective genotype was tested; two copies of UAS-*p35* were expressed throughout the embryo using a stock that carries the *daGAl4* driver and *YET-1* (to visualize the AS). Live imaging these embryos using a Leica stereomicroscope revealed a persistent AS in this genotype with normal gut development. This technique, unlike confocal imaging, was not sensitive enough to clearly expose the motile GFP-expressing macrophages, if any existed.

3.3.3 Global expression of *reaper* and Tissue Dissociation

The over expression of *reaper*, a pro-apoptotic protein, resulted in premature tissue dissociation. This was evaluated in two different ways: first via stereoscopic live imaging of the progeny of cross no.15 (*UAS-rpr X YET-1;daGAL4* x, Table 2.1); and second, via *in situ* hybridization using CG12011 probe on the progeny of cross no.16 (*UAS-rpr X Ubi-DEcad-GFP;daGAL4* x, Table 2.1). Live imaging revealed that the AS ripped during DC (data not shown). The results of *in situ* hybridization are shown in Figure 3.9 where CG12011 positive cells are scattered abnormally over the dorsal surface of the embryos. In both live and fixed embryos, midgut development was abnormal as embryos failed to show midgut constrictions. Although confocal live imaging of this background displayed normal dorsal closure event, the cuticle preparation revealed a penetrant dorsal hole phenotype (Figure 3.6). Moreover, the GFP-expressing apoptotic corpses of the perimeter cells labeled by *YET-1* expression were visible inside the macrophages, indicative of a premature dissociation of the AS in this background.

Figure 3.9 *In situ* hybridization on global expression of *reaper*. The AS cells are labeled with a specific AS probe, CG12011. Wild-type embryos exhibit normal tissue dissociation, following DC (A). The global expression of *reaper*, however, displayed an early tissue dissociation and dorsal hole (B) and (C)

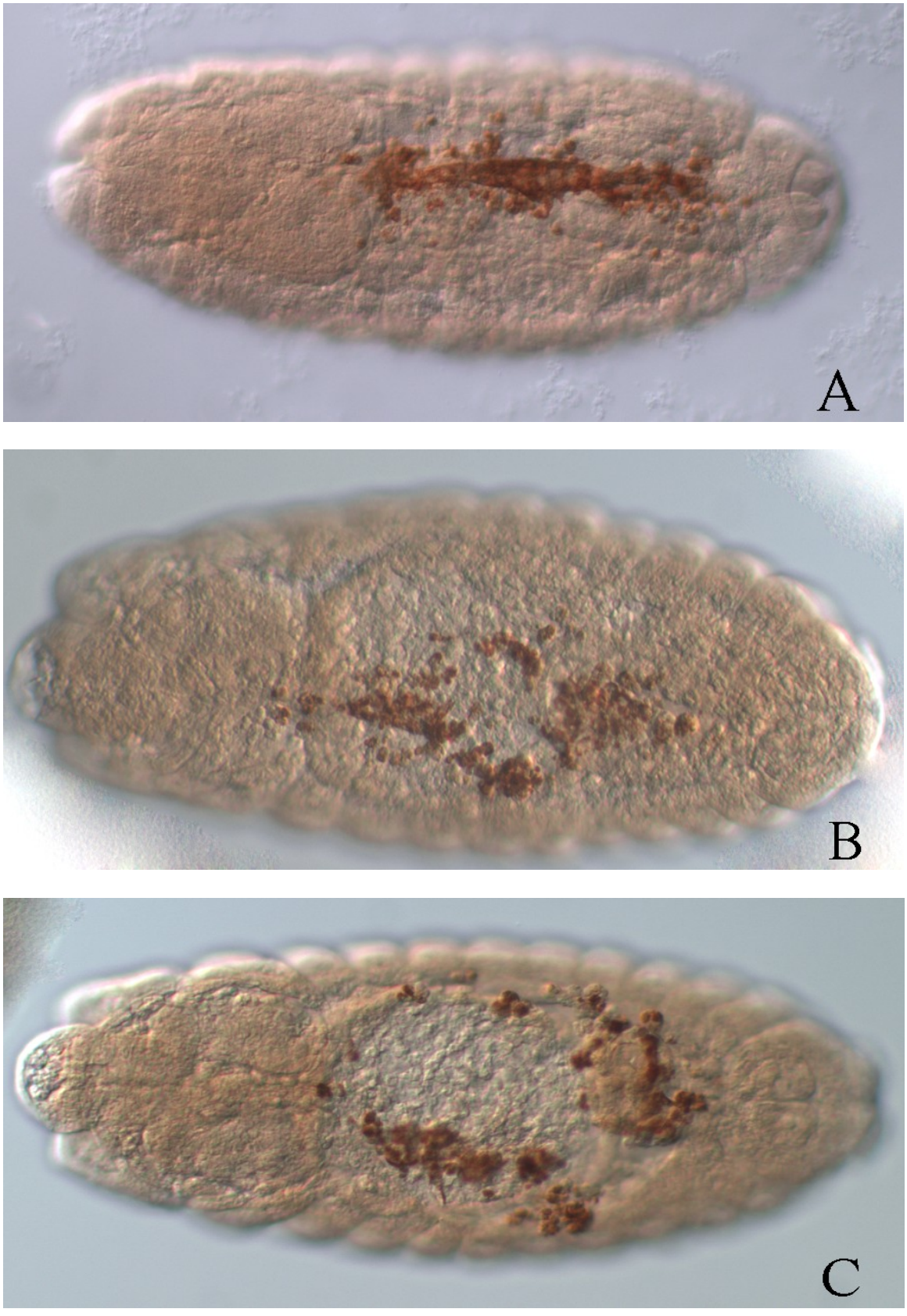
A
B
C

3.4 Autophagy and the AS Degeneration

The AS persists much longer than normal lifespan in *H99* mutants and in global expression of *p35* embryos, yet continues to shrink and eventually breaks apart (Figure 3.10). The next objective was to evaluate the role of autophagy in the degeneration of the AS. LC3 (yeast homolog ATG8) contributes to autophagosome formation and is sequestered inside the autophagosomes. Therefore to examine if autophagy occurs simultaneously with apoptosis in the AS, the distribution of LC3-GFP in the AS was studied using *UAS-LC3-GFP* driven in the AS with $GAL4^{LP\text{-}1}$. The preliminary observations of the wild-type background signified some punctate LC3-GFP in the AS at the very early stage of DC, and increasing punctate LC3-GFP as the DC neared completion (Figure 3.11). An attempt to place *UAS-LC3-GFP* construct in the *H99*, *ED225*, or *p35* backgrounds proved problematic. In addition, we noticed that wild-type controls having no GFP in the background displayed autofluorescence in the AS, making it impossible to differentiate between the LC3-GFP and the autofluorescence from the AS cells (Figure 3.11). This observation led to the conclusion that searching for the existence and pattern of LC3-GFP in the AS is not a reliable method to study autophagy in this tissue. Therefore, to examine the occurrence and accumulation of the autophagic vacuoles in the AS, TEM was adopted.

The ultra-structure of the AS in the control (yw^{67}), *Df(3L)H99/Df(3L)ED225*, and the global expression of two copies of *p35* by *daGAL4* clearly revealed autophagic vacuoles in the AS cells (Figures 3.12, 3.13, 3.14). The ultra-structure of the latter two genotypes was consistent with the persistent AS in these backgrounds, since many AS cells were still visible at very late embryonic stage, compared with the wild-type. Moreover, LysoTracker staining on the same backgrounds produced the same result, as observed via ultra-structure: yw^{67}, *Df(3L)H99/Df(3L)ED225* and the global expression of *p35* with *daGAL4* exhibited high LysoTracker staining in the AS, suggesting the presence of acidic autophagic compartments in

the tissue in these backgrounds (Reed Lab, unpublished data).

Figure 3.10 Live imaging of the late AS in *H99* mutants. To study the fate of the AS in the *H99* mutants, 16 hour old *H99* embryos were live imaged. The AS was visualized by expressing *UAS-mCD8GFP*, driven with $GAL4^{LP\text{-}1}$, in the AS. In wild-type, the AS is completely dissociated by this time; in the *H99* mutants, the AS is persistent (A) but continues to shrink (B) suggesting that autophagy is probably involved in the AS degeneration. amnioserosa (AS), Yolk (YK).

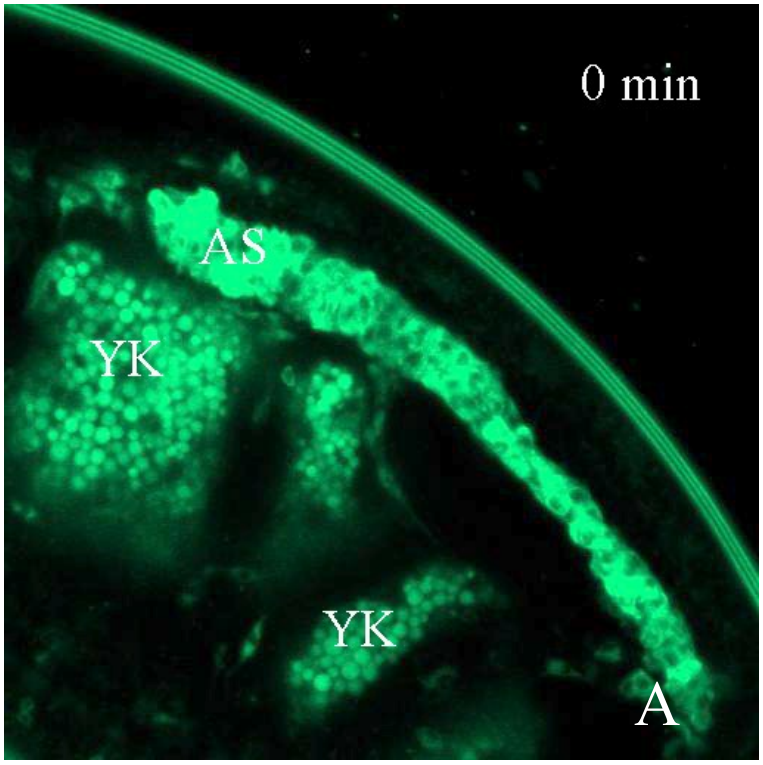
0 min
AS
YK
YK
A

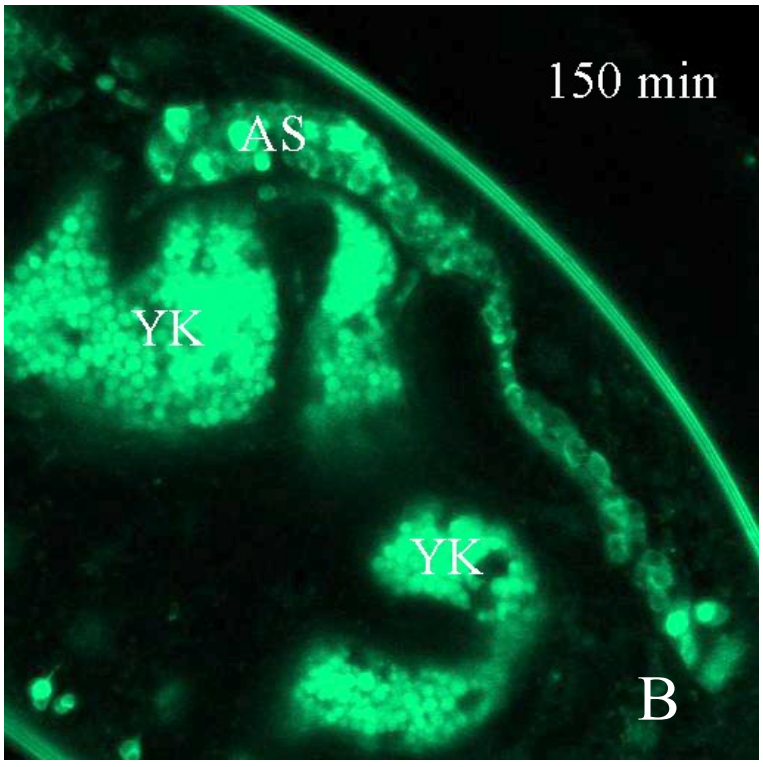
150 min
AS
YK
YK
B

Figure 3.11 The existence and pattern of LC3-GFP expression in the AS. To determine if autophagy occurs in the wild-type AS, *UAS-LC3-GFP*, is expressed in the AS using, $GAL4^{LP\text{-}1}$, an AS specific driver. LC3-GFP expression is uniform in the AS cells during early DC (A), indicating that autophagy is not prominent in the AS during this stage. But a few LC3 punctea are visible at this stage, which suggests that autophagy is occurring at a very low level during this time. During mid DC (B), many LC3 punctae are visible in the AS, signifying an elevated rate of autophagy at this stage. It is noticed, however, that the AS with no GFP in the background is autofluorescent itself, and in the wild-type embryos with no GFP in the background, still some autofluorescence is visible (C) which can be misjudged with LC3 punctae. The AS region is highlighted with a yellow line in all three panels.

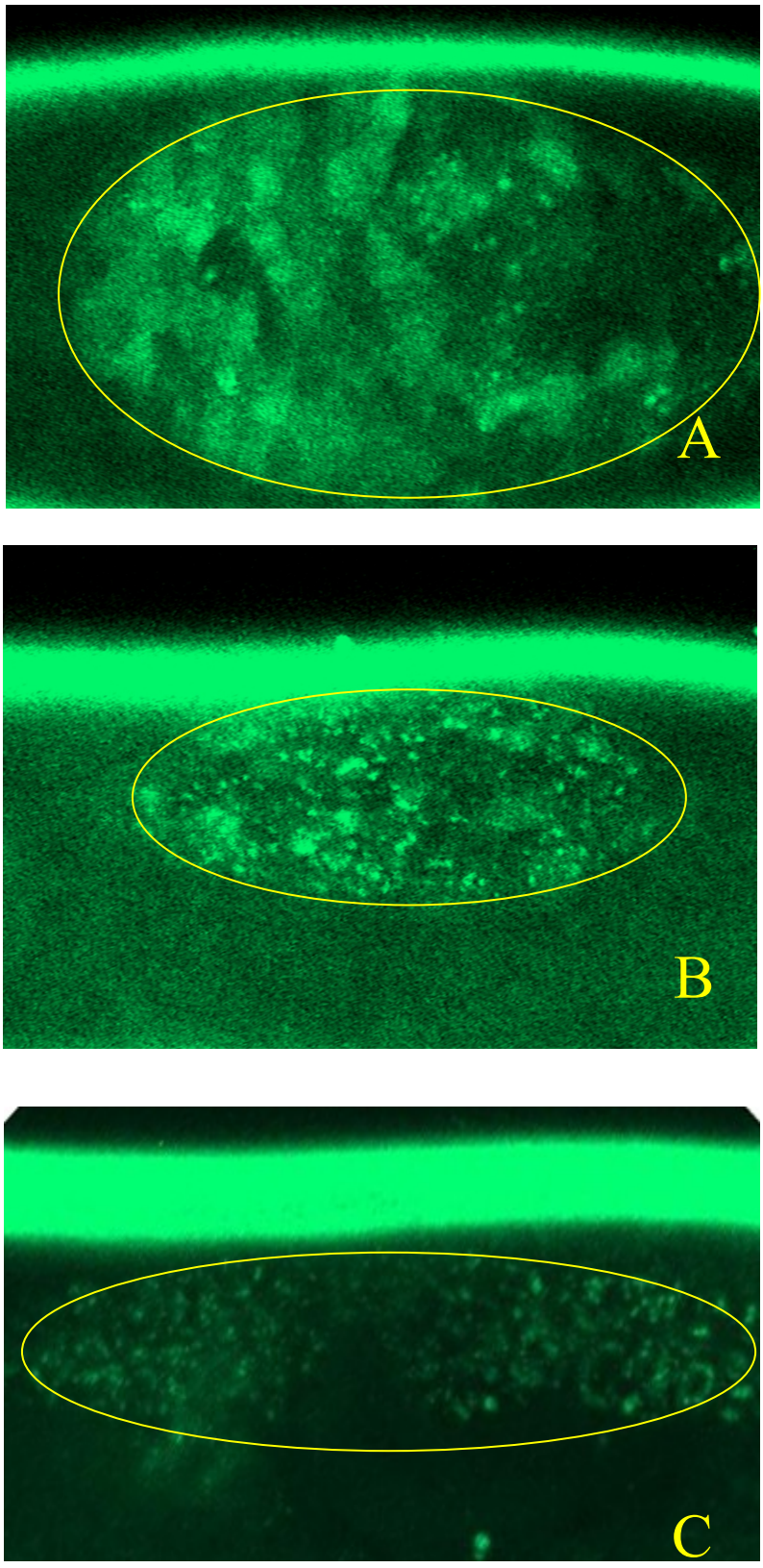
A
B
C

Figure 3.12 Autophagy proceeds normally in the AS in the Control Embryos. TEM of the AS in *yw*^{67} embryos (A) to (C). (A) The presence of autophagic structures (autophagosome or autolysosome) in the AS. Autophagic structures are represented by arrows. (B) and (C) The enlargements of the representative autophagic structures from the panel (A). AS, amnioserosa; PC, amnioserosa perimeter cells; MG, mid-gut; YK, yolk; MP, macrophage; N, nucleus; and the asterisk indicates mitochondria. The scale bar is 2 μm in (A) and 1 μm in (B) and (C).

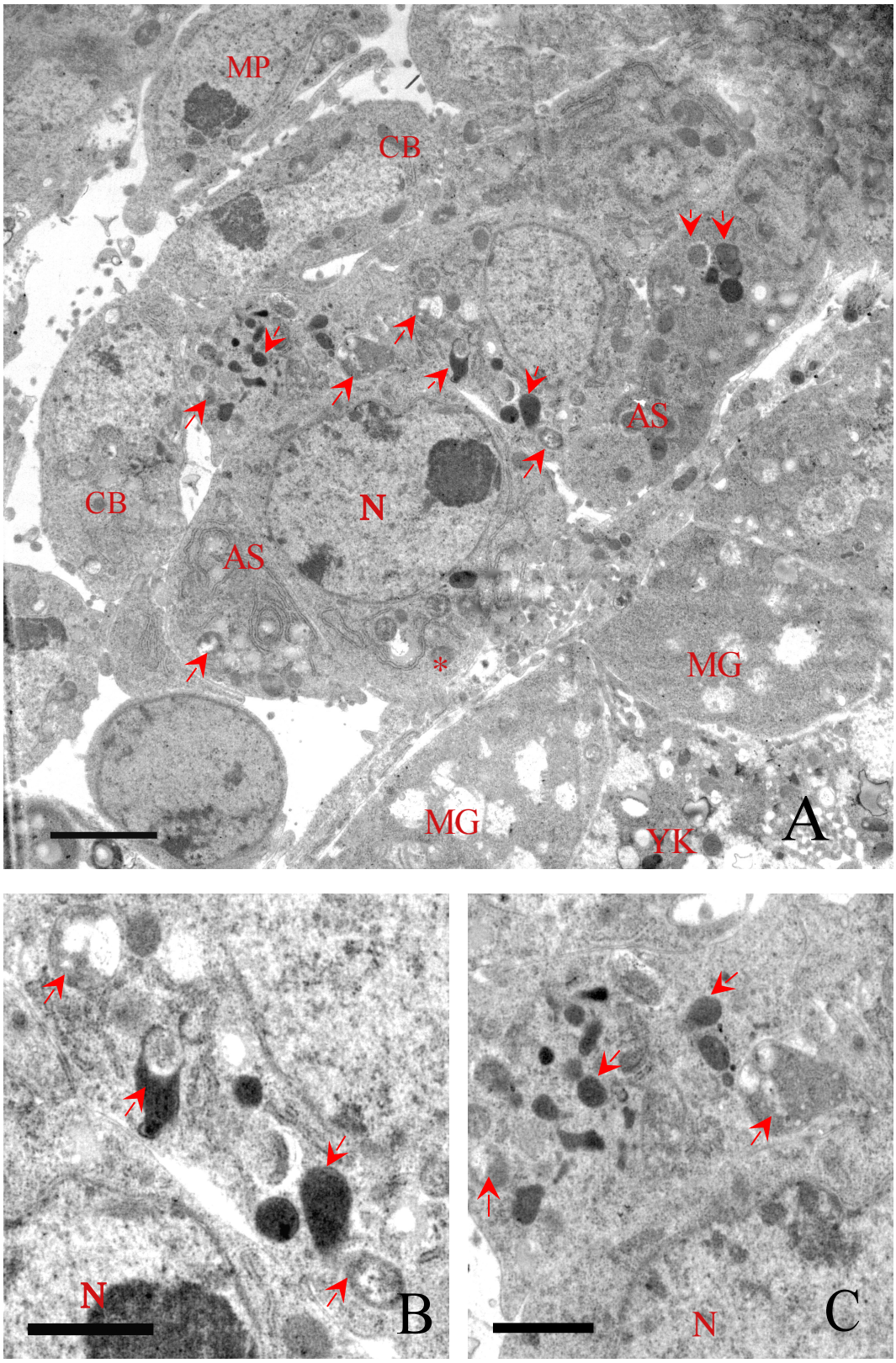
MP
CB
AS
CB
N
AS
MG
MG
YK
A
N
B
N
C

Figure 3.13 Autophagy proceeds normally in the AS in *H99/ED225* mutant Embryos. The ultra-structure of the AS in the *H99/ED225* mutant embryos (A) to (C). (A) The presence of autophagic structures (autophagosome or autolysosome) in the AS. Autophagic structures are represented by arrows. (B to C) The enlargements of the representative autophagic structures from panel (A). AS, amnioserosa; PC, amnioserosa perimeter cells; N, nucleus; CB, cardioblast; asterisk indicates mitochondria. Scale bar: 2 μm in panel (A), and 1 μm in panel (B) and (C).

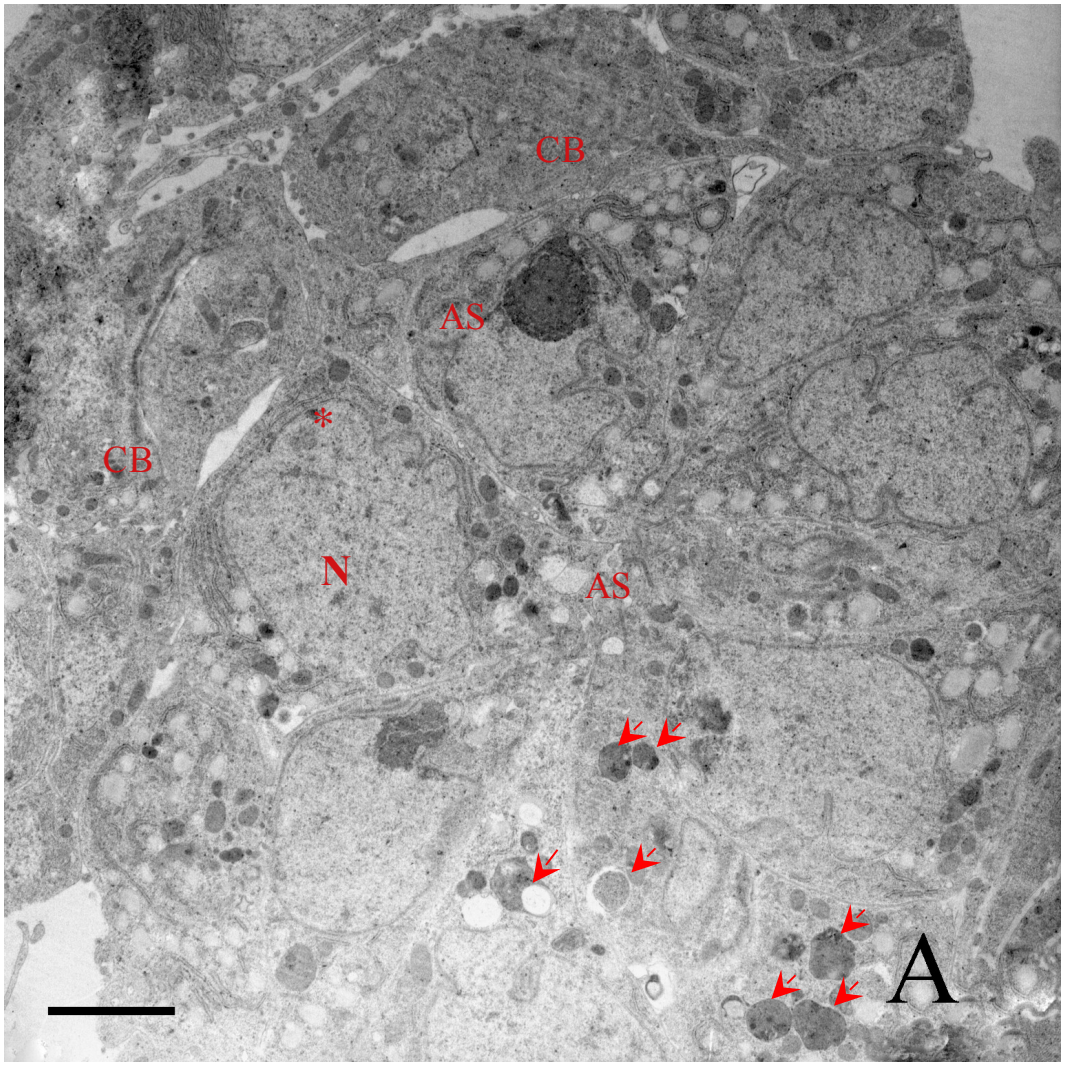
CB
AS
CB
N
AS
A

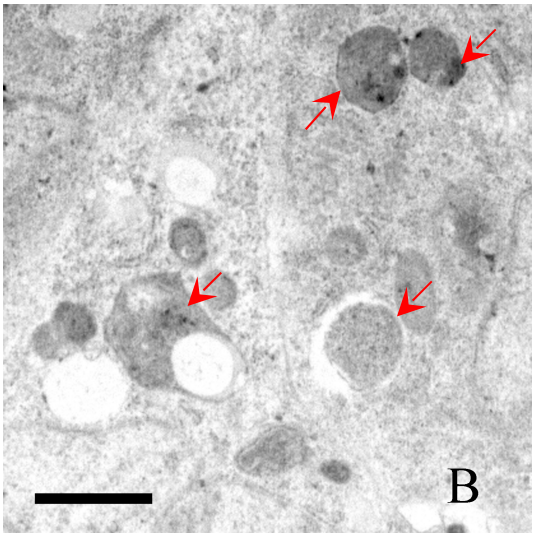
B

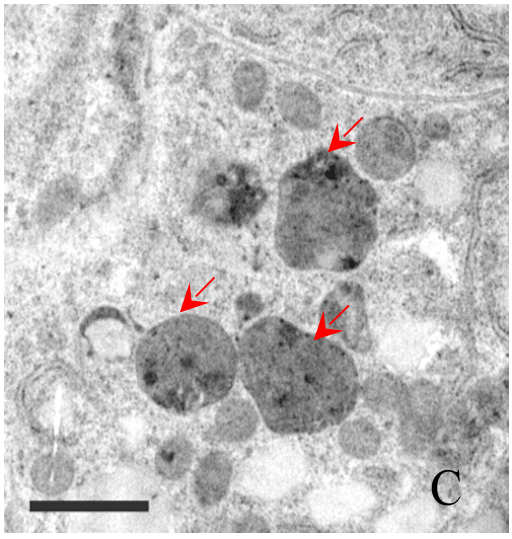
C

Figure 3.14 Autophagy proceeds normally in the AS in globally expressed *p35* Embryos. The ultra-structure of the AS in the global expression of two copies of *p35* backgrounds (A) to (C). (A) The presence of autophagic structures (autophagosome or autolysosome) in the AS. Autophagic structures are represented by arrows. (B) and (C) The enlargements of the representative autophagic structures from panel (A). AS, amnioserosa; N, nucleus; CB, cardioblast; asterisks indicate mitochondria. Scale bar: 2 μm in (A) and,1 μm in (B) and (C).

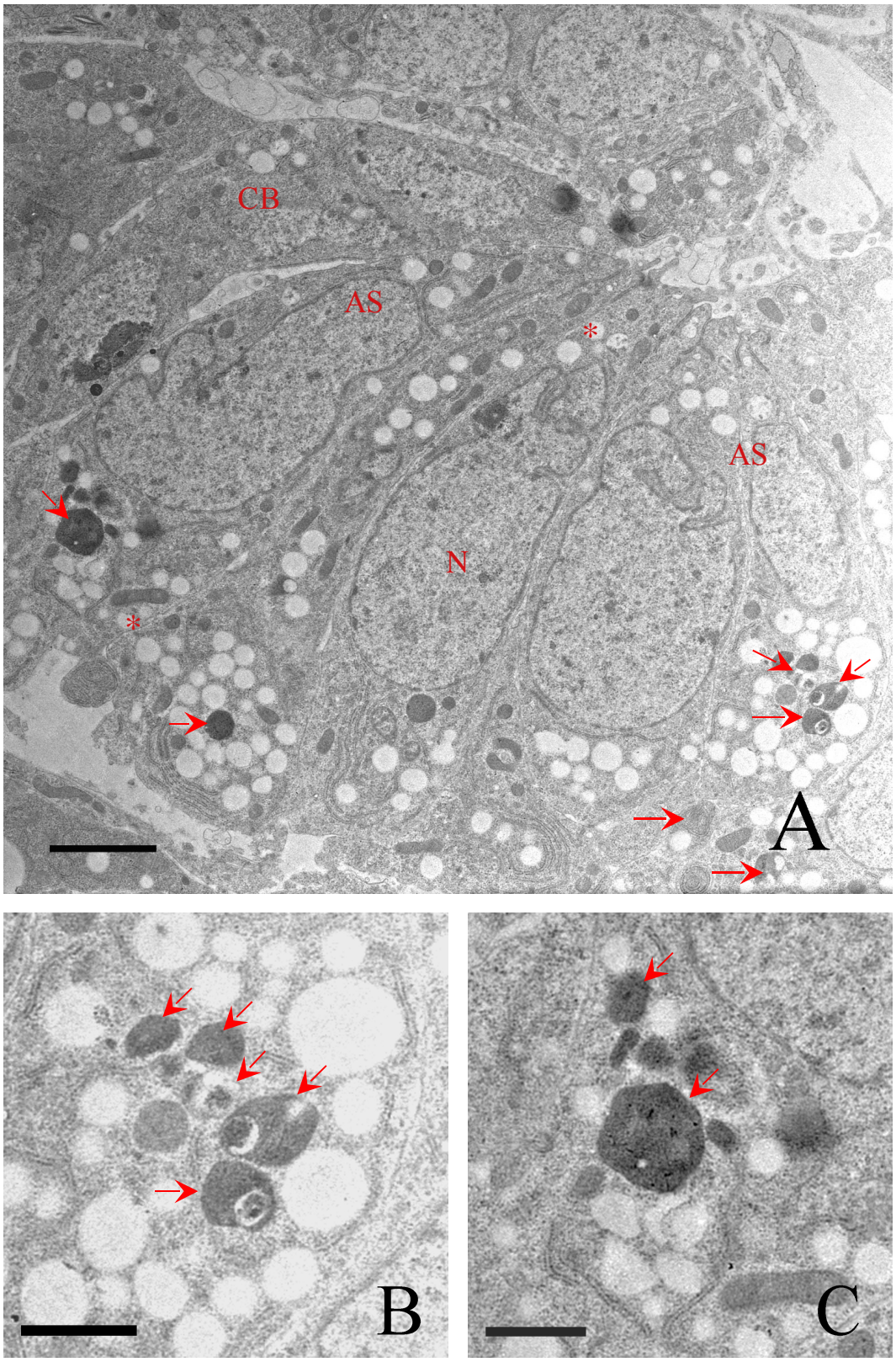
CB
AS
AS
N
A
B
C

3.5 Inhibition of Autophagy in the AS

Live imaging of embryos, expressing activated Insulin Receptor (ΔαInR) driven by either *bsgGAL4* or $GAL4^{LP\text{-}1}$+GFP^{nls}, and *Ubi-DEcad-GFP* demonstrated a very low extrusion rate. Moreover, embryos, expressing *UAS-ΔαInR* in the AS using $GAL4^{LP\text{-}1}$+GFP^{nls}, displayed a fully persistent AS. The activated insulin receptor is believed to inhibit autophagy (Scott et al., 2004). To confirm that autophagy is interrupted in the AS, an ultra-structure on *UAS-ΔαInR*, $GAL4^{LP\text{-}1}$ embryos was performed (Figure 3.15). It was noticed that no autophagic vacuole structures exist in this background, but many abnormally large vacuoles resembling huge lipid droplets, were seen in the AS. LysoTracker staining did not detect a significant acidic compartments in the AS, suggesting the lack of autolysosomal activity in this tissue. Morphogenetic events of GBR, DC, and HI occurred normally in the embryos expressing *Δ*αInR"G" in the AS. Global expression of *UAS-ΔαInR* using *daGAL4* produced highly abnormal AS, having disorganized apical membranes. Interestingly, all other epidermal tissues appeared normal.

3.6 Does Autophagy Lead to Apoptosis?

Following the observation of a persistent AS in an inhibited autophagy background, we tried to activate autophagy in the AS to examine if autophagy affects the rate of extrusion and causes premature death. Live imaging on globally expressing $ATG1^{6A}$ (one or two copies) driven by either *bsgGAL4* or *daGAL4* did not display a high rate of extrusion in almost all embryos but, to our surprise, displayed a very low rate of extrusion. Interestingly, one embryo of six imaged showed an elevated rate of extrusion; the other five embryos showed a reduced level of extrusion. It is not clear if the embryo having the elevated rate of extrusion was an anomaly within this genetic background or if it reflects an alternate phenotype that may be attributable to different levels of ATG1 expression (possible with the UAS-GAL4 system). Without further analysis of this genotype, we are interpreting the reduced extrusion rate as the phenotype of the global

expression of ATG1. Moreover, the AS tore towards the end of DC, possibly indicating a need for healthy cells to facilitate extrusion (see discussion). A premature AS death was also observed in this background (data not shown). The acridine orange staining on this background displayed enhanced AO positive corpses. Therefore, an increased rate of apoptosis in a background with activated autophagy appears to be possible.

Figure 3.15 Autophagy does not proceed normally in ectopic expression of Δ*αInR* (activated insulin receptor) in the AS. Panels display the TEM of the AS in ectopic expression of Δ*αInR* embryos using $GAL4^{LP\text{-}1}$. Note the absence of autophagic structures. There are very few lysosomes (arrow head) in the amnioserosa compared with those in the other backgrounds. Panel (B) is the enlargements of the representative lysosomes (arrow heads), from panel (A). AS, amnioserosa; DH, dorsal hole; EP, epidermis; N, nucleus;. The scale bar is 4 μm in (A) and 2 μm in (B).

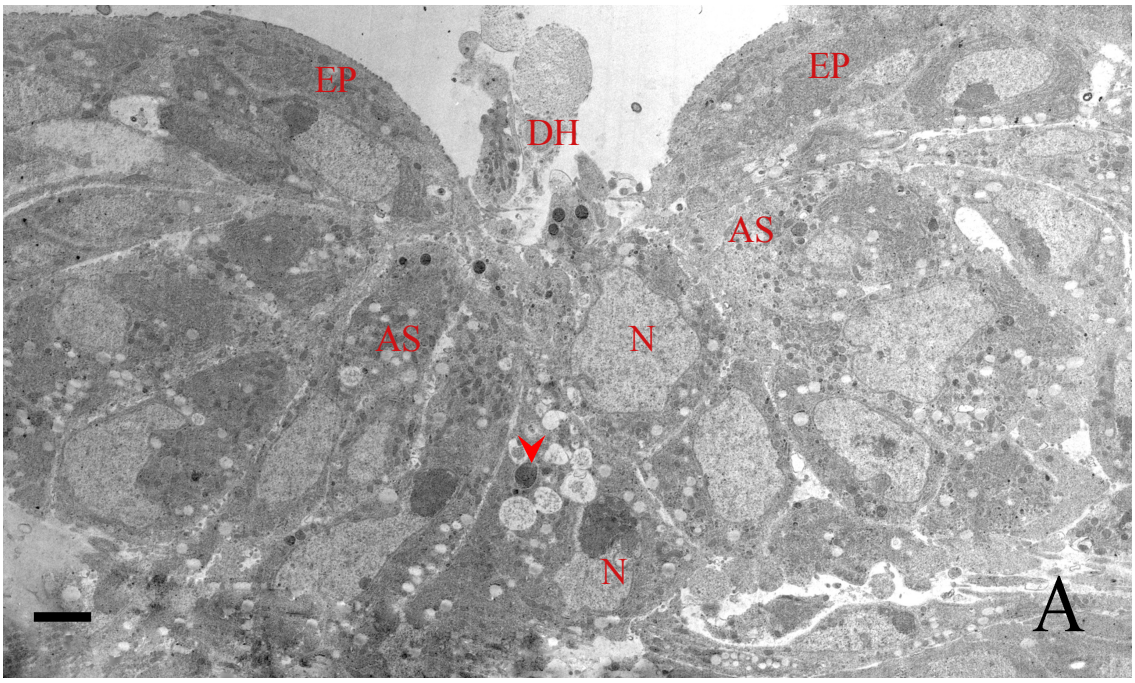
EP
DH
EP
AS
AS
N
N
A

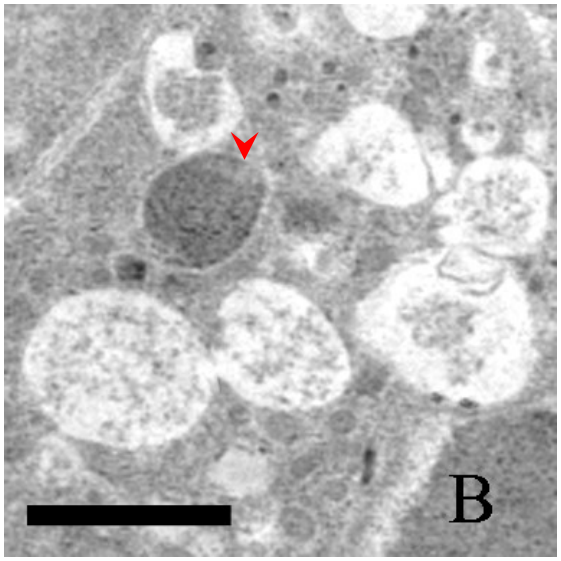
B

Chapter 4

Discussion

The primary objective of this study was to determine the nature of the degeneration of the extra-embryonic AS. The AS, a monolayer epithelium derived from dorsal blastoderm, is required for certain morphogenetic processes in developing *Drosophila* embryos. On the completion of DC, the AS is no longer needed and eventually dissociates (Hartenstein, V. and Jan, Y. N., 1992). The primary mechanism of AS degeneration, whether by PCD or otherwise, was not clearly understood prior to this study.

4.1 contribution of Extrusion to Maintain Epithelial Integrity

Our GFP-based time lapse confocal live imaging in the control (yw^{67}) embryos reveal that 10% of the AS cells are basally extruding from the epithelium during DC. Cell extrusion is a common theme for the removal of the apoptotic epithelial cells in different organisms. Examples of epithelial extrusion include retinal pigment epithelial cells in chick embryos (Nagai and Kalnins, 1996), the MDCK (Madin-Darby canine kidney)monolayer epithelial cell line (Rosenblatt et al., 2001), wing disc epithelia in *Drosophila* (Janody and Treisman, 2006; Shen and Dahmann, 2005), and murine intestine epithelium (Madara, 1990).

Based on studies using the MDCK monolayer epithelium system, Rosenblatt *et al*. have proposed a model for the epithelial extrusion. According to this model, a cell which is doomed to die sends signals to neighboring cells, subsequently inducing the formation of an actin/myosin contractile ring in the baso-lateral side of neighboring cells, as well as within the dying cell. The actin/myosin rings in the apoptotic cell and the neighbors contract, eventually squeeze the dying cell out of the epithelium, efficiently closing the remaining gap left by the extruded cell without disrupting the barrier function of the epithelium.

To investigate the role of actin in the extrusion of the AS, actin-GFP was expressed in the AS, however, no actin accumulation appeared in the extruding or neighboring cells which may be due to the lack of a full wild-type function of the actin-GFP fusion protein. Surprisingly, phalloidin staining showed the accumulation of actin around the extruding cell. This system was not sensitive enough to determine if the accumulation of actin occurs inside the dying cell, the neighboring cells or both (Reedlab, unpublished data).

The preservation of a barrier function is an essential role for any epithelium. Clearly, to maintain a barrier function, the epithelium should remain intact. The death and phagocytic engulfment of apoptotic cells within an epithelium represents a threat to the monolayer integrity. Therefore, it is suggested that in an epithelium, extrusion functions as the primary apoptotic cell removal mechanism. The phagocytosis engulfment of apoptotic corpses still occurs following extrusion, and so, here, phagocytosis can be considered secondary to extrusion. Cell death is common in epithelia, as well as other tissues, during development. It seems reasonable that apoptotic cell extrusion is required, and plays a critical role during the development of all the epithelial tissues (Rosenblatt et al., 2001).

4.2 Contribution of Extrusion to Dorsal Closure

Interactions between the lateral epidermis and the AS are pivotal to the regulation of the morphogenetic events of GBR and DC. During the initiation of DC the leading edge cells of the lateral epithelium, which flank the dorsal hole, become rich in filamentous actin and non-muscle myosin II, and elongate along the dorsal-ventral axis. Through generating a “purse-string” force, the leading edge actin-myosin contraction assists in bringing the two lateral epithelial sheets towards one another and leads to the closing of the dorsal hole (Mizuno et al., 2002). Although this and other evidence demonstrate that the leading edges of the lateral epidermis generate forces required for a successful dorsal closure (Kiehart et al., 2000), the AS is an additional force-

producing tissue, drawing the lateral epidermis towards the dorsal midline (Kiehart et al., 2000); the loss of AS integrity before the completion of the DC, either genetically or mechanically (laser ablation), leads to the interruption of this process (Kiehart et al., 2000). Although it is noteworthy that if the AS disruption occurs late in the DC, the purse string force can achieve DC (Hutson et al., 2003; Scuderi and Letsou, 2005; Kiehart et al., 2000). In this thesis, AS cells were observed to exhibit pulsating contractions, and 10% of the AS cells on average, are extruded during the DC in wild-type embryos. This pulsating contractile AS cell behavior is also observed in the inhibited or activated apoptotic backgrounds; the rate of extrusion in these backgrounds was either negligible or increased two-fold in these genotypes, respectively. DC in apoptotic defective backgrounds was found to be slower than the rate observed in control embryos. The absence of extrusion in our apoptotic defective animals might result in reduced tension in the AS tissue, and this, as a consequence, may result in a slower DC rate. In an elevated rate of extrusion genotype (global expression of *rpr*), however, the rate of DC was similar to the wild-type and displayed no increase. Live imaging and cuticle preparation in this background confirmed that the embryos complete GBR, and DC, but it appeared that the closed dorsal hole subsequently recoiled, as cuticle preparation revealed a consistent dorsal hole phenotype. The recoiling event is probably due to the fact that *rpr* over-expression suppresses the final suturing of the lateral epidermal sheets, which although contact each other, fail to fuse into a coherent epidermal sheet. This thesis supports the interpretation that extrusion, in general, contributes towards the generation of tension in the AS which is required for the normal rate of dorsal closure.

4.3 Apoptosis Leads to Extrusion

To test if apoptosis leads to extrusion we measured the frequency of extrusion in different genetic backgrounds. We examined the rate of AS cell extrusion in apoptotic defective embryos as well as apoptosis induced genotypes, and compared these results with those of the control. Acridine orange staining was initially performed in all of these backgrounds to confirm that theses animals exhibited inhibited or elevated apoptosis, respectively.

Our experimental observations indicate that the extrusion of AS cells is a caspase-dependent process, since the two apoptotic defective backgrounds (*Df(3L)ED225* mutants and global expression of *p35*) portray negligible extrusion. In addition, the global expression of *reaper* leads to an elevated rate of extrusion by more than two-fold. The attempt to over-express the other pro-apoptotic genes: *grim*, *hid*, or *rpr+hid* with *daGAL4*, turns out to be devastating to the embryos, and yielded severely developmentally defective embryos. Targeting the expression of *reaper* or *grim* to the AS by using either $GAL4^{LP\text{-}1}$ or *bsgGAL4* drivers, does not cause premature AS death, or even a considerable elevated rate of extrusion, as expected. These observations suggest that the induction of apoptosis, particularly through *reaper* or *grim*, is highly dependent on the level of expression of these proteins; a low level of expression is not fatal to the AS, but a high level causes premature AS cell death, consequently, the embryos fail in GBR or DC. These findings are consistent with the results obtained from the ectopic expression of *rpr* in adult fly eye retina. The size of the eye is reduced by increasing the number of copies of *rpr*, expressed in this organ. Although one copy of *rpr* does not seem to affect the size of the eyes, four copies of *rpr* completely eliminate the eyes. The eye ablation is rescued by the ectopic expression of *p35* in this organ: two copies of *p35* have rescued the ablated eye phenotype better than one copy (White K, 1996).

Studies on the embryonic CNS also support the notion that the level of expression of *rpr* (and *hid*) affects the extent of cell death induction. The number of surviving midline glia in each

embryonic segment of CNS, which are normally removed during development, is increased by the ectopic expression of two copies of either *rpr* or *hid*, relative to the expression of using only one copy of the same transgenes (Zhou et al., 1997).

The over-expression of *hid* or *rpr+hid* using $GAL4^{LP\text{-}1}$ or *bsgGAL4* drivers led to GBR failure due to an premature AS death. Moreover, the global over-expression of *hid* or *rpr+hid* using the *daGAL4* driver resulted in fully destroyed embryos. Compared with *reaper*, the over-expression of *hid*, has a stronger effect on the cells and causes malformed embryos with all three of GAL4 drivers tested. While we can not be absolutely certain without quantitative analysis on the levels of expression in these different backgrounds, our preliminary data suggest that AS cells are more sensitive to *hid* over-expression. This is interesting because *hid* expression has also been linked with Egfr signaling through MAPK pathway (Bergmann et al., 2002). Curiously, Egfr mutants have been found to fail in GBR due to premature AS death.

It was recently reported that the inhibition of caspases through either p35 or DIAP1 does not inhibit the extrusion of wing disc epithelial cells in which the apoptotic program has been activated (Treisman, 2006). A separate study on MDCK (cell line treated with Z-VAD-fmk, a caspase inhibitor peptide, also reported no block of epithelial extrusion (Rosenblatt et al., 2001). Treisman *et al*, proposed that the inhibition of apoptosis, through p35 or DIAP1, acts downstream of an extrusion signal, and the same interpretation was made by Rosenblatt *et al*.; that is the extrusion signal precedes the activation of the caspases. In the wing disc study, however, it is not clearly shown if the expression of either p35 or DIAP1 inhibits the endogenous pattern of apoptosis in this tissue. Our experiments provide evidence that the levels of either p35 or DIAP1 expression can often be insufficient to completely block apoptosis. In our apoptotic defective backgrounds, we were able to demonstrate a complete block of apoptotic cell death by AO staining. In these other studies it is not clear that the blockage was complete. It is possible that partial caspase activation may activate extrusion without execution of full-blown apoptosis. Indeed, our observation led us to suggest that the apoptotic program (the activation of the

caspases) is primed in individual AS cells that are destined to be extruded. We suggest that the apoptotic pathway does not become fully activated, while the AS cells are still contacting neighboring cells. It is interesting to speculate that the apical contact between the extruding cell and its neighbors may create an inhibitory signal with respect to the full induction of apoptosis. Strikingly, we found that three minutes after the loss of apical contact fragmentation, blebbing and engulfment by macrophages were readily evident. This is consistent with some of the observations on MDCK cells where annexin V labels only those cells that have completely left the tissue; once extruded, the fully apoptotic cells expose phosphatidylserine to signal for the macrophages' uptake (Rosenblatt et al., 2001).

4.4 AS Tissue Dissociation

While it was found that 10 % of the AS cells are eliminated through extrusion during DC in the wild-type embryos, the remaining 90% of the AS cells dissociate following DC. The global expression of p35 and *H99* deficient embryos display a persistent AS; the global expression of *rpr* results in a faster tissue dissociation than that of the wild-type. Our data suggest that phase two of the AS elimination is also a caspase-dependent process.

4.5 Autophagy and Caspase Activation in the AS

In persistent AS backgrounds, such as *Df(3L)H99*, the AS eventually shrinks as embryogenesis proceeds. Previous studies suggest that autophagy is often prominent when an entire tissue is eliminated (Lockshin and Zakeri, 2004). We decided to investigate the possible role of autophagy in the removal of the AS. In the Introduction of this thesis four models of the regulatory pathways concerning apoptosis and autophagy were proposed (Figures 1.5 to 1.8).

In the first model, caspase activation is upstream of both apoptosis and autophagy (and consequently autophagic death), but downstream of the *H99* genes. In the second model, the *H99*

genes activate both caspases and autophagy. The third model places autophagy (high level) upstream of both the apoptotic pathway as well as autophagic cell death (here it is important to distinguish autophagy and autophagic cell death as separate processes). The fourth model suggests that apoptosis and autophagy (and autophagic cell death) function independently.

TEM analysis reported in this thesis indicates that autophagy is prominent in the AS of wild-type, *p35*, and *H99*/*Df(3L)ED225* genetic backgrounds. All genotypes demonstrate abundant autophagosome/autolysosome structures. These observations convey two facts: first, autophagy occurs in the AS; and second, autophagy can occur without caspase activation and independent of *H99* genes. Therefore the first two models were ruled out.

To examine the third model, we tested if the inhibition of autophagy would affect the progression of apoptosis in the AS. It has been previously shown that activated insulin receptor ($\Delta\alpha$InR) inhibits autophagy in the larval fat body (Scott et al., 2004) and we confirmed the lack of autophagy in the AS by ultra structure and LysoTracker staining in this background. Surprisingly, the expression of activated InR in the AS results in no extrusion and yields a strong persistent AS phenotype. Given the absence of apoptosis through the inhibition of autophagy, these striking data suggest that autophagy could activate apoptosis in the AS. This supports model three.

To confirm model three, the next goal was to test if over-expression of an essential autophagy gene would lead to apoptosis activation in the AS. It has been shown that over-expression of ATG1 can induce autophagy in wing disc clones in *Drosophila* and that these cells enter apoptosis (Scott et al., 2007). We used the same approach and examined embryos in which ATG1 was globally over-expressed. AO staining suggests that there is elevated apoptotic cell death in this background. The rate of extrusion in this background, however, was very low; AS cells were irregularly contracted in appearance and the entire AS tissue tore apart prior to the completion of DC. The AO staining and the massive macrophage activity that followed AS ripping led us to suggest that ATG1 expression is associated with premature AS death. The

surprising reduced extrusion rate (we expected an increased rate) in this background could be explained by the massive cell death observed in the AS. The massive AS death could indicate a possible requirement for living neighbors to co-ordinate extrusion. Therefore, the absence of healthy living cells within the AS of this background could explain the lack of extrusion in such backgrounds.

The definitive experiment to confirm model three would involve co-expressing ATG1 and p35 in the AS. These experiments are in progress. If the premature AS death associated with ATG1 expression is suppressed by p35, model three will be confirmed. Otherwise, a lack of suppression would favor model four.

4.6 Possible Role of Autophagy in Regulating Ecdysone Biosynthesis

Cuticle preparation on global expression of ATG1 was performed to search for any possible GBR or DC failure indicative of premature AS death. To our surprise, cuticle preparation on this background and on ectopically expressed ATG1 in the AS with $GAL4^{LP\text{-}1}$ exhibited a thin cuticle formation in the embryos. This phenotype is known as the "Halloween group" phenotype and is considered a hallmark of defective ecdysone biosynthesis.

Ecdysone has been demonstrated to be necessary for cuticle deposition in late embryogenesis (Kozlova and Thummel, 2003) and the embryonic pulse of the ecdysone is thought to initiate during GBR. The AS has been favored to be the main site of ecdysone biosynthesis. The Halloween group genes encode several enzymes, required for ecdysone biosynthesis (Ono et al., 2006). The thin cuticle phenotype we observed in global or ectopical expression of ATG1 may indicate that autophagy induction either downregulates protein synthesis or acts selectively; that is, the ecdysosteroid hormone can be selectively chosen for degradation in an enhanced autophagy background. Curiously, we also observed a similar thin cuticle phenotype for the over-expression of DFOXO in the AS (data not shown).

In a further experiment we tried to kill the AS and eliminate the putative embryonic source ecdysone by expressing ricin, a toxic protein which acts through the inhibition of protein synthesis, in this tissue with $GAL4^{LP\text{-}1}$. Although a thin cuticle phenotype in these embryos was anticipated, cuticle deposition was normal but the embryos failed GBR. A possible reason is the timing of the destruction of the AS by UAS-ricin and $GAL4^{LP\text{-}1}$. $GAL4^{LP\text{-}1}$ is not expressed in the AS very early, and the ricin induced death may not have been sufficiently early to prevent ecdysone production in the AS. Another possibility is that the ring glands, another possible source of embryonic ecdysone may be sufficient for cuticle deposition (Kozlova and Thummel, 2003).

4.7 Conclusions

The studies described in this thesis, described AS dissociation as occurring in two phases: phase I or cell extrusion, during which 10% of the AS cells are eliminated; and phase II or tissue dissociation where the remaining 90% of the cells are removed. Both phases are caspase-dependent processes, since they are inhibited in apoptotic defective backgrounds, and elevated in apoptotic-induced genotypes and the lack of extrusion is correlated with the persistent AS. The two phases are likely manifestations of the same cellular event. Our data suggest that the activation of caspases is primed in individual AS cells that are destined to be extruded, and that apoptosis is not fully activated while the apical contacts still present. Three minutes after losing apical contact, we observed that extruding cells fragment, bleb and are rapidly engulfed by macrophages. Since the rate of DC is slower in the backgrounds lacking extrusion, it is also concluded that extrusion typically, generates adequate tension in the AS which is required for a normal rate of dorsal closure. Moreover, our data suggest that autophagy is also prominent in the AS degeneration and acts upstream of caspase activation and high level of autophagy can possibly trigger apoptosis.

4.8 Future Directions and Relevance of this Research

Although we obtained evidence indicating that high levels of autophagy leads to apoptosis, it was not unambiguously demonstrated in this study that over-expression of autophagy leads to apoptosis. To prove this possibility, it should be clearly shown that first, the over-expression of ATG1 leads to premature AS death, and second, this premature death can be interrupted by caspase inhibition through ectopic expression of *p35*.

The current view of autophagy is that this process acts non-selectively. Our results may indicate that the biosynthetic machinery responsible for ecdysone biosynthesis and /or activation could be a selective target of autophagy. Interestingly, while much is known of the regulation of the rise in ecdysone titre in insects, relatively little is known of how ecdysone levels fall following the peaks in titre.

Future studies regarding the selective nature of autophagy and the possible relationship between autophagy and apoptosis is of general interest to certain neurodegenerative diseases in humans, Alzheimer's and ALS, in particular. It is generally accepted that the excessive neuronal death presented in the pathologies of these debilitating disorders is the consequence of excessive abnormal protein aggregation. Autophagy is the normal cellular function that clears cells of such aggregates and it is thought that excessive autophagy may, in these diseases, activate neuronal apoptosis. Clearly, a strategy for the prevention of apoptosis in cells with high levels of autophagy represents a novel and exciting therapeutic approach. Our model system of AS death in *Drosophila* may ultimately contribute towards the hope of developing effective treatments for these diseases. There is currently no treatment for patients suffering from ALS, and this disease is invariably fatal.

Appendix A

A.1 *Drosophila* Heart Morphogenesis and the Amnioserosa

The heart or dorsal vessel in *Drosophila* is a long and narrow tube that spans from thorasic segment T2 to abdominal segment A8, and is located mid-dorsally under the epidermis (Figure A.1). Three kinds of cells form the dorsal vessel: cardioblasts, pericardial cells, and alary muscles. The precursors of both cardioblasts and pericardial cells originate from the lateral mesoderm during stage 12 (Figure A.2). A mature embryonic dorsal vessel consists of two layers; the inner layer is formed by cardioblasts and the outer one is created by pericardia cells. Cardioblasts are the contractile myoendothelial cells that meet the two layers, and join along the dorsal midline and create a hollow tube (Figure A.2). Cardioblasts are flanked by nonmuscular pericardial, which are responsible for haemolymph excretion (Figure A.2). Alary muscles, the third form of dorsal vessel cells, connect the dorsal vessel to the dorsal epidermis.

During stage 13, the precursors of the carioblasts and pericardial cells, located beneath the epidermis, begin to move dorsally and become close to the position of the AS (Figure A.2). During stage 15 immediately before DC, the AS cells are almost fully internalized, and the cardioblasts are located between the AS cells and the dorsal epidermis, and are in contact with both cell types. At stage 16, following DC, the leading edges of the cardioblasts meet along the dorsal midline, beneath the location, where the leading edge of the epidermal cells converge upon achieving DC. At this stage, the AS cells are still attached to the cardioblasts, and eventually undergo apoptosis. At the end of stage 16 joint cardioblasts begin to bend and join at the other end, forming a lumen (Hartenstein V., 1994). By this time, almost all of the AS cells are eliminated by apoptosis.

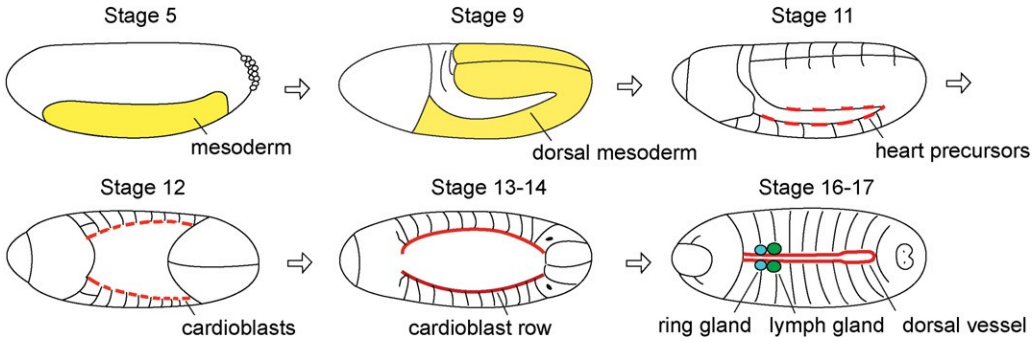

Figure A.1 Dorsal vessel morphogenesis. The heart precursors (red) originate from the lateral mesoderm (yellow) during stages 5 to 9, the arrangement and migration of the cardioblast cells (red) during stages 12-15 are essential for heart morphogenesis. The dorsal vessel/heart is formed by stage 16. The cardioblasts are in close proximity to the AS perimeter cells between stages 11 to 16. Embryos are anterior left, lateral view (stages 5-11) and dorsal view (stages 12-17) (Tao and Schulz, 2007).

Many genes are involved in the *Drosophila* cardiogenesis; among them, *tin* or *tinman*, the vertebrates' homologue of NK-2 class, plays an important role in the specification of the heart precursors. The expression of the homeodomain transcription factor, tin, is initiated early in the entire embryonic mesoderm, but is restricted later, to the dorsal mesoderm. *tinman* is required for the specification of the heart, visceral, and dorsal somatic muscles derivatives. The loss of function of this gene leads to the absence of mesodermal progenitors (Bodmer, 1993; Azpiazu and Frasch, 1993).

$tinman^{EC40}$ is a null, and embryonic lethal mutant of the *tinman* gene, obtained by the chemical mutagen ethyl-methanesulfonate (Bodmer, 1993).

Figure A.2 Dorsal vessel formation in *Drosophila*. At stage 12, heart precursors are located in the Cardiogenic Region (CR), the lateral part of the mesoderm (ms) (A). At stage 13, the precursors of the cardioblasts (ca) and pericardial cells (pe) move dorsally (B). During stage 15, just prior to the DC, the AS (as) internalizes; the cerdoblasts are located between the AS and the epidermis (ep) (C). At the early phase of stage 16, immediately following the DC, the leading edges of the cardioblasts join along the dorsal midline; the AS cells are still attached to the cardioblasts (D). The lumen of the dorsal vessel is formed in a late stage 16 embryo, when the edges of the cardioblasts bend and join. Most of the AS cells are removed by this stage (E). At the stage 17, the formation of the lumen is complete and macrophages (mc) has engulfed the apoptotic AS corpses (F). Adheren junctions are indicated as short thick double lines (Adopted from (Hartenstein v., 1994).

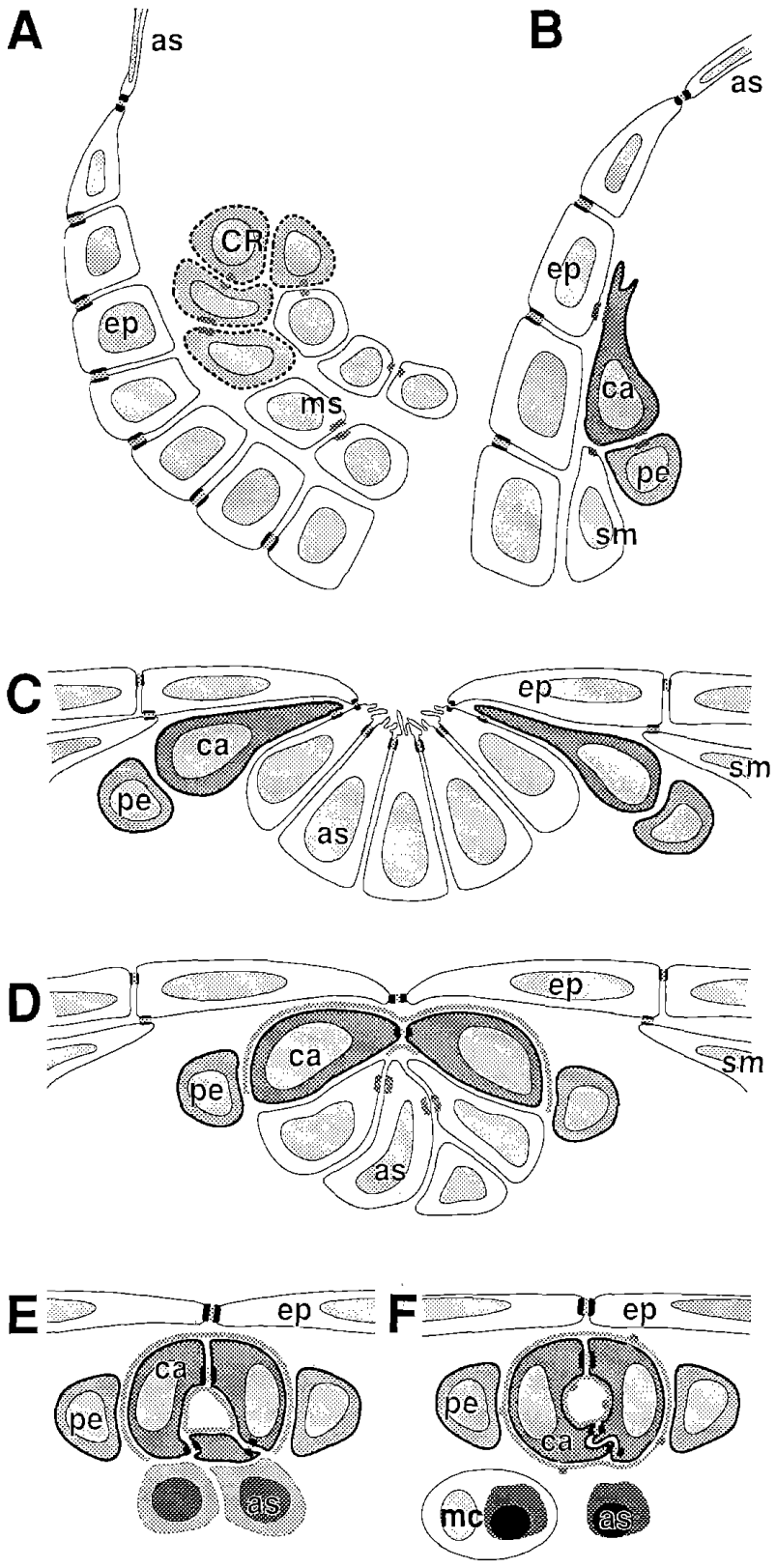
A
as
CR
ep
ms
B
as
ep
ca
pe
sm
C
ep
ca
sm
pe
as
D
ep
ca
sm
pe
as
E
ep
ca
pe
as
F
ep
pe
ca
mc
as

A.2 *Df(3L)ED225*, *tinman*^{EC40} Mutants

Following DC in the *Df(3L)H99* homozygous mutants, *Df(3L)ED225* homozygous mutants or globally expressing *p35* the internalized AS gradually stretched out and formed an elongated tube beneath the epidermis. We assumed that the final elongated shape of the persistent AS in the apoptotic defective backgrounds is dependent on the persistent contact between the AS cells and the cardioblasts. Therefore, the hypothesis was tested by constructing a double mutant recombinant between *tinman*^{EC40}, a mutant suffering the from lack of a heart formation and *Df(3L)ED225***.** Since the heart/dorsal vessel formation occurs after DC, and the AS perimeter cells are in close contact with the cardioblasts, we speculated that the contacts between the AS cells and the cardioblasts in the *H99* , *ED225* or globally expressing *p35* mutants did not break, probably since the breakage of the AS and cardioblasts contacts is a caspase dependent process. Therefore in the absence of caspase activity the AS and cardioblasts remain connected. As the dorsal vessel formed, the attached AS also elongates. RNA *in situ* hybridization on these double mutant embryos, using a specific AS probe, CG12011, disproved this assumption, since the long tube-like AS was still observed in the double mutant background (Figure A.3). These data suggest that the terminal AS shape in the apoptotic defective backgrounds is not related to the caspase dependent contacts between the AS perimeter cells and the cardioblasts of the developing embryonic heart.

Figure A.3 *In situ* hybridization of the AS in *tinman*^{EC40} and *ED225* double mutants indicates elongated AS phenotype. *in situ* on control (*ED225*, *tinman*^{EC40} heterozygous embryos) using a specific AS probe demonstrates that the AS cells start to disperse at approximately, 13 hr AEL (A). The AS dissociation dose not occur in *H99* mutants, and the persistent AS begins to gradually form an elongated tube (B). A double mutant including t*inman*^{EC40}, which fails to form dorsal vessel, and *ED225*, portrays the similar elongated AS phenotype, observed in single *ED225* mutants (C). Head defect is clearly visible in both single or double mutants. Embryos are anterior left, dorsal up.

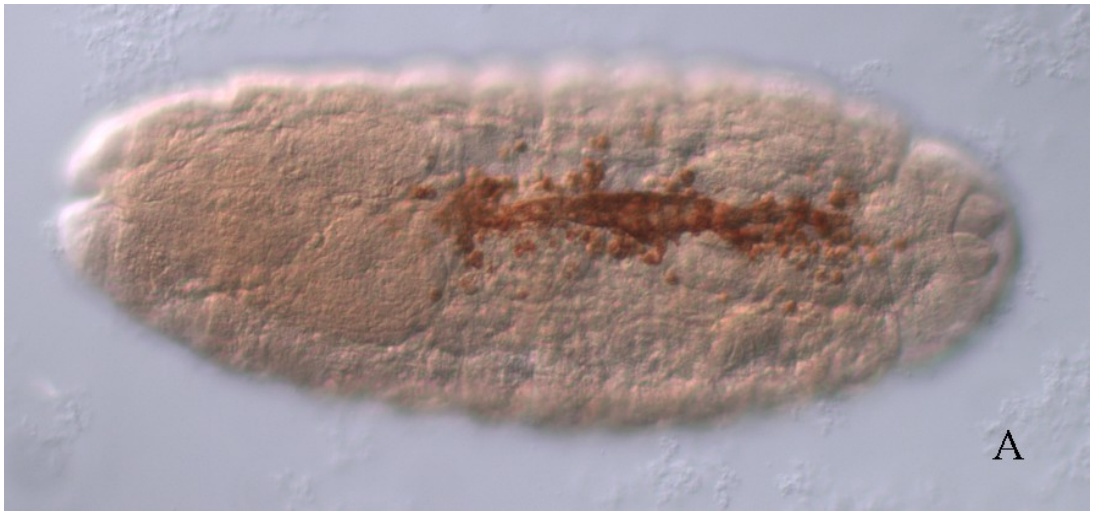
A


B


C

References

Abrams, J. M., White, K., Fessler, L. I. and Steller, H. (1993). Programmed Cell Death during Drosophila Embryogenesis. *Development* **117,** 29-43.

Azpiazu, N. and Frasch, M. (1993). Tinman and Bagpipe: Two Homeo Box Genes that Determine Cell Fates in the Dorsal Mesoderm of Drosophila. *Genes Dev.* **7,** 1325-1340.

Baehrecke, E. H. (2002). How Death Shapes Life during Development. *Nat. Rev. Mol. Cell Biol.* **3,** 779-787.

Baehrecke, E. H. (2003). Autophagic Programmed Cell Death in Drosophila. *Cell Death Differ.* **10,** 940-945.

Bangs, P., Franc, N. and White, K. (2000). Molecular Mechanisms of Cell Death and Phagocytosis in Drosophila. *Cell Death Differ.* **7,** 1027-1034.

Bao, Q. and Shi, Y. (2007). Apoptosome: A Platform for the Activation of Initiator Caspases. *Cell Death Differ.* **14,** 56-65.

Bergmann, A., Tugentman, M., Shilo, B. Z. and Steller, H. (2002). Regulation of Cell Number by MAPK-Dependent Control of Apoptosis: A Mechanism for Trophic Survival Signaling. *Dev. Cell.* **2,** 159-170.

Berry, D. L. and Baehrecke, E. H. (2007). Growth Arrest and Autophagy are Required for Salivary Gland Cell Degradation in Drosophila. *Cell* **131,** 1137-1148. **Bodmer, R.** (1993). The Gene Tinman is Required for Specification of the Heart and Visceral Muscles in Drosophila. *Development* **118,** 719-729.

Bodmer, R. (1993). The Gene Tinman is Required for Specification of the Heart and Visceral Muscles in Drosophila. *Development* **118,** 719-729.

Campos-Ortega JA. (1997). The Embryonic Development of Drosophila Melanogaster.

Chan, T. O., Rittenhouse, S. E. and Tsichlis, P. N. (1999). AKT/PKB and Other D3 Phosphoinositide-Regulated Kinases: Kinase Activation by Phosphoinositide-Dependent Phosphorylation. *Annu. Rev. Biochem.* **68,** 965-1014.

Chavez, V. M., Marques, G., Delbecque, J. P., Kobayashi, K., Hollingsworth, M., Burr, J., Natzle, J. E. and O'Connor, M. B. (2000). The Drosophila Disembodied Gene Controls Late Embryonic Morphogenesis and Codes for a Cytochrome P450 Enzyme that Regulates Embryonic Ecdysone Levels. *Development* **127,** 4115-4126.

Christich, A., Kauppila, S., Chen, P., Sogame, N., Ho, S. I. and Abrams, J. M. (2002). The Damage-Responsive Drosophila Gene Sickle Encodes a Novel IAP Binding Protein Similar to but Distinct from Reaper, Grim, and Hid. *Curr. Biol.* **12,** 137-140.

Chung, J., Kuo, C. J., Crabtree, G. R. and Blenis, J. (1992). Rapamycin-FKBP Specifically Blocks Growth-Dependent Activation of and Signaling by the 70 Kd S6 Protein Kinases. *Cell* **69,** 1227-1236.

Clarke, P. G. (1990). Developmental Cell Death: Morphological Diversity and Multiple Mechanisms. *Anat. Embryol. (Berl)* **181,** 195-213.

Clerc, S. and Barenholz, Y. (1998). A Quantitative Model for using Acridine Orange as a Transmembrane pH Gradient Probe. *Anal. Biochem.* **259,** 104-111.

Delic, J., Coppey, J., Magdelenat, H. and Coppey-Moisan, M. (1991). Impossibility of Acridine Orange Intercalation in Nuclear DNA of the Living Cell. *Exp. Cell Res.* **194,** 147-153.

Deveraux, Q. L. and Reed, J. C. (1999). IAP Family Proteins--Suppressors of Apoptosis. *Genes Dev.* **13,** 239-252.

Dorstyn, L., Mills, K., Lazebnik, Y. and Kumar, S. (2004). The Two Cytochrome c Species, DC3 and DC4, are Not Required for Caspase Activation and Apoptosis in Drosophila Cells. *J. Cell Biol.* **167,** 405-410.

Du, C., Fang, M., Li, Y., Li, L. and Wang, X. (2000). Smac, a Mitochondrial Protein that Promotes Cytochrome c-Dependent Caspase Activation by Eliminating IAP Inhibition. *Cell* **102,** 33-42.

Dunn, W. A.,Jr. (1990). Studies on the Mechanisms of Autophagy: Formation of the Autophagic Vacuole. *J. Cell Biol.* **110,** 1923-1933.

Earnshaw, W. C., Martins, L. M. and Kaufmann, S. H. (1999). Mammalian Caspases: Structure, Activation, Substrates, and Functions during Apoptosis. *Annu. Rev. Biochem.* **68,**

383-424.

Fesik, S. W. and Shi, Y. (2001). Structural Biology. Controlling the Caspases. *Science* **294,** 1477-1478.

Franc, N. C., Dimarcq, J. L., Lagueux, M., Hoffmann, J. and Ezekowitz, R. A. (1996). Croquemort, a Novel Drosophila hemocyte/macrophage Receptor that Recognizes Apoptotic Cells. *Immunity* **4,** 431-443.

Frank, L. H. and Rushlow, C. (1996). A Group of Genes Required for Maintenance of the Amnioserosa Tissue in Drosophila. *Development* **122,** 1343-1352.

Gorski, S. M., Chittaranjan, S., Pleasance, E. D., Freeman, J. D., Anderson, C. L., Varhol, R. J., Coughlin, S. M., Zuyderduyn, S. D., Jones, S. J. and Marra, M. A. (2003). A SAGE Approach to Discovery of Genes Involved in Autophagic Cell Death. *Curr. Biol.* **13,** 358-363.

Goyal, L., McCall, K., Agapite, J., Hartwieg, E. and Steller, H. (2000). Induction of Apoptosis by Drosophila Reaper, Hid and Grim through Inhibition of IAP Function. *EMBO J.* **19,** 589-597.

Hanahan, D. and Weinberg, R. A. (2000). The Hallmarks of Cancer. *Cell* **100,** 57-70.

Hartenstein, V. (1993). Atlas of Drosophila Development. Cold Spring Harbor Laboratory Press

Hartenstein, V (1994). Embryonic Origin and Differentiation of the Drosophila Heart. **203,** 266-280.

Hartenstein, V. and Jan, Y. N. (1992). Studying Drosophila Embryogenesis with P-lacZ Enhancer Trap Lines. **201,** 194-220.

Huang, H., Joazeiro, C. A., Bonfoco, E., Kamada, S., Leverson, J. D. and Hunter, T. (2000). The Inhibitor of Apoptosis, cIAP2, Functions as a Ubiquitin-Protein Ligase and Promotes in Vitro Monoubiquitination of Caspases 3 and 7. *J. Biol. Chem.* **275,** 26661-26664.

Hutson, M. S., Tokutake, Y., Chang, M. S., Bloor, J. W., Venakides, S., Kiehart, D. P. and Edwards, G. S. (2003). Forces for Morphogenesis Investigated with Laser Microsurgery and Quantitative Modeling. *Science* **300,** 145-149.

Janody, F. and Treisman, J. E. (2006). Actin Capping Protein Alpha Maintains Vestigial-

Expressing Cells within the Drosophila Wing Disc Epithelium. *Development* **133,** 3349-3357.

Jiang, C., Baehrecke, E. H. and Thummel, C. S. (1997). Steroid Regulated Programmed Cell Death during Drosophila Metamorphosis. *Development* **124,** 4673-4683.

Jiang, C., Lamblin, A. F., Steller, H. and Thummel, C. S. (2000). A Steroid-Triggered Transcriptional Hierarchy Controls Salivary Gland Cell Death during Drosophila Metamorphosis. *Mol. Cell* **5,** 445-455.

Kabeya, Y., Kamada, Y., Baba, M., Takikawa, H., Sasaki, M. and Ohsumi, Y. (2005). Atg17 Functions in Cooperation with Atg1 and Atg13 in Yeast Autophagy. *Mol. Biol. Cell* **16,** 2544-2553.

Kiehart, D. P., Galbraith, C. G., Edwards, K. A., Rickoll, W. L. and Montague, R. A. (2000). Multiple Forces Contribute to Cell Sheet Morphogenesis for Dorsal Closure in Drosophila. *J. Cell Biol.* **149,** 471-490.

Klionsky, D. J. and Emr, S. D. (2000). Autophagy as a Regulated Pathway of Cellular Degradation. *Science* **290,** 1717-1721.

Kornbluth, S. and White, K. (2005). Apoptosis in Drosophila: Neither Fish nor Fowl (nor Man, nor Worm). *J. Cell. Sci.* **118,** 1779-1787.

Kozlova, T. and Thummel, C. S. (2003). Essential Roles for Ecdysone Signaling during Drosophila Mid-Embryonic Development. *Science* **301,** 1911-1914.

Kozma, S. C. and Thomas, G. (1994). P70s6k/p85s6k: Mechanism of Activation and Role in Mitogenesis. *Semin. Cancer Biol.* **5,** 255-260.

Krause. H. M (2006)., FISH Protocols for Drosophila. http://www.utoronto.ca/krause/FISH.html. Accessed 2008 January 10.

Lamka, M. L. and Lipshitz, H. D. (1999). Role of the Amnioserosa in Germ Band Retraction of the Drosophila Melanogaster Embryo. *Dev. Biol.* **214,** 102-112.

Lee, C. Y. and Baehrecke, E. H. (2001). Steroid Regulation of Autophagic Programmed Cell Death during Development. *Development* **128,** 1443-1455.

Lee, C. Y., Clough, E. A., Yellon, P., Teslovich, T. M., Stephan, D. A. and Baehrecke, E. H. (2003). Genome-Wide Analyses of Steroid- and Radiation-Triggered Programmed Cell Death in Drosophila. *Curr. Biol.* **13,** 350-357.

Lee, C. Y., Wendel, D. P., Reid, P., Lam, G., Thummel, C. S. and Baehrecke, E. H. (2000). E93 Directs Steroid-Triggered Programmed Cell Death in Drosophila. *Mol. Cell* **6,** 433-443.

Lee, S. B., Kim, S., Lee, J., Park, J., Lee, G., Kim, Y., Kim, J. M. and Chung, J. (2007). ATG1, an Autophagy Regulator, Inhibits Cell Growth by Negatively Regulating S6 Kinase. *EMBO Rep.* **8,** 360-365.

Levine, B. and Yuan, J. (2005). Autophagy in Cell Death: An Innocent Convict? *J. Clin. Invest.* **115,** 2679-2688.

Li, P., Nijhawan, D., Budihardjo, I., Srinivasula, S. M., Ahmad, M., Alnemri, E. S. and Wang, X. (1997). Cytochrome c and dATP-Dependent Formation of Apaf-1/caspase-9 Complex Initiates an Apoptotic Protease Cascade. *Cell* **91,** 479-489.

Lockshin RA and Zakeri Z. (2004). When Cells Die II: A Comprehensive Evaluation of Apoptosis and Programmed Cell Death.

Luo, X., Puig, O., Hyun, J., Bohmann, D. and Jasper, H. (2007). Foxo and Fos Regulate the Decision between Cell Death and Survival in Response to UV Irradiation. *EMBO J.* **26,** 380-390.

Madara, J. L. (1990). Maintenance of the Macromolecular Barrier at Cell Extrusion Sites in Intestinal Epithelium: Physiological Rearrangement of Tight Junctions. *J. Membr. Biol.* **116,** 177-184.

Martin, D. N. and Baehrecke, E. H. (2004). Caspases Function in Autophagic Programmed Cell Death in Drosophila. *Development* **131,** 275-284.

Meier, P., Silke, J., Leevers, S. J. and Evan, G. I. (2000). The Drosophila Caspase DRONC is Regulated by DIAP1. *EMBO J.* **19,** 598-611.

Mizuno, T., Tsutsui, K. and Nishida, Y. (2002). Drosophila Myosin Phosphatase and its Role in Dorsal Closure. *Development* **129,** 1215-1223.

Mizushima, N., Yamamoto, A., Hatano, M., Kobayashi, Y., Kabeya, Y., Suzuki, K.,

Tokuhisa, T., Ohsumi, Y. and Yoshimori, T. (2001). Dissection of Autophagosome Formation using Apg5-Deficient Mouse Embryonic Stem Cells. *J. Cell Biol.* **152,** 657-668.

Montagne, J., Stewart, M. J., Stocker, H., Hafen, E., Kozma, S. C. and Thomas, G. (1999). Drosophila S6 Kinase: A Regulator of Cell Size. *Science* **285,** 2126-2129.

Mukae, N., Enari, M., Sakahira, H., Fukuda, Y., Inazawa, J., Toh, H. and Nagata, S. (1998). Molecular Cloning and Characterization of Human Caspase-Activated DNase. *Proc. Natl. Acad. Sci. U. S. A.* **95,** 9123-9128.

Nagai, H. and Kalnins, V. I. (1996). Normally Occurring Loss of Single Cells and Repair of Resulting Defects in Retinal Pigment Epithelium in Situ. *Exp. Eye Res.* **62,** 55-61.

Neufeld, T. P. (2003). Body Building: Regulation of Shape and Size by PI3K/TOR Signaling during Development. *Mech. Dev.* **120,** 1283-1296.

Oda, H. and Tsukita, S. (2001). Real-Time Imaging of Cell-Cell Adherens Junctions Reveals that Drosophila Mesoderm Invagination Begins with Two Phases of Apical Constriction of Cells. *J. Cell. Sci.* **114,** 493-501.

Ono, H., Rewitz, K. F., Shinoda, T., Itoyama, K., Petryk, A., Rybczynski, R., Jarcho, M., Warren, J. T., Marques, G., Shimell, M. J. et al. (2006). Spook and Spookier Code for Stage-Specific Components of the Ecdysone Biosynthetic Pathway in Diptera. *Dev. Biol.* **298,** 555-570.

Pattingre, S., Espert, L., Biard-Piechaczyk, M. and Codogno, P. (2007). Regulation of Macroautophagy by mTOR and Beclin 1 Complexes. *Biochimie*.

Pattingre, S., Tassa, A., Qu, X., Garuti, R., Liang, X. H., Mizushima, N., Packer, M., Schneider, M. D. and Levine, B. (2005). Bcl-2 Antiapoptotic Proteins Inhibit Beclin 1-Dependent Autophagy. *Cell* **122,** 927-939.

Peterson, C., Carney, G. E., Taylor, B. J. and White, K. (2002). Reaper is Required for Neuroblast Apoptosis during Drosophila Development. *Development* **129,** 1467-1476.

Phelps, C. B. and Brand, A. H. (1998). Ectopic Gene Expression in Drosophila using GAL4 System. *Methods* **14,** 367-379.

Pyo, J. O., Jang, M. H., Kwon, Y. K., Lee, H. J., Jun, J. I., Woo, H. N., Cho, D. H., Choi, B.,

Lee, H., Kim, J. H. et al. (2005). Essential Roles of Atg5 and FADD in Autophagic Cell Death: Dissection of Autophagic Cell Death into Vacuole Formation and Cell Death. *J. Biol. Chem.* **280,** 20722-20729.

Qin, H., Srinivasula, S. M., Wu, G., Fernandes-Alnemri, T., Alnemri, E. S. and Shi, Y. (1999). Structural Basis of Procaspase-9 Recruitment by the Apoptotic Protease-Activating Factor 1. *Nature* **399,** 549-557.

Rao, L., Perez, D. and White, E. (1996). Lamin Proteolysis Facilitates Nuclear Events during Apoptosis. *J. Cell Biol.* **135,** 1441-1455.

Reed, B. H., Wilk, R. and Lipshitz, H. D. (2001). Downregulation of Jun Kinase Signaling in the Amnioserosa is Essential for Dorsal Closure of the Drosophila Embryo. *Curr. Biol.* **11,** 1098-1108.

Reed, B. H., Wilk, R., Schock, F. and Lipshitz, H. D. (2004). Integrin-Dependent Apposition of Drosophila Extraembryonic Membranes Promotes Morphogenesis and Prevents Anoikis. *Curr. Biol.* **14,** 372-380.

Rosenblatt, J., Raff, M. C. and Cramer, L. P. (2001). An Epithelial Cell Destined for Apoptosis Signals its Neighbors to Extrude it by an Actin- and Myosin-Dependent Mechanism. *Curr. Biol.* **11,** 1847-1857.

Rusten, T. E., Lindmo, K., Juhasz, G., Sass, M., Seglen, P. O., Brech, A. and Stenmark, H. (2004). Programmed Autophagy in the Drosophila Fat Body is Induced by Ecdysone through Regulation of the PI3K Pathway. *Dev. Cell.* **7,** 179-192.

Scott, R. C., Juhasz, G. and Neufeld, T. P. (2007). Direct Induction of Autophagy by Atg1 Inhibits Cell Growth and Induces Apoptotic Cell Death. *Curr. Biol.* **17,** 1-11.

Scott, R. C., Schuldiner, O. and Neufeld, T. P. (2004). Role and Regulation of Starvation-Induced Autophagy in the Drosophila Fat Body. *Dev. Cell.* **7,** 167-178.

Scuderi, A. and Letsou, A. (2005). Amnioserosa is Required for Dorsal Closure in Drosophila. *Dev. Dyn.* **232,** 791-800.

Shen, J. and Dahmann, C. (2005). Extrusion of Cells with Inappropriate Dpp Signaling from Drosophila Wing Disc Epithelia. *Science* **307,** 1789-1790.

Shi, Y. (2004). Caspase Activation: Revisiting the Induced Proximity Model. *Cell* **117,** 855-858.

Shimizu, S., Kanaseki, T., Mizushima, N., Mizuta, T., Arakawa-Kobayashi, S., Thompson, C. B. and Tsujimoto, Y. (2004). Role of Bcl-2 Family Proteins in a Non-Apoptotic Programmed Cell Death Dependent on Autophagy Genes. *Nat. Cell Biol.* **6,** 1221-1228.

Shiozaki, E. N. and Shi, Y. (2004). Caspases, IAPs and Smac/DIABLO: Mechanisms from Structural Biology. *Trends Biochem. Sci.* **29,** 486-494.

Srinivasula, S. M., Hegde, R., Saleh, A., Datta, P., Shiozaki, E., Chai, J., Lee, R. A., Robbins, P. D., Fernandes-Alnemri, T., Shi, Y. et al. (2001). A Conserved XIAP-Interaction Motif in Caspase-9 and Smac/DIABLO Regulates Caspase Activity and Apoptosis. *Nature* **410,** 112-116.

Staveley, B. E., Ruel, L., Jin, J., Stambolic, V., Mastronardi, F. G., Heitzler, P., Woodgett, J. R. and Manoukian, A. S. (1998). Genetic Analysis of Protein Kinase B (AKT) in Drosophila. *Curr. Biol.* **8,** 599-602.

Stromhaug, P. E., Berg, T. O., Fengsrud, M. and Seglen, P. O. (1998). Purification and Characterization of Autophagosomes from Rat Hepatocytes. *Biochem. J.* **335 (Pt 2),** 217-224.

Talbot, W. S., Swyryd, E. A. and Hogness, D. S. (1993). Drosophila Tissues with Different Metamorphic Responses to Ecdysone Express Different Ecdysone Receptor Isoforms. *Cell* **73,** 1323-1337.

Tao, Y. and Schulz, R. A. (2007). Heart Development in Drosophila. *Semin. Cell Dev. Biol.* **18,** 3-15.

Thompson, C. B. (1995). Apoptosis in the Pathogenesis and Treatment of Disease. *Science* **267,** 1456-1462.

Tschopp, J., Thome, M., Hofmann, K. and Meinl, E. (1998). The Fight of Viruses Against Apoptosis. *Curr. Opin. Genet. Dev.* **8,** 82-87.

Ueno, T., Muno, D. and Kominami, E. (1991). Membrane Markers of Endoplasmic Reticulum Preserved in Autophagic Vacuolar Membranes Isolated from Leupeptin-Administered Rat Liver. *J. Biol. Chem.* **266,** 18995-18999.

Van Cruchten, S. and Van Den Broeck, W. (2002). Morphological and Biochemical Aspects of Apoptosis, Oncosis and Necrosis. *Anat. Histol. Embryol.* **31,** 214-223.

Verhagen, A. M., Ekert, P. G., Pakusch, M., Silke, J., Connolly, L. M., Reid, G. E., Moritz, R. L., Simpson, R. J. and Vaux, D. L. (2000). Identification of DIABLO, a Mammalian Protein that Promotes Apoptosis by Binding to and Antagonizing IAP Proteins. *Cell* **102,** 43-53.

Walker NI, Harmon B V, Gobe G C and Kerr J F. (1988). Patterns of Cell Death. **13,** 18-54.

Wang, S. L., Hawkins, C. J., Yoo, S. J., Muller, H. A. and Hay, B. A. (1999). The Drosophila Caspase Inhibitor DIAP1 is Essential for Cell Survival and is Negatively Regulated by HID. *Cell* **98,** 453-463.

Wieschaus, E. and Nusslein-Volhard, C. (1986). Drosophila:A Practical Approach., 215.

Williamson, P., van den Eijnde, S. and Schlegel, R. A. (2001). Phosphatidylserine Exposure and Phagocytosis of Apoptotic Cells. *Methods Cell Biol.* **66,** 339-364.

Wyllie, A. H. (1980). Glucocorticoid-Induced Thymocyte Apoptosis is Associated with Endogenous Endonuclease Activation. *Nature* **284,** 555-556.

Yin, V. P. and Thummel, C. S. (2004). A Balance between the diap1 Death Inhibitor and Reaper and Hid Death Inducers Controls Steroid-Triggered Cell Death in Drosophila. *Proc. Natl. Acad. Sci. U. S. A.* **101,** 8022-8027.

Yin, V. P. and Thummel, C. S. (2005). Mechanisms of Steroid-Triggered Programmed Cell Death in Drosophila. *Semin. Cell Dev. Biol.* **16,** 237-243.

Yu, L., Alva, A., Su, H., Dutt, P., Freundt, E., Welsh, S., Baehrecke, E. H. and Lenardo, M. J. (2004). Regulation of an ATG7-Beclin 1 Program of Autophagic Cell Death by Caspase-8. *Science* **304,** 1500-1502.

Yuan, J., Shaham, S., Ledoux, S., Ellis, H. M. and Horvitz, H. R. (1993). The C. Elegans Cell Death Gene Ced-3 Encodes a Protein Similar to Mammalian Interleukin-1 Beta-Converting Enzyme. *Cell* **75,** 641-652.

Yuan, J. and Yankner, B. A. (2000). Apoptosis in the Nervous System. *Nature* **407,** 802-809.

Zamzami, N., Hirsch, T., Dallaporta, B., Petit, P. X. and Kroemer, G. (1997). Mitochondrial Implication in Accidental and Programmed Cell Death: Apoptosis and Necrosis. *J. Bioenerg. Biomembr.* **29,** 185-193.

Zhang, H., Stallock, J. P., Ng, J. C., Reinhard, C. and Neufeld, T. P. (2000). Regulation of Cellular Growth by the Drosophila Target of Rapamycin dTOR. *Genes Dev.* **14,** 2712-2724.

Zhou, L., Schnitzler, A., Agapite, J., Schwartz, L. M., Steller, H. and Nambu, J. R. (1997). Cooperative Functions of the Reaper and Head Involution Defective Genes in the Programmed Cell Death of Drosophila Central Nervous System Midline Cells. *Proc. Natl. Acad. Sci. U. S. A.* **94,** 5131-5136.